An-Najah National University

Faculty of Graduate Studies

IMPROVING CONCRETE PROPERTIES USING WASTE MATERIALS

By

Raja K. Sabra

Supervisors

Dr. Monther Dwaikat

Dr. Mahmoud Dwaikat

This thesis is Submitted in Partial Fulfillment of the Requirements for the Degree of Master of Structural Engineering, Faculty of Graduate Studies, An-Najah National University, Nablus, Palestine.

2023

IMPROVING CONCRETE PROPERTIES USING WASTE MATERIALS

By

Raja K. Sabra

This thesis was Defended Successfully on 08/10/2023 and approved by

Dr. Monther Dwaikat Supervisor	Signature
Dr. Mahmoud Dwaikat Co-Supervisor	Signature
Dr. Abdulsamee Halahla External Examiner	Signature
Dr. Mohammad Samaaneh Internal Examiner	Signature

Dedication

This thesis is dedicated to my parents for their infinite support, as well as to my whole family and friends.

With respect and love

Acknowledgment

I would like to express my sincere gratitude to my supervisor Dr. Mahmoud Dwaikat and Dr. Monther Dwaikat for their helpful gaudiness and efforts.

Declaration

I, the undersigned, declare that I submitted the thesis entitled:

IMPROVING CONCRETE PROPERTIES USING WASTE MATERIALS

I declare that the work provided in this thesis, unless otherwise referenced, is the researcher's own work, and has not been submitted elsewhere for any other degree or qualification.

Student's Name: Raja. K. Sabra

Signature: 

Date: 08/10/2023

Table of Contents

List of Tables

List of Figures

List of Appendices

IMPROVING CONCRETE PROPERTIES USING WASTE MATERIALS

By
Raja. K. Sabra
Supervisors
Dr. Monther Dwaikat
Dr. Mahmoud Dwaikat

Abstract

Background: Fiber-reinforced concrete is a material of choice for enhancing the performance of concrete structure by improving their mechanical properties.

Objectives: The study aims to understand the effects of adding waste fiber material, such as rivet mandrels and wire fibers, on the behavior of concrete and how it influences the workability, compressive strength, tensile strength, modulus of elasticity, and stress-strain relationship of concrete.

Methodology: Experiments were conducted to observe the effects of adding fiber material on the workability, density, compressive strength, and tensile strength of concrete, while finite element analysis tested the effects of adding the same proportions of the previous material to the elastic modulus and stress-strain relationship of concrete.

Results: The study shows that adding waste fibers generally enhances the mechanical properties of concrete up to a certain percentage, beyond which these benefits start to decline. Wires gave better results due to their higher aspect ratio compared to the revit mandrels.

Conclusion: The study concludes that it is possible to enhance various mechanical properties of concrete by making use of waste fiber material and reduce the costs of producing traditional concrete.

Keywords: fiber reinforcement, waste material, mechanical properties workability, density, compressive strength, tensile strength.

Chapter One
Introduction

1.1 General

Concrete is one of the most commonly used materials in the construction industry. The percentage of concrete structures is significantly higher in Palestine due to its effectiveness, flexibility in use, high strength, durability, low costs, low maintenance requirements, and availability in many forms. Despite all these advantages and features, its use is limited in many cases (e.g., large floor spans, high-rise buildings, or elements that are exposed to tensile stresses). This prompted researchers to work on developing and improving concrete to meet the needs of various structures.

Many studies were conducted to develop and produce high-performance concrete to meet architectural requirements. These studies have made excellent progress in this field. Very high compressive strength, noticeable improvement in tensile strength, and ductility in concrete were achieved. Many studies aimed to investigate the effect of using fibers from different materials on concrete behavior; all types of fibers shared a longitudinal shape, high tensile strength, and high elasticity. Adding fibers to the concrete helps to hold it together and reduce cracks in it. Consequently, it increased its tensile strength and ductility, making concrete usable in new areas, such as tensile elements and high-rise buildings, as well as in the connection between beams and columns. The use of high-performance concrete remained limited in most countries and was not used in Palestine at all due to its high cost.

In this research, to overcome the high cost, an attempt is made to produce high-performance concrete using waste materials, and it will be compared to the concrete used in our country.

1.2 Definition of High-Performance Concrete (HPC)

High-performance concrete is a type of concrete that comes with enhanced characteristics than the ordinary concrete material, including the strength, durability, ductility, and other properties. It evolved around 1980 in the production of concrete with higher strengths (up to 120MPa at that time). The definition of HPC has evolved over the history.

There are different types of high-performance concrete, such as:

- Self -consolidating concrete (SCC):

Which is a type of HPC that flows and settles under its own weight, without the need of an external vibrator.[1]

- High-strength concrete (HSC):

It's a type of HPC that has high compressive strength (usually greater than 60MPa)[2]

- Ultra-high-performance concrete (UHPC):

It has extremely high compressive strength (typically exceeds 150MPa), with high durability and resistance to environmental factors [3].

The enhanced properties of HPC depend on the specific mix design and additives used in it.

1.3 Scope of Research

As mentioned previously, there are many researches to produce high-performance concrete that tended to use fibers, which in turn improve the performance of concrete in terms of tensile strength and ductility.

In this research, the focus will be on producing concrete with improved properties in the field of compressive strength, tensile strength, modulus of fracture, and ductility using two specific waste materials: steel mandrel of aluminum blind rivets and building wire waste.

Steel mandrel of aluminum blind rivets *(Figure A1 in the appendix)* are obtained from any aluminum fitting store. They were measured, and their length and diameter are found to be 41mm and 2.1mm respectively.

On the other hand, wires *(Figure A2 in the appendix)* are used to bind formwork together and in large quantities, then they are cut when the formwork is loosened, and they are not used any more. wire thickness is 1.25 mm [4] [5] [6], they are cut to a length of 41 mm.

Those materials were chosen for the following reasons:

1. They are available in acceptable quantities
2. The low cost of their collection, processing and use
3. They have the properties of steel. For example they have a high tensile strength and they are a ductile material.
4. These rivets are coated, which delays rust.
5. Wires can easily be manipulated and cut in various lengths.

These materials, while improving the overall mechanical properties of the concrete, they also promote recycling and waste management, hence contributing to sustainability in construction.

1.4 Research Objectives

This study aims mainly to produce high performance concrete material from local materials. This will have a great impact on the development of structures. It will verify the aspirations of structural engineers and architects and will allow us to increase the distances of spans and use smaller sections.

This research will study the adding of materials to concrete to improve its strength. The main advantages of these materials are that they are cheap, easily obtainable, and waste materials. Finally, it will obtain a material with the required specifications and reasonable cost.

The behavior of the material will then be described under static loads (compressive and tensile strength and modulus of rupture).

To achieve these main targets, the following sub objectives and tasks will be performed:

1. Literature review: literature review will be conducted to study and collect published information on this topic. This information will be taken to know the characteristics of the high-performance concrete material produced by researchers. The characteristics of the materials to be added is also considered. The methods of experimenting and researching are studied.
2. Experiment test: A set of tests described in the previous section will be done on a set of samples on special devices and the required readings will be taken. Experiments

will be done to determine the concrete behavior variation in terms of workability, density, compressive strength, tensile strength and the modulus of elasticity. After accumulating the results of experiment tests, a set of calculations will be performed to convert the readings taken from the devices into values that express the material properties.

3. Numerical Modeling: This step involves conducting simulations to predict the behavior of the studied mixtures. These models will provide characteristics that could not be provided with in the experiments with available tools (step 2). It will also help ensuring the results of the experiments by comparing the experiments with the models results. ABAQUS software is used for numerical modeling.
4. Conclusion: The research findings are identified, and the results are summarized.

1.5 Research Significance

This research studies the effect of adding waste material to concrete mixes, examining how it may improve concrete characteristics, reduce production costs, and consequently, promote its use in various areas and countries. It also studies the improvement of its properties like the compressive and tensile strength, and its ductility.

Waste has rapidly accumulated in large quantities over the past few decades due to population growth, industrial development, technology, and increased consumption. These factors, in return, have led to the consumption of natural resources. The research also aims to recycle a portion of this waste and use it in the production of special types of concrete to preserve non-renewable natural resources.

1.6 Overview

The use of concrete is rising. In 1996, there was an annual consumption of 5.3 billion cubic meters worldwide[7]. In response to the growing demand from engineers and architects, researchers are continuously developing concrete to improve its properties. Some focus on increasing compressive strength, while others work on enhancing tensile strength or ductility. Thanks to these advancements, concrete has found new applications in areas such as bridges, roads, windmills, towers, and utility structures in the oil and gas industry.

Other researchers have worked on using fiber-reinforced concrete in the joints between columns and beams.

High-Performance Concrete (HPC) can offer a durable and sustainable solution for construction. HPC possesses exceptional strength properties, better fatigue performance, and negligible porosity, thereby making it highly resistant to harsh environmental conditions [8] [9]. The attainment of HPC's properties involves meticulous evaluation of its raw components and utilization of specialized techniques for mixing and curing.

For example, in terms of materials[10]:

a. Coarse aggregate is removed to enhance homogeneity.
b. High quantities of superplasticizer or water reducing agents are used to achieve low water/cement (w/c) ratios and hence improve strength.
c. Specially graded sands, silica fume and glass powders are used to reduce porosity, improve particle packing density and improve strength.

1.7 Performance Development in Concrete Material

In recent years, researchers and engineers in the field of construction have significantly improved the development of concrete by adding various materials to the mixtures. These materials aim to improve the performance, durability, and other characteristics of concrete structures. Some of the improved concrete mixtures are self-compacting concrete, fiber reinforced concrete, and high-performance concrete. Those products have developed the construction industry by offering unique properties and overcoming traditional limitations.

1.8 Research examples of Concrete

Many researchers studied concrete and its properties and worked on adding special materials to concrete for many purposes, including enhancing its characteristics, or replacing lacking and costly cement materials.

Some researches studied the effect of adding steel fibers, like Yuliarti, Susilorini, & Aboubakr [11], who studied the addition of gold colored steal fibers to the concrete with a length of 10 mm and a diameter of 0.2 mm in the ultra-high performance concrete (UHPC) mixture. The fiber properties were obtained from the factory and include a

density of 7850 kg/m^3, tensile strength of 1250 MPa, and a modulus elasticity of 200000 MPa. The study noted that the UHPC concrete used had an average flexure strength of 11.63 MPa (for UHPC with 0% fiber), 13.77 MPa (for UHPC with included 1% of fiber), and 14.23 MPa (for UHPC with 2% fiber used).

On the other hand, Wille, Naaman & Parra-Montesinos [12] reported that the incorporation of deformed fibers at a volume fraction of 1.5% leads to a direct tensile strength of 13.3 MPa, which was 8.3 MPa, which is 60% higher than that of UHP-FRC smooth steel fibers. Moreover, the tensile stress at a peak strain of 0.6% is approximately three times greater than that observed with smooth fibers. On the other hand, the addition of high strength steel fibers at a percentage of 8% volume fraction of high strength steel fibers results in a compressive strength of up to 292 MPa (42 ksi), along with a tensile strength of up to 37 MPa (5.4 ksi) and stress at peak strain of up to 1.1%, after 28 days of casting.

Other researchers made comparison between steel and carbon fibers. They used four mixes: reference mix (REF), mix with carbon fibers (C), mix with steel fibers (S) and composite mix of carbon fibers together with steel fibers (C+S) [13]. Used carbon fibers are characterized by density of 1.82 g/cm^3, tensile strength of 4275 MPa, tensile modulus of 225 GPa and ultimate elongation of 1.9%. Fiber length is 12 mm and diameter 7 μm; therefore, aspect ratio of selected fiber is very high: 1714. Used steel fibers are fibers with hooked ends, having length 30 mm and diameter 0.5 mm, therefore aspect ratio of selected fibers is: 30/0.5 = 60. Long steel fibers were used to provide quasi-plastic behavior and crack bridging effect during bending test. At the same time, “wall effect” is possible, where the moulds walls direct the fibers, which are too long compared to the mould size (40 mm^3). Volumetric concentration of carbon and steel fibers in experimental mixes was provided 1% from the total volume of concrete. They found that the compressive and bending tests proved an increase of strength value in the case of use both steel and carbon fibers. Carbon fibers decreased the effect of explosive collapse of the UHPC cement matrix, at the same time the bending behavior was take still brittle. Steel fibers considerably improved bending ductility thanks to a pull-out mechanism of steel fibers. The best results were achieved in the case of combined application of both carbon and steel fibers.

Meng & Khayat made a research about including steel and hybrid fiber in concrete mixes and concluded that when compared to the UHPC mixture containing 2% steel fiber (SF), the use of 1% SF and 1% hybrid fiber (HF) in the mixture results in a considerable increase of approximately 25%, 30%, and 20% in flexural strength, toughness, and tensile strength, respectively[14]. Additionally, it reduces autogenous shrinkage by 25%. The addition of 1.5% SF and 0.5% polyvinyl alcohol (PVA) fibers to the mixture enhances flexural strength and toughness by 10% and 15%, respectively, while it reduces autogenous shrinkage by 40%. Despite the fact that increasing the SF content from 2% to 5% does not significantly improve the flexural properties, it significantly reduces autogenous shrinkage.

Meng & Khayat also studied adding glass fiber-reinforced polymer grids and reported that the utilization of GFRP grids with dimensions of 25 × 25 mm and a unit weight of 225 g/m^2, possessing a Young's modulus of 25 GPa and a Poisson's ratio of 0.26, offers numerous benefits, including superior tensile strength and exceptional corrosion resistance[15]. When single- and dual-layer GFRP grids are incorporated into UHPC panels, they can increase the flexural strength by 20% and 23%, respectively.

Chen, Yu & Tang[16] studied the production of UHPC mixtures with polypropylene fibers which has water-binder ratio of 0.195, a mass of 196 kg/m^3, with and 39 kg/m^3 steel fiber, 167 kg/m^3 silica fume, 21 ultra-fine silica powder and 1 viscous agent was found to exhibit a compressive strength of 155.8 MPa after 56 days at room temperature. During the same time and under identical conditions of temperature and mixture composition, the flexural strength was 13 MPa.

A group of researchers made some studies on the mechanical properties of high-performance concrete, and found that incorporating the basalt fibers of 2% of the concrete volume, in combination with mineral admixtures, enhanced the compressive strength of concrete[17]. The enhancement in the strains that correspond to the maximum compressive strength and splitting tensile strength outcomes were evident across all fiber volumes, but there was minimal impact on the elastic modulus as a result of the fiber addition.

Some researchers tried to reuse waste material and include them concrete mixes to enhance the properties of concrete or overcome the lack of some important material.

The human hair for example was included in a study to report its effects on the concrete characteristics when used as a fiber material.

The study stated that the annual production of human hair reached about $6.9*10^5$ tons. The length of human usually ranges between 8mm and 100mm, and its diameter is 0.04-0.12mm. The modulus of elasticity of human hair is around 4GPa.

The study tested the mechanical properties of concrete with 0%, 1%, 2%, 3% and 4% of human hair to the volume of cement, using 180 of concrete specimens. The results showed that the compressive strength of concrete had better value at 1% of hair, as it improved by 8.15%, while the tensile and flexural strengths had their maximum values at 2% of hair and improved by 21.83% and 12.7% respectively compared to the plain concrete.[18]

Through an extensive study[19], it was found that UHPC made with partial replacement of cement by rice husk ash (RHA) resulted in a significant reduction in autogenous shrinkage compared to those made with silica fume. RHA particle size varied from 3.6 μm to 9 μm, and it was observed that a combination of 10% RHA and 10% silica fume yielded a higher compressive strength than the control samples with either 20% RHA or 20% silica fume replacement, offering a synergic effect.

Further, the study explored the effect of RHA's fineness on the strength and autogenous shrinkage of the mixtures, concluding that RHA was not just a viable but a superior replacement for silica fume in the UHPC production, even when the packing density of the silica fume mixtures was higher. It was found that mixtures with RHA (having a mean particle size of 3.6 to 5.6 μm) displayed higher strength compared to those with 20% silica fume. Furthermore, RHA proved effective in mitigating autogenous shrinkage, with RHA particles (mean size of 5.6 μm) outperforming other sizes in reducing shrinkage, due to their optimal ability to absorb water during the self-desiccation process. This makes RHA an excellent low-cost material for producing ultra-high-performance materials, replacing the expensive silica fume.

Given the limited stock of natural sand in the country, a paper investigated iron tailings as a viable alternative. The utilization of iron tailings not only addresses the issues of tailings storage, sand supply, and raw material cost, but also converts waste into useful materials, thereby benefitting the environment and contributing to economic development. The paper further presents test results indicating that the optimal sand rate for the concrete mix is approximately 24.4%, with the particle size between 0.15-0.30mm corresponding to the best proportion of iron tailings.

The study finds that while the use of iron tailings could be beneficial, it may also reduce the workability of concrete to a certain extent. For instance, when the volume of coarse aggregate is 0.0044m^3, the mixture's workability decreases with increasing tailings volume. Moreover, the research reveals that under normal curing conditions, the compressive strength of concrete prepared by substituting natural sand with iron tailings first increases, then decreases. Optimal sand strength is achieved when the proportion of iron tailings is between 13% and 23%. The research concludes that with a sand rate of 24.4%, the corresponding slump (a measure of concrete's workability) is around 36, indicating better flow of the designed concrete. [20]

A paper was prepared by Rao, Reddy and Ghorpade to report the study result of adding manufactured sand to as a replacement for the natural one, which was extracted from riverbeds, as it can contain harmful inorganic materials, chlorides, sulphates, silt, and clay. The study indicated that these substances can compromise the strength and durability of concrete and, if used in excess, can impact the environment and groundwater levels. In addition, river sand is becoming rare, and finding an alternative source is becoming necessary. Therefore, manufactured sand (M-Sand) has been developed as a replacement for river sand. It is made from crushed granite stone, and the shape and texture of these crushed sand particles can enhance the strength of concrete by improving interlocking between particles, reducing issues such as segregation, bleeding, honeycombing, voids, and capillarity. M-Sand also has the appropriate particle size distribution and can be dust-free, further reducing the corrosion of reinforcement steel by limiting permeability, moisture ingress, and freeze-thaw effects, thereby enhancing the durability of concrete structures.

Research has led to several important conclusions about the use of M-Sand. For instance, as the percentage of M-Sand in High Performance Concrete increases, the slump values decrease, suggesting a decline in workability. However, the Compressive Strength of HPC also increases with the age of the concrete and as the percentage replacement with M-Sand grows. The study also found that chloride permeability decreases as the age of the concrete increases, with a 28-day-old sample showing the highest permeability and a 90-day-old sample showing the lowest. This indicates that the durability of concrete improves with age. For all percentages of M-Sand replacements, Chloride Ion Permeability was very low. When looking at 28, 60, and 90 days of curing, 100% replacement with M-Sand exhibited the lowest chloride ion permeability compared to other percentage replacements. Thus, M-Sand is deemed suitable for replacing river sand in order to conserve natural resources. [21]

Some researches were also made on concrete material modeling and its mechanical properties under different behaviors.

The mechanical properties of concrete depend on a complex interaction on multiple length scales, ranging from the micro-scale to the macro-scale [22]. At the micro-scale, the behavior of concrete is governed by the properties and interactions of its constituent materials, such as cement, aggregates, and water. The micro-structure of concrete, which includes the pore structure and the interfacial transition zone between the cement paste and the aggregates, also plays a crucial role in determining its mechanical properties. At the meso-scale, the behavior of concrete is influenced by the arrangement and distribution of the aggregates, as well as the presence of cracks and other defects. The meso-scale structure of concrete can be represented using various approaches, including discrete element modeling and lattice models. At the macro-scale, the behavior of concrete is determined by the overall geometry and boundary conditions of the structure. The macro-scale behavior of concrete can be analyzed using finite element modeling, which considers the interaction between different parts of the structure and the external loading conditions.

The multi-scale modeling of concrete involves integrating information from the micro-scale, meso-scale, and macro-scale to predict the behavior of concrete under different loading conditions. This approach is essential for understanding the complex behavior

of concrete and designing structures that can withstand different types of loads, including static, dynamic, and impact loads. Several studies have been conducted to develop multi-scale models of concrete that can accurately capture its behavior at different length scales. For example, Marcello, Eleazar, Deane and Ederli [23] developed numerical models on fiber reinforced concrete to compare the material behavior at the macroscale and mesoscale. Similarly, Bernard, Kamali and Prince [24] developed 3D multi-scale models to study the mechanical behaviour of sound and leached mortar.

The previous studies aimed to add materials to enhance the concrete and/or overcome the lack of some ingredients. It's noted that most of those studies aimed to produce high tensile strength concrete with high ductility. Most of these studies produced the best characteristics of concrete at 1% to 2% of fibers. This research aimed to testify adding more ratio of waste fiber materials to the concrete mix to ensure at which ratio produces the best performance of concrete. The following chapters study the effects of adding rivet and wire fibers to the concrete and its characteristics.

Chapter Two
Experimental Work

In this chapter, the experimental methodologies are discussed, and their results. The Palestinian standards [25] were used, and in some fields, the ASTM code was used in the experiments. The experimental tests were used to study the effect of adding fiber to the concrete characteristics. The mixes were prepared in the required proportions (1:2:4).[26] Water was used at a ratio of 0.67, and a superplasticizer at a rate of 2.7%. Fibers were added in different proportions (1%, 2%, 3%) to the volume of the mix without fibers. These percentages of different fibers were added separately to result in 7 different mixtures, which were tested for workability. For the other tests, four samples were used for each mix. Those tests studied the change of concrete behavior in terms of density, compressive strength, tensile strength and modulus of elasticity.

2.1 Workability

The workability property of concrete refers to its ability to be easily mixed, placed, compacted, and finished without segregation or bleeding[27]. It is an important property for ensuring the quality and durability of concrete structures.

There are several methods used to measure the workability of concrete, including slump test, compaction factor test, vee-bee test, flow table test, and Kelly ball test.

The Palestinian specifications were used to measure the workability with the slump test[25]. A mould of the shape of a frustum of a cone with a bottom diameter of 20cm, a top diameter of 10cm and a height of 30cm is used in this test. Samples were taken from different mixes immediately after mixing, then they were placed on four equal layers and each layer was compacted separately with the tamping rod (16mm diameter steel rod). According to the Palestinian specifications 2015, the slump readings indicate the workability as shown in *Table 3.1*

Table 2.1

Workability Levels

Work conditions	Workability	Slump (mm)
Using excess vibration	Very low	0-10
Lightly reinforced with vibration	Low	10-30
Medium reinforcement with vibration	Medium	30-60
Heavy reinforcement with vibration	High	60-180

Then the slump readings of the mixture were taken, as shown in Figure A3 in the appendix.

The addition of fiber, regardless of its material type and shape, reduces the slump readings according to the added ratio. Table 3.2 shows the different slump readings for the different mixes.

Table 2.2

Slump test results for adding different fiber types and ratios

Concrete mix.	**Slump (mm)**
1. Plain concrete without added fiber	140
2. With 1% fiber rivet mandrels	130
3. With 2% fiber rivet mandrels	50
4. With 3% fiber rivet mandrels	15
5. With 1% fiber wires	55
6. With 2% fiber wires	20
7. With 3% fiber wires	10

It is clear from the results that the slump of concrete containing wires is less than that of concrete containing rivets, and that the greater the percentage of fibers in both types, the lower the slump states. This is due to the increase of overlapping between fiber pieces as the quantity increases, and the quantity of wires is more than the quantity of rivets at the same percentage, which causes more overlapping of fiber wires, and leads to a decrease in the slump level.

Figure 3.1 shows a comparison between adding rivet mandrels and wires at different ratios. According to the Palestinian specifications [25], it's not recommended to have a slump less than 30mm. This means that adding 2% of wires or 3% of rivet mandrels starts to cause problems during concrete casting.

Figure 2.1

Comparison of slump test results between adding rivet mandrels and wires

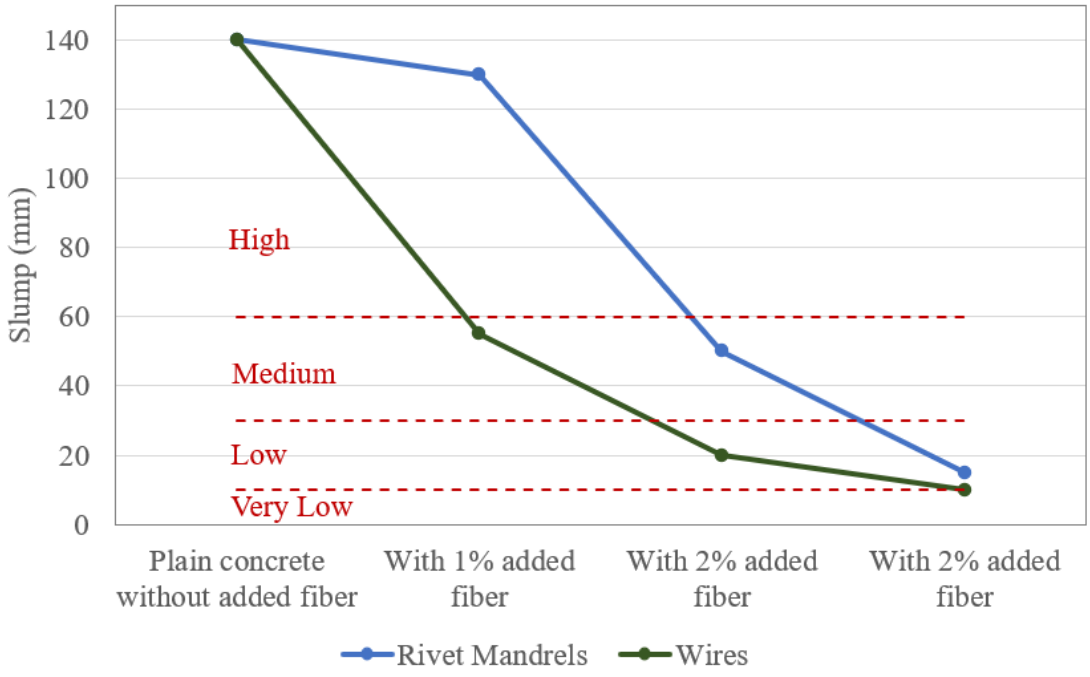

2.2 Density

The density of normal concrete typically ranges from about 2240– 2430 kg/m^3. The exact density of concrete depends on several factors, including the mix design, the size and shape of aggregates, and the amount of entrained air. [28]

After the 28-day curing period of the cubic samples (which were obtained to be tested in for compressive strength), the saturated samples were removed from water and allowed to drain for any excess water [29]. The surfaces of the concrete cubes were then carefully dried using a clean, absorbent fabric, ensuring that no excess water was present on the surfaces. This step was crucial to obtain accurate mass and density measurements. The cleaned and dried samples were then subjected to the density measurement process.

The two fiber types utilized in this study were steel fibers, which have a higher density compared to the plain concrete. As a result, incorporating them into concrete mixtures was expected to increase the concrete's density, which was confirmed by the research findings. Table 3.3 presents the results.

Table 2.3

Density results for adding different fiber types and ratios

Concrete mix.	Densities (ton/m^3)	Individual Deviation	Average density (ton/m^3)
1. Plain concrete without added fiber	2.32, 2.33, 2.28, 2.32	1.25%	2.31
2. With 1% fiber rivet mandrels	2.41, 2.42, 2.41, 2.42	0.37%	2.42
3. With 2% fiber rivet mandrels	2.45, 2.43, 2.44, 2.43	0.45%	2.44
4. With 3% fiber rivet mandrels	2.49, 2.47, 2.48, 2.50	0.48%	2.48
5. With 1% fiber wires	2.42, 2.39, 2.41, 2.43	0.79%	2.41
6. With 2% fiber wires	2.52, 2.48, 2.42, 2.46	1.9%	2.50
7. With 3% fiber wires	2.52, 2.50, 2.53, 2.47	1.16%	2.50

The table shows that the density of concrete increased by 4.46%, 5.36% and 7.4% when adding 1%, 2% and 3% of rivet fibers respectively, while it showed increases of 4.28%, 6.83% and8.26% when adding the same amount of wires.

Figure A4 in the appendix It shows that the readings on rivet mandrels gave less deviation, which means more accurate results than those with added wires. Table 3.3 shows the individual deviations of the results

2.3 Compressive Strength

The compressive strength of concrete is the maximum amount of compressive stress that it can withstand after 28 days of casting, before failure [30]. It is typically measured in megapascals (MPa) or pounds per square inch (psi). It depends in concrete on many factors, such as, the water/cement ratio, the type and size of aggregates, the humidity and the cement type.

The compressive strength can be tested for cubical or cylindrical specimens of a standard size and curing them under controlled conditions.

It has been stated in the Palestinian specifications [25], that for compression, at least 3 samples are required for to be tested after 28 days. 4 samples were used in this test. These samples are cubic in shape with dimensions of 10 x 10 x 10 cm. According to the specifications, the result shall be multiplied by a factor of 0.975 for transforming the 10 x 10 x 10 cm cube to the 15 x 15 x 15 cm dimensions.

A reliable test machine is used, and the rate of loading is approximately 15 N/mm^2/min.

The dimensions are confirmed to the nearest 0.1 mm. The compressive stress is calculated by dividing the load on the loading area, and the result is confirmed to the nearest 0.5N/mm^2.

The average strength is taken for the four samples to be a representative result and then multiplied by 0.8 to find $f'c$ (The compressive stress when using a cylindrical sample with a diameter 15cm and a height of 30cm) to be used in further calculations, provided that none of the samples differs from 15% of the compressive strength, otherwise the test must be repeated.

Figure 2.2

An image of the compressive strength testing process

The test results demonstrate that incorporating fibers of both varieties generally enhanced the concrete's compressive strength. However, when the slump ratios were extremely low, the opposite effect occurred, and the strength started to diminish. More details are shown in Table 3.4.

Table 2.4

Compression test results for adding different fiber types and ratios

Concrete mix.	Actual Compressive Strengths for 10x10x10 cubes (MPa)	Average (MPa)
Plain concrete without added fiber	16.66, 17.19, 18.59, 17.71	17.54
With 1% fiber rivet mandrels	25.11, 23.42, 23.27, 22.77	23.64
With 2% fiber rivet mandrels	30.82, 30.81, 31.00, 28.85	30.37
With 3% fiber rivet mandrels	24.46, 26.46, 26.45, 25.54	25.73
With 1% fiber wires	38.18, 37.55, 37.43, 39.91	38.27
With 2% fiber wires	35.85, 36.61, 36.17, 36.73	36.34
With 3% fiber wires	31.43, 30.64, 31.03, 30.20	30.83

The readings were multiplied by 0.975 to convert them and automate the cubic strengths with dimensions of 15x15x15 cm (the standard dimension in the Palestinian specifications [25]).

The average compressive strength for the plain mix was 17.10MPa. The compressive strength of the four samples ranged between 16.24MPa and 18.12MPa, meaning that the highest individual deviation was 6%.

When adding 1% of the rivet mandrels, the compressive strength increased to 23.05MPa, i.e., by 34.81% compared to the plain mixture. The values for the different samples ranged between 22.20MPa and 24.48MPa, and the highest individual deviation was 6.19%.

When adding 2% of the rivets, the compressive strength increased to 29.61MPa, meaning the percentage of increase was 73.18%. The values for the different samples ranged between 28.12MPa and 30.23MPa, and the highest individual deviation amounted to 5.03%.

The addition of 3% of the rivets resulted in a 46.67% increase compared to the mixture, i.e., the average compressive strength of the four samples reached 25.08MPa. This value is lower than the strength shown by the mixture containing 2% fiber, due to the agglomerations and the formation of pores as mentioned previously. Regarding the distribution of the compressive strength values for different samples, the compressive strength ranged between 23.85MPa and 25.80MPa, with the highest individual deviation being 4.92%.

The compressive strength of concrete reaches its peek when adding about 2% of rivets. Adding more rivets leads to an increase in the segregation and porosity of concrete, and thus a reduction in the compressive strength.

When adding 1% of wires, the average compressive strength of the four samples was 37.31MPa, meaning that the percentage increase was 118.21%. This increase, compared to the same percentage of rivets, is explained by the smaller size of the wires, which led to a greater number of fibers in the samples. This, in turn, led to better distribution within the sample. The compressive strength values of the four samples ranged between 36.50MPa and 38.91MPa, and the highest individual deviation was 4.49%.

When adding 2% of wires, the percentage of increase decreased for the same reasons previously mentioned, with the percentage of increase reaching 107.23%, meaning that the average compressive strength was 35.44MPa. The values of the four samples ranged between 34.96MPa and 35.81MPa, with the highest individual deviation reaching 1.35%.

With a 3% increase in wires percentage, there was a further decline in the increase rate, reaching 75.77%. This meant that the average compressive strength reached 30.05MPa, while the values for the four samples ranged between 29.44MPa and 30.64MPa. The highest individual variation reached 2.03%.

When adding the fiber wires, the maximum possible obtained compressive strength was at about 1%. The fall in compressive strength after this value was due to the same reason as in adding more than 2% of rivet mandrels, however, the compressive strength has fallen earlier in the case of wires because the wires have smaller volume, which leads to increased number of wires in the same quantity of concrete, and thus leads to faster conglomeration of fibers.

Although the effect on adding wires to the concrete on its compressive strength started to fall earlier than adding rivet mandrels because of its relatively small volume, due to the same reason, it gave better results in general because it caused more separation of fibers. Also, the high aspect ratio of wires, gave it higher coherence with concrete, which resulted in more increase in the compressive strength.

Figure A5 in the appendix shows the deviations of the compressive strength for each set of samples. Figure 3.3. displays the comparison between the average compressive strength of the samples containing rivets and those containing wires.

Figures 2.3

Concrete compressive strength when adding different ratios of rivet mandrels and wires

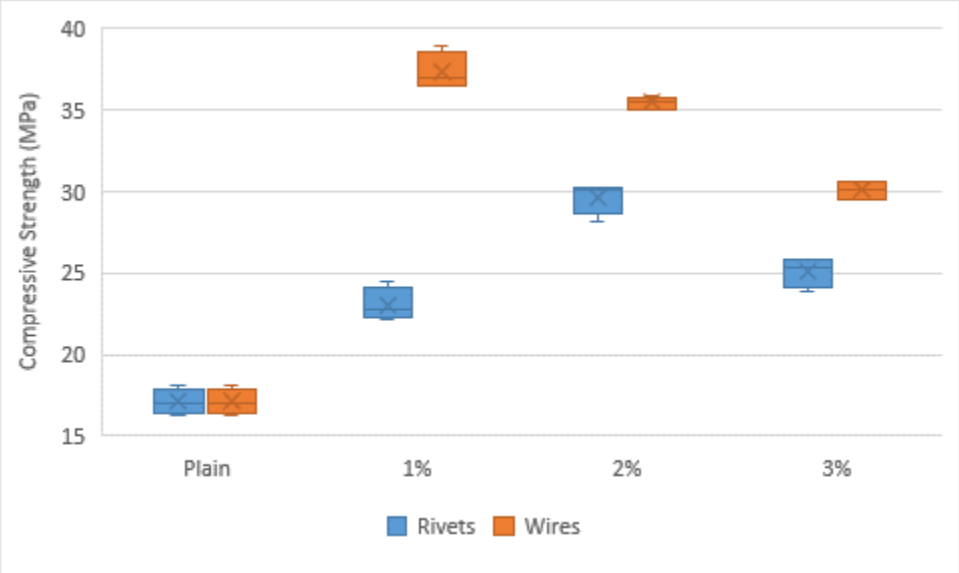

The addition of fibers led to a general increase in the compressive strength of the concrete. This was due to three factors:

1. Fiber has higher compressive strength than concrete, which increases the strength as a result.
2. The existence of fiber within the concrete, breaks the longitudinal shape of the crack, and thus increased the surface area on the crack.
3. Due to the poison ratio, tension stresses are caused on the perpendicular directions. The high tensile strength of fibers assists in the resistance of those tensile stresses.

2.4 Tensile Strength:

The tensile strength of concrete is relatively low compared to its compressive strength. Similar to compressive strength, the tensile strength depends on the water/cement ratio, the quality and size of aggregates, and the age of concrete [31]. There are several methods for examining and calculating the tensile strength of concrete, including direct tension tests, flexural tests, splitting tests [32] [33] [34]. These testing methods typically

involve applying a force to the concrete sample and measuring the resulting deformation of fracture.

Two testing methods were used to calculate the tensile strengths of the samples, which are:

1. Split test:

A split test was made to obtain the tensile strength of cylinder samples with a diameter of 100 mm and a height of 200 mm. [35]

The cylinder was placed on its side in a machine and exposed to a roll on its side at a loading rate of 0.7 ~ 1.4 MPa/min. [33]

The following equation is used to calculate the split tensile strength.

$$f_t = \frac{2*P}{\pi dL} \qquad Eq3.1$$

Where f_t is the split tensile strength, P is the maximum load, d is the diameter of the cylinder, and L is the high of cylinder.[33]

The following table displays the results of the split test.

Table 3.5

Split test results for adding different fiber types and ratios

Concrete mix	Load readings (kN)
1. Plain concrete without added fiber	48.67, 53.10, 50.54, 51.55
2. With 1% fiber rivet mandrels	62.47, 68.45, 61.57,63.53
3. With 2% fiber rivet mandrels	87.69, 83.19, 94.97, 87.83
4. With 3% fiber rivet mandrels	82.91, 76.82 75.60, 85.94
1. With 1% fiber wires	93.74, 104.80 102.59, 97.60
2. With 2% fiber wires	106.54, 114.80 121.59, 115.43
7. With 3% fiber wires	114.46, 120.36, 120.23, 113.42

The load readings of the samples were taken and converted to the tensile strength of the cracking using the relationships shown previously. The tensile strength of the split test for the plain mixture ranged from 1.55MPa to 1.69MPa, with an average of 1.62MPa, meaning the highest individual deviation was 4.4%. A relationship between the split cylinder tensile strength f_t and the compressive strength f_c' of the cylinder from the compression test was established by multiplying the compressive strength by 0.8 for conversion, as mentioned previously of this research. The relationship was $0.44\sqrt{f_c'}$.

With the addition of 1% rivet mandrels, the split cylinder tensile strength increased by 25.47% compared to the plain mixture. The average split cylinder tensile strengths reached 2.04 MPa, and its value in the four samples ranged from 1.96 MPa to 2.18 MPa, meaning the highest individual deviation was 7%. The relationship constant between f_t and $\sqrt{f_c'}$ was 0.47.

When adding 2% of rivet mandrels, the average tensile strength was 2.81 MPa, which represented a 73.44% increase compared to the plain mixture. The value for different samples ranged from 2.65MPa to 3.02MPa, with the highest individual deviation at 7.41%. The relationship constant was 0.58.

The addition of 3% of rivet mandrels led to a 57.54% increase compared to the plain mixture, with an average tensile strength of 2.56MPa for the four samples. The distribution of tensile strength in different samples ranged from 2.41MPa to 2.74MPa, with the highest single deviation at 7%. The relationship constant between f_t and $\sqrt{f_c'}$ reached 0.57.

The addition of 1% of wires resulted in an average tensile strength of 3.17MPa, a 95.53% increase compared to the plain mixture. The tensile strength value of the four samples ranged from 2.99MPa to 3.39MPa, with the highest individual deviation at 5.13%. The relationship constant between f_t and $\sqrt{f_c'}$ was 0.58.

When adding 2% of wire, the average tensile strength of different samples reached 3.65MPa, a 124.77% increase. The value for different samples ranged from 3.39MPa to 3.87MPa, with the highest individual deviation at 7.02%. The relationship constant between f_t and $\sqrt{f_c'}$ was 0.69.

The mixture containing 3% of wire exhibited an average strength of 3.73MPa, an increase of 129.75%. The values for different samples ranged from 3.61MPa to 3.83MPa, with the highest individual deviation at 3.17%. The relationship constant between the split cylinder tensile strength and the square root of the compressive strength was calculated to be 0.76.

Figure A6 in the appendix shows the deviations for each set of samples. Figure 3.4(a) shows the relationship constant k_t growth when adding different types and rates of fiber.

Figure 3.4(b). displays the comparison between the average compressive strength of the samples containing rivets and those containing wires.

Figures 2.4

Split cylinder tensile strength of concrete samples when adding different ratios of rivet mandrels and wires

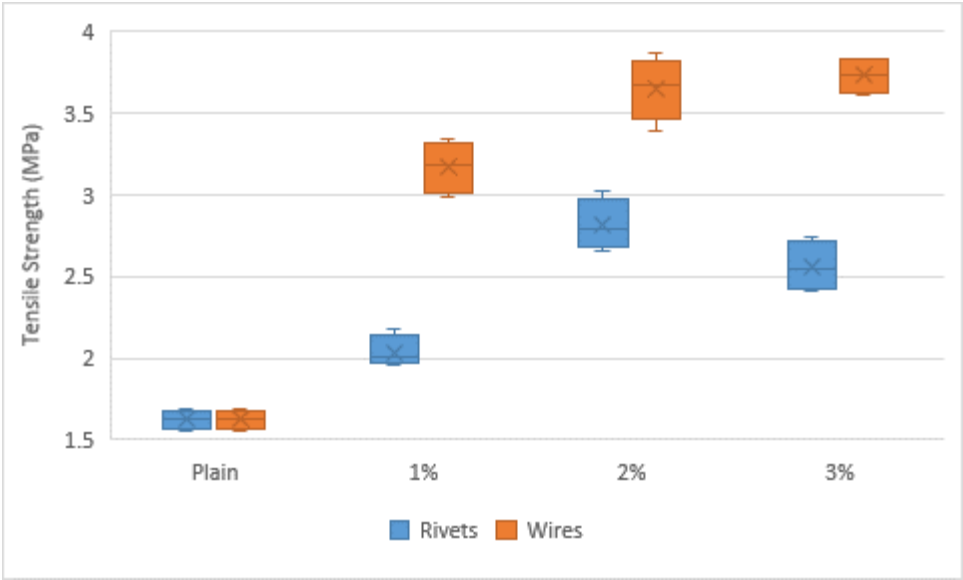

a) Split tensile strength comparison between adding rivet mandrels and wires

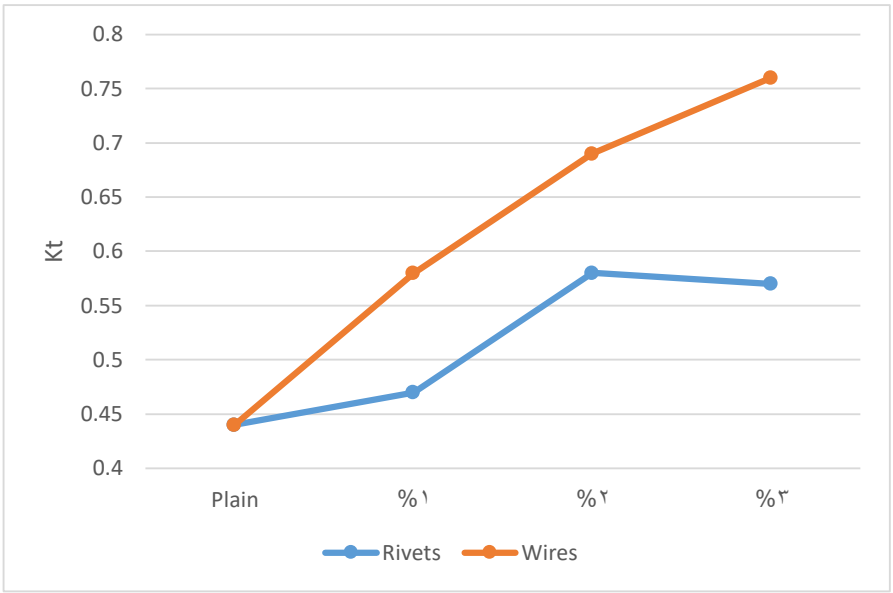

b) Kt comparison between adding rivet mandrels and wires

2. Flexural test:

It is stated in the ASTM codes that for flexural test samples, three samples are required for each age stage in which the test is carried out[32]. A quantity of four samples with the dimensions 50 * 10 * 10 cm were used in the flexural test to find the modulus of rupture of the modified concrete. The test machine must be reliable so that the error does not exceed 1% of the applied load.

The sample is placed in the testing machine, then a load is applied at a rate of 50N/s, then the load at failure is recorded [32].

If the distance between the fracture and the near support, is more than 13.3 cm. We apply the following equation to calculate the rupture factor:

$$f_r = \frac{PL}{bd^2} \qquad Eq3.2$$

Where Fr is the modulus of rupture, P is the load by the Machine, L is the length of space, b is the width of the sample, and d is the depth of the sample.

But if the distance is less than 13.3 cm, and greater than 11 cm, we apply the equation:

$$f_r = \frac{3Pa}{bd^2} \qquad Eq3.3$$

Where a is the distance between the fracture and the support close to it.

If it is less than 11 cm, the test values should be ignored.

Figure 2.5

An image of the flexural strength testing process

The tested results are represented in the following table:

Table 2.6

Flexural test results for adding different fiber types and ratios

Concrete mix	Load readings (kN)
1. Plain concrete without added fiber	7.15, 6.9, 7.52, 7.19
2. With 1% fiber rivet mandrels	9.11, 10.19, 9.27, 9.52
3. With 2% fiber rivet mandrels	11.66, 11.36, 11.31, 10.59
4. With 3% fiber rivet mandrels	10.45, 11.77, 10.67, 11.1
3. With 1% fiber wires	12.72, 13.76, 12.72, 12.85
4. With 2% fiber wires	13.6, 14.41, 12.94, 13.33
7. With 3% fiber wires	19.07, 17.26, 17.82, 19.77

The value of the Rapture modulus for the reference samples ranged between 2.76MPa and 3.01MPa, and the mean for the four samples was 2.88 MPa, and the largest individual variance was 4.59%. The relationship modulus between rupture modulus f_r and compressive strength $\sqrt{f_c'}$ was found to be 0.78.

The peak of the rapture coefficient for the mixture containing 1% rivet mandrels ranged between 3.78 MPa and 4.10 MPa, and the average for the four values was 3.96 MPa, meaning that the percentage increase was 37.47% compared to the plain mixture, and the highest individual deviation amounted to 4.55%. The relationship constant was 0.89.

When adding 2%, the values were between 4.24 MPa and 4.66 MPa, with an average of 4.49 MPa, and the percentage of increase compared to the plain mixture was 56.23%, and the highest individual deviation was 5.67%. The relationship constant with root f_c' was 0.92

As for the mixture with 3% rivet, the values of the Rapture coefficient ranged between 4.18 MPa and 4.71 MPa, and the average for the four samples was 4.40 MPa, meaning that the percentage increase was 52.97%, and the highest individual deviation was 7.01%. The relationship constant with root f_c' was 0.98

The addition of 1% of the wire to the concrete mixture showed an increase in the rapture coefficient, as the values ranged between 5.09 MPa and 5.50 MPa, and the average was 5.20 MPa, and the percentage increase compared to the reference mixture was 81%, and the largest individual deviation was 5.74%. The relationship constant with root f_c' was 0.95

As for the mixture containing 2% of the wires, the values ranged between 5.18 MPa and 5.76 MPa, and its average was 5.43 MPa, i.e. the percentage of increase compared to the reference mixture was 88.76%, and the highest individual deviation was 6.21%. The relationship constant with f_c' was 1.02

As for the mixture containing 3%, it showed a new increase in the rapture coefficient, as its values ranged between 6.91 MPa and 7.91 MPa, and its average was 7.39 MPa, meaning that the percentage of increase reached 157.08%, and the highest individual deviation was 7%. The relationship constant with root fc was 1.51.

Figure A7 in the appendix shows the distribution of the rapture coefficient for the each set of samples. Figure 3.6(a) shows the relationship constant k_t growth when adding different types and rates of fiber. Figure 3.6(b). displays the comparison between the average compressive strength of the samples containing rivets and those containing wires.

Figures 2.6

Modulus of rupture of concrete samples when adding different ratios of rivet mandrels and wires

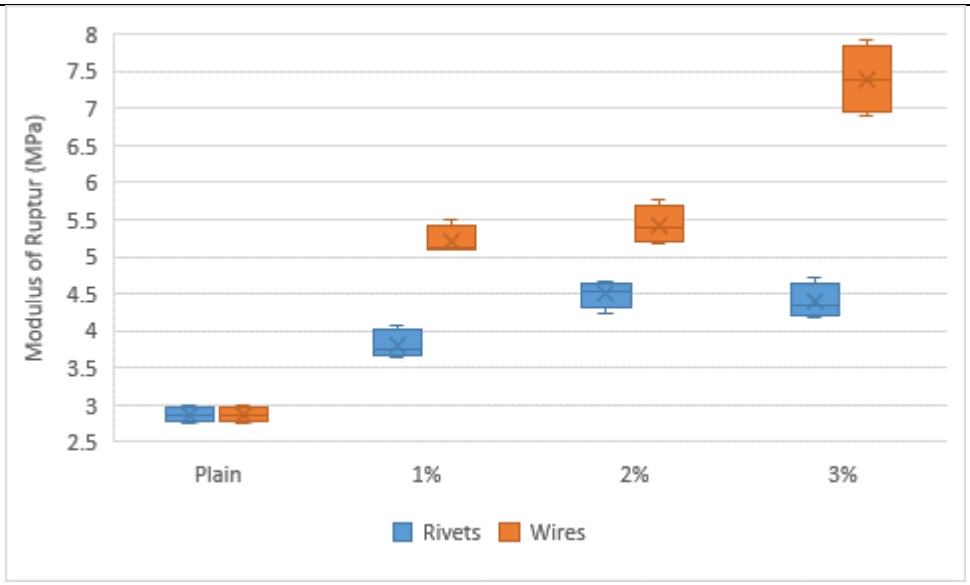

a) Modulus of rupture comparison between adding rivet mandrels and wires

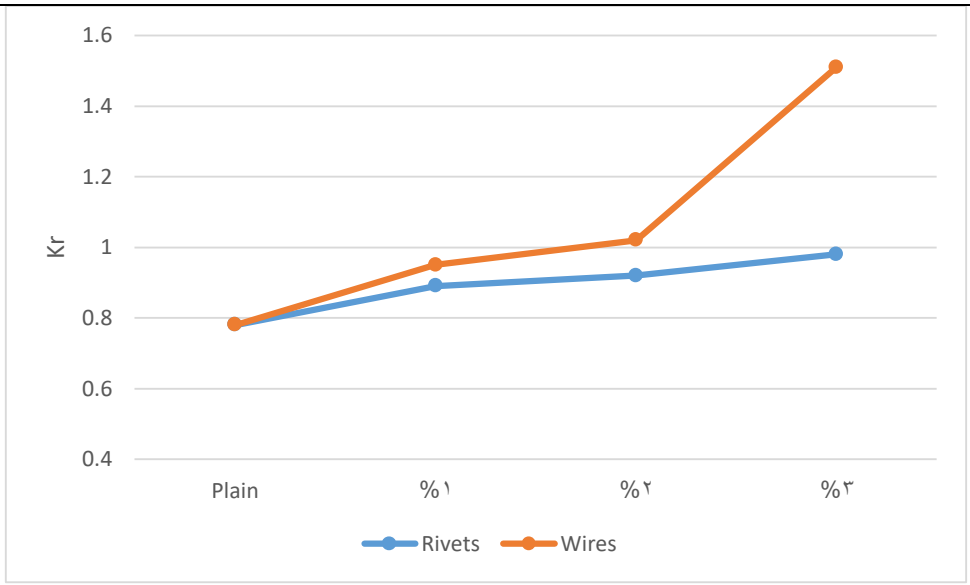

b) Kt comparison between adding rivet mandrels and wiress

The results show that the tensile strength is improved when adding fibers to the concrete mix. The increase of tensile strength is cause by the following factors:

1- Fiber material has higher tensile strength than concrete, which increases the strength as a result.
2- The existence of fiber within the concrete, breaks the longitudinal shape of the crack, and thus increased the surface area on the crack.

Wires fibers generally gives better tensile strengths due to the following reasons:

1- Wire fibers have less volume than rivets, and this causes them to distribute better.
2- The diameter of wires is low compared to rivet mandrels, which means more aspect ratio and that leads for a better cohesion with concrete and less possibility to be pulled out.

2.5 Modulus of elasticity

The modulus of elasticity can be defined as the direct relation between stress and strain with the following equation,

$$E = \frac{\sigma}{\varepsilon} \qquad Eq3.4$$

Where E is the modulus of elasticity, σ is the stress applied to the material, and ε is the strain resulted to the applied stress

Note that the above equation, is only applicable to the material under elastic behavior. The elastic behavior of concrete starts when stress is 0 and ends at $0.45f'c$[28].

The device used for the flexural test, produces a load per time graph. The graph is then scanned and passed into AutoCAD software to extract a table of the load per time.

During the test, a tool is installed to check the deflection in the sample at the loading points, and a camera is attached to this tool to link the deflection with time, and then a table is made with the deflection values at different times. A table of the deflection per time was concluded, and linked with the load per time extracted above. The value of the elastic modulus of the material is calculated through the following relationship.

$$E_{\emptyset} = \frac{(5Pl^3)}{162\Delta I} \qquad Eq3.5$$

Where, Δ is the deflection at the load, P is half of the load applied by the machine, l is the sample length (40cm), and I is the moment of inertia of the sample. Figure A8 in the appendix illustrates more information

The value of the elastic modulus of the four samples is calculated for each ratio, then an average of the four samples is taken and approved as the elastic modulus of the material. This process is repeated for the seven mixes of this research.

For plain concrete, the E_c was found to be 17541MPa, the load/deflection relationship is plotted in the Figure A9(a) in the appendix.

The modulus of elasticity $E_\emptyset$ for the concrete containing 1% of rivets increased by 2.9% to reach 18041MPa. Figure A9(b) shows the load/deflection diagram.

The elastic modulus of concrete samples containing 2% of rivets had an increase of 3.9%, which reached 18224MPa. Figure A9(c) shows the load/deflection diagram.

For the concrete samples containing 3% of rivets, the elastic modulus reached 18433MPa, which is 105% of the elastic modulus of the plain concrete. Figure A9(d) plots the load/deflection relationship.

The effect of inserting wires had more effect on the concrete elastic modulus than the rivet when the ratio increases. The modulus of elasticity reached 18012MPa (2.7% increase), 18266MPa (4.1% increase) and 18595MPa (6% increate) when inserting 1%, 2% and 3% ratio of fiber wires respectively. The relationships between load & deflection for those samples are plotted in Figures A9(e-g).

Chapter Three
Numerical Analysis

Because of the cost and time constraints, real specimen testing is not always feasible. Finite element analyses is therefore a widely used computer-based method for solving a range of boundary problems. By defining the mechanic qualities, boundary conditions, and interfaces between model components and loads, it can provide precise findings for deflections, the growth and development of cracks, and potential RC element failure processes.

This chapter discusses the numerical analysis applied to the mixes models. The modulus of elasticity and stress-strain relationship characteristics where calculated during this process. ABAQUS software was used to simulate and perform the finite element analysis to the models and compare them with the results taken from the experiments.

3.1 Assumptions

The plain concrete is assumed to be fully homogenous, and the cohesive between fiber and concrete is perfect. This leads us to analyse the meso-scale modeling to better understand and capture the complex behavior of concrete. The meso-scale model considered the arrangement and distribution of aggregates, as well as the presence of cracks and other defects. By integrating the meso-scale model with the 3D non-linear finite element model in ABAQUS, we were able to simulate the behavioral response more accurately, accounting for the inherent heterogeneity of concrete and fiber.

One eighth of the cube was modelled and considered that it is identical to the other parts of the cube. Within the one part, the fibers are assumed to be distributed randomly.

The stress-strain diagram of fiber is assumed to be elastic perfect-plastic. The fibers are assumed to be very thin and thus they are modeled as linear rods.

3.2 Modelling methodology

A cube of concrete (100 mm x 100 mm x 100 mm) is modelled, which goes through the following stages:

1. Elements Definitions

- **Concrete:**

A concrete cube of 50 mm x 50 mm x 50 mm (i.e., 1/8 of the real size) to make use of the symmetric behavior of concrete, and is drawn with coordinates.

- **Fibers:**

The fibers are distributed randomly in the bock, and their lengths are 41 mm. A python script is used for this purpose. The quantity of fibers required for each mixture is calculated through the following steps:

1- Calculation of the volume of concrete:

Concrete volume = $50\ \text{mm} * 50\ \text{mm} * 50\ \text{mm} = 125{,}000\ mm^3$

2- Calculation of the volume of fiber:

Fiber volume = concrete volume * fiber ratio = $125{,}000\ \emptyset\ mm^3$

3- Calculation of the amount of fiber

The number of fiber pieces = the calculated total volume of fiber / the volume of a single fiber.

The number of fibers for the different mixtures should be as follows:

Table 3.1
Concrete cube models

Mixture So.	Size of a single fiber	Number of fibers in a 50x50x50 concrete cube
1. Plain concrete without fiber	-	0
2. With 1% fiber rivet mandrels		9
3. With 2% fiber rivet mandrels	142.01	18
4. With 3% fiber rivet mandrels		27
5. With 1% fiber wires		25
6. With 2% fiber wires	50.31	50
7. With 3% fiber wires		75

Figures 3.1

Material definitions in ABAQUS

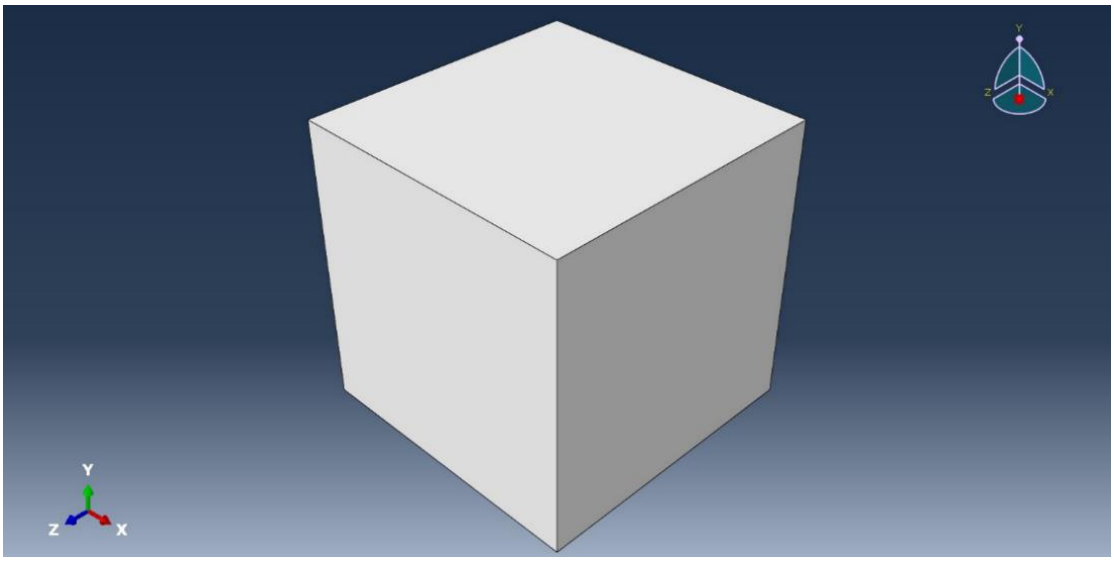

a) Concrete element model

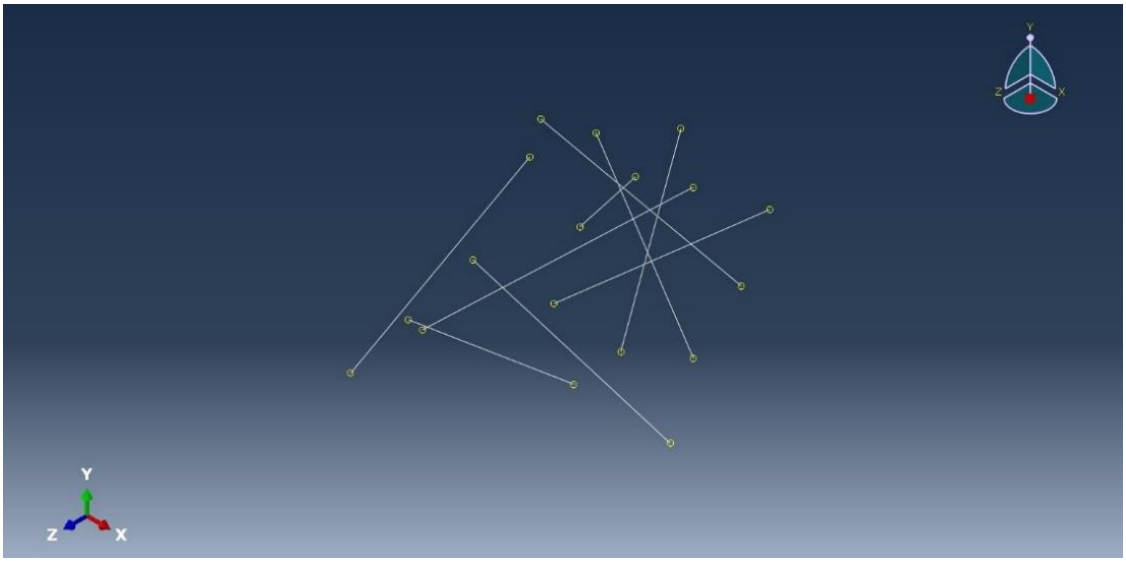

b) Programmatically generated 1% of river fiber elements with Python (see figures A12 in Appendix B for the remaining fibers)

2. Material Properties:

The model consists of 2 types of materials, namely:

- **Concrete:**

Difference in the material response at different stages of loads in both tension & compression happens because the concrete is a non-homogenous material and is thus difficult to simulate. Different models may be used to simulate how concrete's strength and stiffness are affected by crushing and cracking.

Most FEA software include 3 models to simulate the concrete, which are, brittle crack, smeared crack, and concrete damage plasticity. [36]

- Brittle Crack model

It is applicable only to linear-elastic material with tensile crack. For that, it cannot represent real concrete behavior accurately.

- Smeared Crack Model

The cracks here form wherever the stresses in concrete reach beyond the failure surfaces, whether in area of biaxial tension or the area of combined tension and compression. The crack presence is determined by how the crack affect material stiffness & stress. The model is mainly limited by mesh size dependence, stress locking (due to distribution across widely open crack), and loading instability at late stage [37].

- Concrete Damage Plasticity (CDP)

Permanent strain remains in concrete because of the friction and sliding of micro cracks due to the loading and unloading on the material. Those inelastic deformations and stiffness degrading cause the failure mechanism of concrete in tension and compression [38].

The CDP model is based on plastic flow theory and encompasses continuous damage, dmechanisms, concrete compressive crushing and tensile cracking. The CDP model is suitable for modeling concrete material under cyclic and static loads in both ABAQUS/Standard and ABAQUS/Explicit scenarios [36].

For that, we used Concrete damage plasticity model to represent the concrete material plastic behavior.

There are various CDP assumptions to define the characteristics of the concrete material, which are:

- **Strain Rate Decomposition**

It assumes that the rate-independent model is calculated through the following equation:

$$\dot{\varepsilon} = \dot{\varepsilon}^{el} + \dot{\varepsilon}^{pl} \qquad Eq3.7$$

Where, $\dot{\varepsilon}$ is the total strain rate, $\dot{\varepsilon}^{el}$ is the elastic strain rate, and $\dot{\varepsilon}^{pl}$ is the plastic strain.

- **Stress-Strain Relationship**

It is based on a scalar damaged elasticity, which is defined by the following equation:

$$\sigma = (1 - d)D_0^{el}.(\varepsilon - \varepsilon^{pl}) \qquad Eq3.8a$$

$$D^{el} = (1 - d)D_0^{el} \qquad Eq3.8b$$

Where, D_0^{el} is the initial (undamaged) elastic stiffness, D^{el} is the degraded elastic stiffness, and d is the scalar stiffness degradation variable, which ranges from 0 (undamaged) to 1 (completely damaged). [39]

When we substitute *Eq3.8b* into *Eq3.8a*, when get the following equation:

$$\sigma = D^{el}.(\varepsilon - \varepsilon^{pl}) \qquad Eq3.9$$

The decrease in the elastic stiffness of concrete is caused by damage to the material, which occurs as a result of the failure mechanism of concrete. The scalar-damage theory (eq3.8) states that the degradation of stiffness in concrete is isotropic and can be characterized by a single parameter (d).

We can then conclude to the following 2 equations, which show the relation between the Cauchy stress and the effective stress through the scalar degration:

$$\bar{\sigma} = D_0^{el}.(\varepsilon - \varepsilon^{pl}) \qquad Eq3.10a$$

$$\sigma = (1 - d)\bar{\sigma} \qquad Eq3.10b$$

Where, $\bar{\sigma}$ is the effective stress

As the hardening parameters increase in concrete, micro cracking and crack propagation are initiated. To define the yield surface function, a model was proposed as shown in Figure A13[40][41] in the appendix This model accounted for the various evolutions of concrete's tensile and compressive strength and defined the yield surface function in terms of effective stress, as represented by Equation 3.11.

$$F = \frac{1}{1 - \alpha}(\bar{q} - 3\alpha\bar{p} + \beta(\tilde{\varepsilon}^{pl})\big(\bar{\sigma}_{max} - \gamma(\bar{\sigma}_{max})\big) - \tilde{\sigma}_c\big(\tilde{\varepsilon}_c{}^{pl}\big) \leq 0 \qquad Eq3.11$$

Where, $\bar{q}$ is the equivalent von Mises stress, $\bar{p}$ is the effective hydrostatic pressure. $\bar{\sigma}_{max}$ is the tensor's algebraically maximum eigenvalue. α, β and γ are the dimensionless material constants defined by equations 13.12 [39]

$$\alpha = \frac{\left(\frac{\sigma_{b0}}{\sigma_{c0}}\right) - 1}{2\left(\frac{\sigma_{b0}}{\sigma_{c0}}\right) - 1}, \qquad 0 \leq \alpha \leq 0.5 \qquad \textit{Eq3.12a}$$

$$\beta(\tilde{\varepsilon}^{pl}) = \frac{\bar{\sigma}_c\left(\tilde{\varepsilon}_c^{pl}\right)}{\bar{\sigma}_t\left(\tilde{\varepsilon}_t^{pl}\right)}(1-\alpha) - (1+\alpha) \qquad \textit{Eq3.12b}$$

$$\gamma = \frac{3(1-k_c)}{2k_c - 1} \qquad \textit{Eq3.12c}$$

Where, $(\frac{\sigma_{b0}}{\sigma_{c0}})$ is the ratio of biaxial to uniaxial compressive yield stress, which affects the yield surface in a plane stress state, $\bar{\sigma}_c\left(\tilde{\varepsilon}_c^{pl}\right)$ and $\bar{\sigma}_t\left(\tilde{\varepsilon}_t^{pl}\right)$ are the effective cohesion stress in compression and tension respectively, and k_c is the ratio of the hydrostatic effective stress in tensile meridian to that one the compressive stress in tensile meridian to that one the compressive. [39]

The $(\frac{\sigma_{b0}}{\sigma_{co}})$ ratio typically falls within the range of 1.10 to 1.16 in experimental studies, which leads to a value of α between 0.08 and 0.12.

The connection between the yield surface and stress-strain relationships in concrete is established by the flow rule. The CDP models propose a non-associated Drucker-Prager hyperbolic function for the flow potential function, G, as shown in Equation 3.13.

$$G = \sqrt{(\xi\sigma_{t0}tan\psi)^2 + \bar{q}^2} - \bar{p}tan\psi \qquad \textit{Eq3.13}$$

where ξ: the eccentricity of flow; ψ: the dilation angle and σ_{t0} is the uniaxial tensile stress.

The stress-strain behavior of concrete was simulated using the diagram in figure A14 in the appendix, and the Equations 3.14 that establish the drawing.

$$\sigma_{c,1} = E_c \varepsilon_c, \qquad \varepsilon_c \leq \frac{0.4 f'_c}{E_c} \qquad \textit{Eq3.14a}$$

$$\sigma_{c,2} = \frac{\mu_c \frac{\varepsilon_c}{\varepsilon_0} - \left(\frac{\varepsilon_c}{\varepsilon_0}\right)^2}{1 + (\mu_c - 2)\frac{\varepsilon_c}{\varepsilon_0}} f'_c, \qquad \frac{0.4 f'_c}{E_c} \leq \varepsilon_c \leq 0.0035, \qquad \textit{Eq3.14b}$$

$$\sigma_{c,3} = \left(\frac{2 + \lambda_c f'_c \varepsilon_0}{2 f'_c} - \lambda_c \varepsilon_0 + \frac{\lambda_c \varepsilon_c^2}{2\varepsilon_0}\right)^{-1}, \qquad 0.0035 \leq \varepsilon_c \leq 0.03 \qquad \textit{Eq3.14c}$$

In Equation (3.14a), ε_c represents a variable that ranges from zero to 0.4f'c/Ec, where Ec is the initial modulus of elasticity. This equation represents the linear elastic branch, which ends at a stress level of 0.4f'c. Equation 3.13 describes the second branch, which extends up to a strain level of 0.0035 in the descending branch. At the peak stress, the corresponding strain level is defined as ε_0 = 2f'c/Ec, and μ_c is a material constant. The value of μ_c can be determined by using stress and strain compatibility at the strain level of ε_c = 0.4f'c/Ec for Equations 3.14a and 3.14b. Equation 3.14c represents the third and descending branch, where λ_c is a constant crushing energy as a material property. By using stress and strain compatibility at the strain level of ε_c = 0.0035 for Equations 3.14b and 3.14c, the value of λ_c can be determined. To avoid numerical difficulties, the concrete ultimate strain ε_u was assigned a large value of 0.035. [39]

Here, the assumption of linear uniaxial stress-strain behavior of concrete is employed in the finite element analysis. According to this assumption, the tensile behavior of concrete can be divided into two stages. In the first stage, concrete exhibits linear elastic behavior up to the concrete tensile strength, σ_{t0}. The second stage commences with the occurrence and propagation of cracks in concrete under tension. The softening process of concrete material was modeled using the linear, bilinear, or nonlinear model proposed by Belbarbi and Hsu, as shown in figure A15 in the appendix. The tensile strength of concrete was estimated using Equation 3.15:

$$f'_t = 0.33\sqrt{f'_c} \qquad \textit{Eq3.15}$$

The CDP model takes into account the damage caused by both uniaxial tension and compression during the softening process, which is defined in the finite element

analysis. Damage occurs when the concrete stress reaches the stress level corresponding to the strain level ε_0, which represents the maximum uniaxial compressive strength.

The values of the additional five parameters are utilized to determine the surface yield, and are shown in table 4.2 [39]:

Table 3.2
CDP input parameters

Parameter	σ_{b0}/σ_{co}	K_c	ψ	ξ	μ
Value	1.16	0.667	35	0.1	0

- **Fibers**

Stress-strain diagrams of the steel are derived from monotonic tension tests conducted on steel bars [42]. These curves exhibit a linear elastic region initially, a yield area where there is minimal stress increase despite strain increase, a strain-hardening region where stress increases again with strain, and a final stage where fracture occurs, causing stress to drop off.

The young's modulus of reinforcing steel is assumed to be 200 GPa according to China Steel suppliers.

During the design process, the stress-strain diagram is idealized. Typically, this curve is approximated as two straight lines. The ACI-318 code adopts this stress-strain curve for reinforcement steel, disregarding the higher yield point and the stress increase due to strain hardening, which is referred to as the elastic perfectly plastic curve. Figure A16 in the appendix illustrates the typical stress-strain behavior of fibers.

The rivets are found to be made of carbon steel 1006. Further experiments were done, and from China Steel suppliers it is found that the tensile strength is of 650 – 880MPa, Elongation of 8-25, a yield strength of 350 - 550 MPa and a density 7700 kg/m^3.

The wires are made of low carbon steel Q 195, with tensile strength of 315-430 MPa, elongation of 33, yield strength of 195 MPa, density of 7850 kg/m^3.

3. Modeling of Interfaces

Modeling the concrete-fiber joints requires interface modelling in the elements. ABAQUS software provides multiple options for modeling connection interfaces, referred as constraints. Constraints are represented in various forms, such as Tie, coupling and embedded region constraints. A connection is created between the concrete and the fibers using embedded region. This constraint defines perfect bond surfaces with no slip between elements. Figure A17 in the appendix shows the embedded region constraint modelling.

4. Boundary conditions and Loading

One eighth of the cube is modelled by assuming the symmetry of the concrete and considering it as homogeneous. Movement is prevented in three perpendicular faces, and displacement was applied to the upper surface in a direction perpendicular to the surface, and it is in the direction of compression. Figure A18 in the appendix shows the applied boundary conditions in the model.

5. Mesh Type

To model the concrete element, a 4-nodded linear tetrahedron shape was created (C3D4) for the mesh of the concrete. The initial size of the mesh was 5 mm. Then remeshing role is done by allowing the software to make analysis, and depending on the results, it redefines a new mesh size the is adequate to the resulted stresses. This process is done to prevent the concentrated stresses.

The fibers were modeled using 2-node linear bar elements (T3D2) to reduce the computational running time.

Figures 3.2

Concrete mesh definition

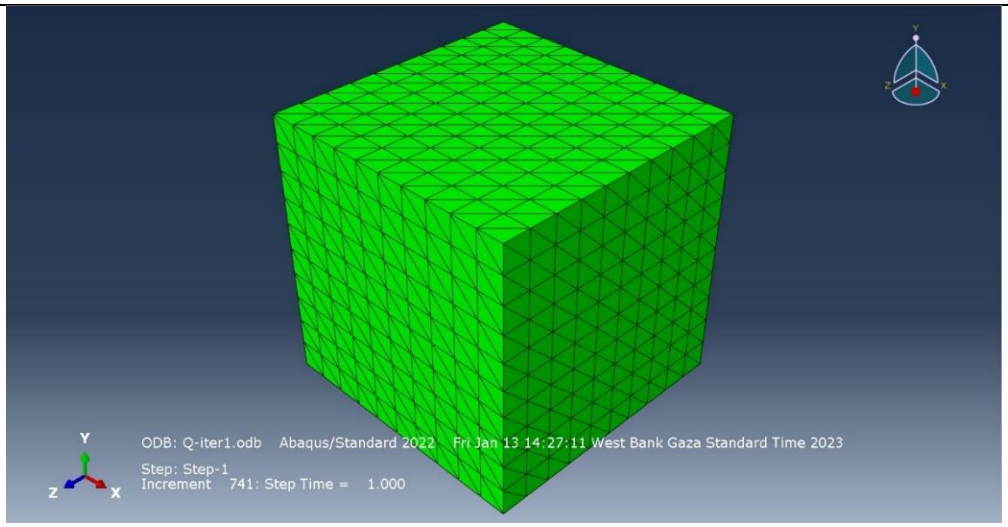

a. The initial defined concrete mesh with a size of 5mm

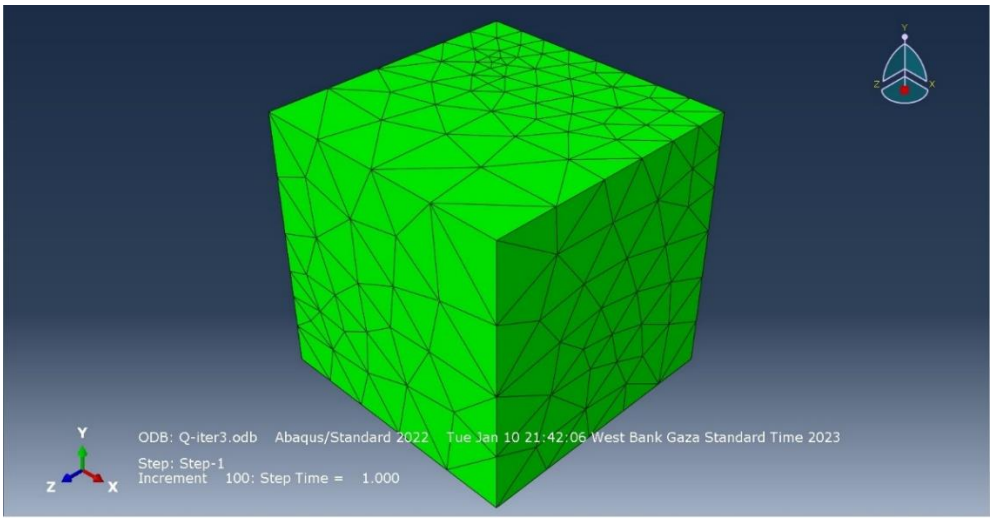

b. Concrete mesh during its redefinition

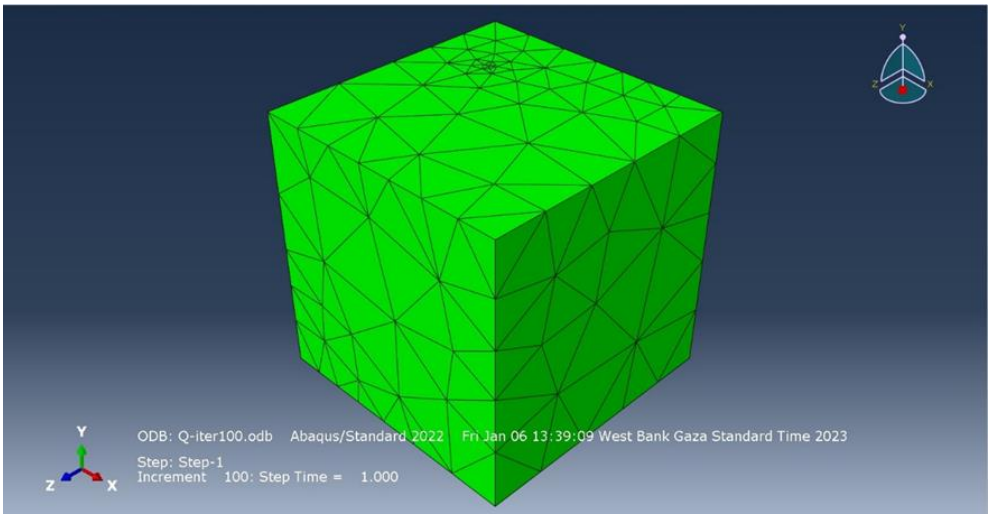

c. Final redefined concrete mesh after the analysis process

6. Analysis and Job Creation

After defining the model, it is ran with an enough number of iterations until the results become nearly fixed.

The results are drawn from the history output as follows:

1. The average displacement of the upper surface is applied and divided by 50 mm (which is the height of the concrete to obtain the strain).
2. The sum is calculated for the reaction on the lower surface and divided by 2500 mm^2 (which is the surface area of the reaction) to find the stress.
3. The relationship between the stress & strain is drawn.

3.3 Obtained Concrete Characteristics

Different characteristics were obtain from the numerical analysis, which are:

3.3.1 Modulus of elasticity

Before modelling the samples on the FEA software, mathematical calculations are done to be compared with the software and experimental results.

Mathematical Calculations

To perform the theoretical calculations, first, it's assumed that the fibers are arrange perpendicular to the direction of the loading. In this case, the modulus values will be calculated through the following equation:

$$E_{\emptyset} = \frac{E_c E_f}{(1 - \emptyset_f)E_f + \emptyset_f E_c} \qquad Eq3.18$$

Where, $E_{\emptyset}$ is the modulus of elasticity for the composite material at a ratio of $\emptyset$, E_c is the modulus of elasticity of concrete, E_f is the modulus of elasticity of fiber, and $\emptyset_f$is the ratio of fiber in the composition.

The second assumption is that the fibers are arranged parallel to direction of the loading, which is the ideal case, which gives the highest value to the elastic modulus. The equation in this case will be as follows:

$$E_{\emptyset} = \emptyset_f E_f + (1 - \emptyset_f) E_c \qquad Eq3.19$$

The third assumption is that the fibers will be distributed randomly (which is the real distribution), which will give us a modulus of elasticity between the ones we calculated in the above two assumptions. [44]

Modelling for Modulus of Elasticity

To obtain the elastic modulus, the steps in *section 4.2* are followed, while defining the material in the elastic region, without defining the plasticity of the material

For concrete, poison ratio = 0.2 and modulus of elasticity is calculated through the equation *Eq3.17*, and is found to be 17,400 MPa.

And $f'c$ value is based on lab results from the fracture test.

As for the fiber characteristics, the following characteristics will be entered:

1- For rivet mandrels

$E = 200{,}000\ MPa$ and obtained by

Poison ratio = 0.3

2- For wire waste:

Poison ratio = 0.3

$E = 200{,}000\ MPa$

$$E_c = w^{1.5}(0.043)\sqrt{f'c} \qquad Eq3.16$$

Where $f'c$ is the compressive strength of the concrete at 28 days, w is the density of the concrete, and E_c is the modulus of elasticity.

When adopting concrete density to be equal to $2300\ kg/m^3$, then the equation becomes:

$$E_c = 4700\sqrt{f'c} \qquad Eq3.17$$

To obtain the modulus of elasticity of the mixes, a final step is performed in the job creation, and then the elastic modulus is calculated from the slope of the elastic region in the graph or from equation *Eq3.4* [43].

To compare with the theoretical calculations, two models are defined for each of the mixtures alongside with the main model containing random distributed fibers. The first model has its fibers distributed horizontally (perpendicular to the load) which is expected to give a result near the value calculated from equation *Eq3.18*. The fibers in the second model are distributed vertically (parallel to the load), which should give a value near to the equation *Eq3.19*. The main model is expected to get a value between the above 2 models. Figure 4.3 shows the 3 models. Table 4.3 compares the results obtained from the experimental, theoretical and FE analysis.

Figures 4.3

Different distributions of fibers in concrete

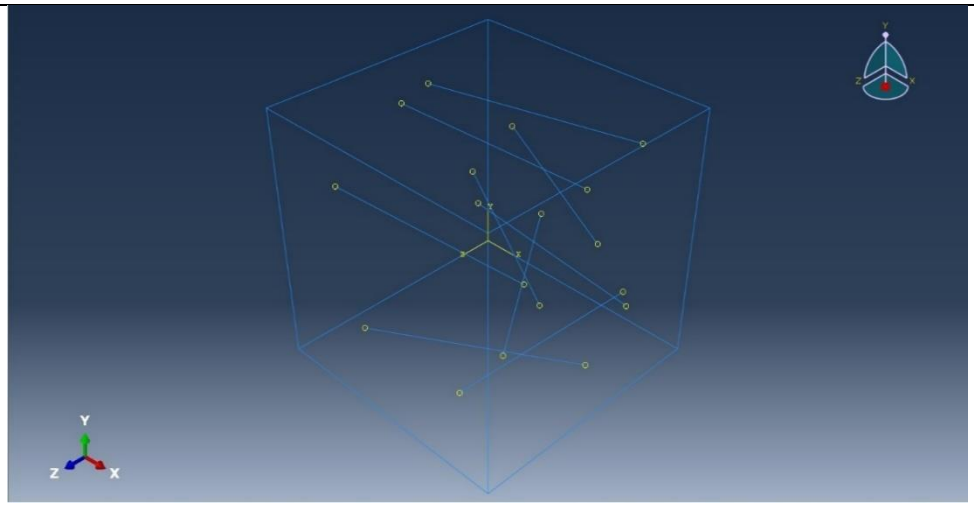

a) Horizontal distribution of fibers

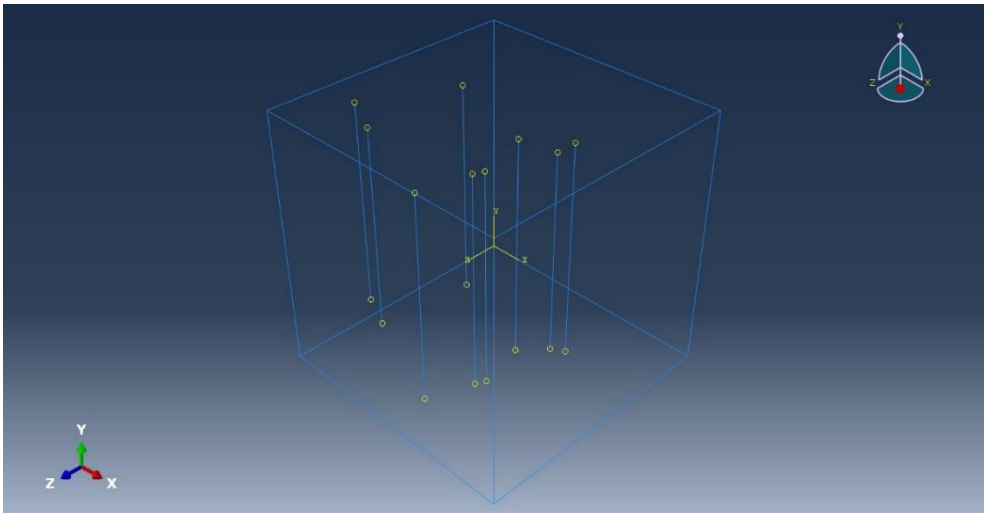

b) Vertical distribution of fibers

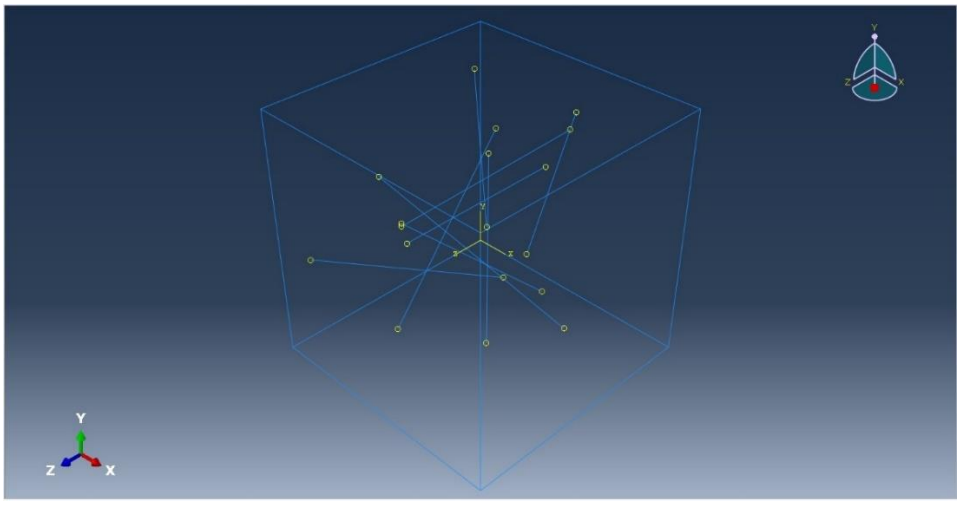

c) Random distribution of fibers

Finite Element Analysis Results

The results collected from the finite element analysis gave less elastic modulus than the experiments, but more effects compared to the plain concrete.

The elastic modulus E_c for the plain concrete calculated to be 17405MPa

For the concrete with 1% rivets included, the modulus of elasticity for the horizontally, vertically and randomly distributed where found to be 17478MPa, 19414MPa and 17912MPa respectively. This had an increase of 2.9% compared to plain concrete.

The results concluded from inserting 2% of rivets were found to be 17546MPa, 21390MPa and 18125MPa for the horizontally, vertically and randomly distributed rivet mandrels. The increase was 4.1% compared to the plain concrete.

The analyses of concrete with 3% of fiber rivet gave a modulus of elasticity 5.2% more modulus of elasticity compared to those of plain concrete without added fiber. The results were found to be 17606MPa, 23310MPa and 18318MPa for the horizontally, vertically and randomly distributed fiber rivets.

As in the experiments, the addition of fiber wires had more increase of modulus of elasticity than those of added rivet mandrels.

The addition of 1% of wires increased $E_{\emptyset}$ by 3.1% with values of 17479MPa, 19409MPa and 17953MPa for the horizontally, vertically and randomly distributed fiber wires.

While the addition of 2% of wires increased $E_{\emptyset}$ by 4.1%. The values were found to be 17549MPa, 21360MPa and 18123MPa for the horizontally, vertically and randomly distributed wires.

The results accumulated from adding 3% of wires for the horizontally, vertically and randomly distributed wires were found to be 17612MPa, 23096MPa and 18472MPa, which means that the increase of the modulus of elasticity was 6.1%.

Table 3.3

$E_{\emptyset}$ Comparison between the different methodologies

Results	Theoretical Results		Experimental Results		Finite Elements Analysis Results			
Mixes	Horizontal	Vertical	Random	Avg. Random	Horizontal	Vertical	Random	Avg. Random
Plain concrete without added fiber	17400	17400	17796 17167 17537 17664	17541	17405	17405	- - - -	17405
With 1% fiber rivet mandrels	17560	19226	17979 18095 18218 17873	18041	17478	19414	17905 18060 18142 17541	17912
With 2% fiber rivet mandrels	17724	21052	18017 18408 18153 18317	18224	17546	21390	17782 18550 18223 17945	18125
With 3% fiber rivet mandrels	17890	22878	18294 18412 18638 18384	18433	17606	23310	18274 18394 17881 18723	18318
With 1% fiber Wires	17560	19226	18286 17794 17945 18023	18012	17479	19409	17909 17740 17915 18249	17953
With 2% fiber Wires	17724	21052	18250 18355 18186 18272	18266	17549	21360	18034 18104 18085 18267	18123
With 3% fiber wires	17890	22878	18569 18758 18373 18681	18595	17612	23096	18232 18442 18582 18631	18472

3.3.2 Stress-Strain Relationship

The stress-strain diagram of concrete is a diagram that shows the relationship between the stress applied to a concrete specimen and the resulting strain that occurs.

It consists of 2 regions, initial linear elastic region followed by a nonlinear region that includes within it the strain hardening. The point that separates the two regions is the yielding of the material. The elastic modulus of concrete is relatively low compared to other construction materials, and the ultimate strength and strain capacity are also relatively low. The shape of the stress-strain curve can vary depending on factors such as the type and mixture of concrete, age, and testing conditions. Additionally, concrete

is known to be brittle, meaning that it typically does not exhibit significant plastic deformation before failure. [28]

Some of the most important values in the stress-strain diagram of concrete include the elastic modulus, the yield stress, the ultimate stress, and the strain at failure. These values are important for designing structures that will withstand expected loads and ensure the safety and reliability of the structure. Those characteristics are measured and represented in the stress-strain diagram later in this thesis.

This time, the plasticity of concrete and fiber material is defined in the model. After getting the stress-strain diagram, some comparisons are made to validate the model. Those comparison are:

1. The modulus of elasticity: The modulus of elasticity is obtained by calculating the slope of the stress-strain diagram, and is compared with the elastic modulus obtain in the above section.
2. Compressive strength: The compressive strength is the highest value in the diagram, and is compared with the experimental results.

The stress-strain relationship was plotted using FEA methodology. The resulted compressive stress f_c' and modulus of elasticity E were compared with those obtained from the previous experiments, to check and ensure that the model was represented correctly.

Using the concrete damage plasticity material model, the characteristics of the plain concrete were included in the model. The model then produced figure 4.4(a) -see Appendix (A)-, which represents the stress-strain diagram of the plain concrete. From the diagram, f_c' was found to be 13.74MPa at 0.00176 strain, and modulus of elasticity was found to be 17377.89MPa. Those resulted characteristics were very close to the input ones.

Figure 4.4(b) -see Appendix (A)- shows the stress-strain diagram for the concrete samples with 1% of fiber rivets. The compressive strength f_c' obtained was 16.93MPa at 0.00325 stain. Compared with the one obtained from the experimental tests (18.44MPa), the calculated error is 8.2%. The linear region ends around 38% of f_c', and the slope of this regions was found to be 18065MPa, which represents the modulus of elasticity, and

it’s very close to the one obtained in the previous section, which was 17912MPa (0.9% difference). The compressive stress drops to 85% of f_c' at a strain of 0.00574.

Figure 4.4 (c) -see Appendix (A)- illustrates the stress-strain diagram for concrete samples containing 2% of fiber rivets. The compressive strength f_c' reached was 22.26MPa at a strain of 0.00403. In comparison with the experimental tests' value (23.69MPa), the calculated error is 6%. The linear region concludes at approximately 39% of f_c', and the slope of this region was determined to be 18169MPa. This value represents the modulus of elasticity and is very close to the result obtained in the previous section, which was 18125MPa (0.2% difference). The compressive stress decreases to 85% of f_c' at a strain of 0.00719.

Figure 4.4 (d) -see Appendix (A)- presents the stress-strain diagram for concrete samples with 3% of fiber rivets. The compressive strength f_c' obtained was 21.30MPa at a strain of 0.00416. Compared to the experimental tests' value (20.07MPa), the calculated error is 6.1%. The linear region ends at around 32% of f_c', and the slope of this region was found to be 18199MPa, which represents the modulus of elasticity. This result is very close to the one obtained in the previous section, which was 18318MPa (0.7% difference). The compressive stress drops to 85% of f_c' at a strain of 0.00802.

Figure 4.4 (e) -see Appendix (A)- depicts the stress-strain diagram for concrete samples reinforced with 1% of wires. The compressive strength f_c' reached was 26.88MPa at a strain of 0.0045. When compared to the experimental tests' value (29.85MPa), the calculated error is 10%. The linear region concludes at approximately 43% of f_c', and the slope of this region was determined to be 17939MPa. This value represents the modulus of elasticity and is very close to the result obtained in the previous section, which was 17953MPa (0.1% difference). The compressive stress decreases to 85% of f_c' at a strain of 0.00835.

Figure 4.4 (f) -see Appendix (A)- displays the stress-strain diagram for concrete samples containing 2% of wires. The compressive strength f_c' obtained was 26.03MPa at a strain of 0.00443. In comparison with the experimental tests' value (35.43MPa), the calculated error is 26.6%. The linear region ends at around 42% of f_c', and the slope of this region was found to be 18063MPa, which represents the modulus of elasticity. This

result is very close to the one obtained in the previous section, which was 18123MPa (0.3% difference). The compressive stress drops to 85% of f_c' at a strain of 0.00867.

Figure 4.4(g) -see Appendix (A)- presents the stress-strain diagram for concrete samples with 3% of wires. The compressive strength f_c' reached was 25.70MPa at a strain of 0.00458. When compared to the experimental tests' value (30.05MPa), the calculated error is 14.5%. The linear region concludes at approximately 36% of f_c', and the slope of this region was determined to be 18351MPa. This value represents the modulus of elasticity and is very close to the result obtained in the previous section, which was 18472MPa (0.7% difference). The compressive stress decreases to 85% of f_c' at a strain of 0.00957.

In summary, the stress-strain diagrams for concrete samples with varying percentages of fiber rivets and wires show different compressive strengths, strains, and modulus of elasticity values. The calculated errors compared to experimental tests vary, but the modulus of elasticity for each sample remains relatively close to the values obtained in the previous sections.

Cost Analysis

From previous results, we conclude that using waste material as fibers resulted in improving the concrete properties, which is the main objective of this study.

An analysis of the cost variations is necessary to conclude the effectiveness of using those materials. This section analyses and discusses the costs of using waste material studied and used in this thesis.

The cost calculations were done on the concrete with 1% wires as it possessed the best results in terms of the compressive strength, and acceptable tensile strengths and workability.

Depending on the market pricing of concrete, the concrete with 20 MPa strength is around 290 ILS while the concrete with 15 MPa strength is about 270 ILS. The studied plain concrete strength was in average 17.5 MPa, which would cost 280 ILS in Palestine.

A ton of wires cost about 700 ILS. Processing of wires including cleaning and cutting could cost about 20%, which is 140 ILS per ton of wires. Considering the density of

fiber wires is 7.85 ton/m^3, the cost of wires is calculated to be 6594 ILS per cubic meter of wires. A 1% ratio of wires costs 66 ILS per cubic meter of concrete.

From the above, a mix of 17.5 MPa of plain concrete with 1% of added fiber wires cost about 345 ILS and leads to a 38.27 MPa compressive strength and 5.20 MPa flexural strength.

Concrete of 40MPa is of 370 ILS and 35MPa costs 350 ILS. From those values, it can be estimated that concrete of 38.27 is about 365 ILS. This concludes that the addition of wires saves around 5% of the concrete cost.

The enhanced tensile strength of concrete produced with the fiber wires are not available in the Palestinian industries as plain concrete. For improving concrete tensile strength, polypropylene fiber of density of 0.91 g/cm^3 is added to the concrete in the Palestinian industries. A backet of 600g is added per cubic meter of cement mix, (0.07% of the concrete volume), which costs, and a price of 395 ILS, which is about 115% of the cost of the concrete with the added 1% of waste wires.

Chapter Four
Conclusions, Recommendations, and Future Work

4.1 Overview

This chapter presents the conclusions derived from the research and the experimental investigation conducted to the performance of concrete by adding different types and rates of fibers, namely rivet mandrels and wire fibers. The chapter also provides design guidelines for practitioners who wish to apply the findings of this research in real-world scenarios. Finally, the chapter concludes with recommendations for future work to enhance the understanding of fiber-reinforced concrete and expand its applicability.

4.2 Research Findings

The experimental investigation conducted in this research yielded significant findings on the mechanical properties of concrete with the addition of rivet mandrels and wire fibers. The study found that:

1. The workability decreases as the fiber ratio increases in the concrete. The effect remains positive until it falls below the limit of medium degree of workability when adding 3% of rivets mandrel or 2% of wires.
2. The compressive strength of concrete increased with the addition of fibers until a specific ratio, then it starts to decrease due to the agglomerations and the formation of pores. In our case, the compressive strength started to degrade when the ratio of rivets reached 3%, and when adding 2% of wire. The highest increase in compressive strength was observed in the samples containing 1% wire fibers with an increase up to 34.81%.
3. The tensile strength of the concrete also improved with the addition of fibers. As in the compressive strength, the tensile strength starts to degrade after certain ratios for the same reasons. The highest tensile strength obtained from the rivet mandrels was at 2%, while in the wires case, the tensile strength continued to increase even at 3%. The highest increase in tensile strength was observed in the samples containing 3% wire fibers with a maximum increase of 129.75% in the split cylinder tensile strength and 157.08% in the flexural tensile strength.

4. The modulus of elasticity increased with the addition of fibers. Wire fibers had a more impact on the modulus of elasticity than rivet mandrels, with very close values.
2. The stress-strain diagrams showed that the addition of fibers increased the ductility of the concrete, and slowed its failure with increased strain at failure. The elastic behaviour of concrete with the added fibers remains in the range of 30% to 45%.

4.3 Design Guidelines

Based on the findings of this research, the following design guidelines are recommended for practitioners who wish to implement fiber-reinforced concrete in their projects:

1. To achieve higher compressive and tensile strength, consider using wire fibers rather than rivet mandrels.
2. The optimal fiber content for wire fibers is between 1% and 3% depending on the structural element. Exceeding this percentage may lead to diminishing returns in mechanical properties and workability.
3. When using rivet mandrels, an optimal content of 2% is recommended to achieve a balance between mechanical properties and workability.
4. When designing fiber-reinforced concrete mixtures, consider the impact of fibers on the stress-strain relationship and adjust the design accordingly.

4.4 Future Work

The current research has opened up several avenues for future investigation in the field of fiber-reinforced concrete. Some recommendations for future work include:

1. Investigate the long-term durability and performance of concrete reinforced with rivet mandrels and wire fibers under various environmental conditions.
2. Study the impact of varying fiber lengths and aspect ratios on the mechanical properties of fiber-reinforced concrete.
3. Investigate the effectiveness of hybrid fiber-reinforced concrete, where two or more types of fibers are used in combination, to optimize mechanical properties and workability.
4. Develop advanced analytical models and simulation techniques to predict the behavior of fiber-reinforced concrete under various loading conditions.

5. Study the effect of the addition of fiber material on different mixtures of concrete with higher workability and less aggregate sizes.
6. In the case that laboratory tests become available, more studies can be done to assure and get more precise mechanical characteristics, such as the modulus of elasticity and stress-strain relationships.

4.5 Conclusion

Study Background: Concrete, which is the most material used in construction faces some problems and limitations when constructing high rise buildings, large floor spans, special floors with high loadings, etc. Materials used to produce high-performance concrete come with high costs, and this created the need to alternatives to the commonly used material to produce this type of concrete.

Objectives: Mandrel of aluminum blind rivets and building wire are widely available as waste material, and the research aims to study the effect of those materials on concrete mechanical properties, to test their appropriability to be used to produce high-performance concrete.

Methodology: Two methodologies were used to study the effect of adding fibers to concrete. The first was by using finite element analysis and simulating the behavior of the concrete material when different ratios of fibers are added. Also, laboratory experiments were conducted to verify the results of the finite element analysis and find some other properties such as the density of the material and its formability.

Results: The results indicate that adding rivets and wires helped to improve the compressive strength, tensile strength, and ductility of the concrete material. However, there are limits that represent the peak of the tensile and compressive strength, and exceeding these limits results in weakening the material.

References

[1] Panarese, W. C., Allen, G. E., & Cumming, S. (1991). Design and control of concrete mixtures. S. H. Kosmatka (Ed.). Canadian Portland Cement Association [CPCA].

[2] Aïtcin, P. C. (1998). High performance concrete. CRC press.

[3] Neville, A., & Aitcin, P. C. (1998). High performance concrete—An overview. Materials and structures, 31, 111-117.

[4] The World Material, https://www.theworldmaterial.com/q195-steel/

[5] SteelonCall, https://steeloncall.com/what-is-the-q195-steel-grade

[6] Haolijinhui Science & Technology Co., Ltd, https://2u.pw/q0nn7f6w

Gjorv, O. E., & Sakai, K. (1999). Concrete technology for a sustainable development in the 21st century. CRC Press.

[8] Amran, M., Huang, S. S., Onaizi, A. M., Makul, N., Abdelgader, H. S., & Ozbakkaloglu, T. (2022). Recent trends in ultra-high performance concrete (UHPC): Current status, challenges, and future prospects. Construction and Building Materials, 352, 129029.

[9] ALTAYEH, N. A. (2021). Mechanical Properties and Durability of Ultra-High-Performance Concrete with Locally Available Materials (Master's thesis).

[10] Ali, M. M. Manufacturing Ultra-High Performance Concrete Utilising Conventional Materials and Production Methods (Doctoral dissertation, The University of Adelaide).

[11] Yuliarti, K., Susilorini, R., & Aboubakr, A. (2015). Properties of Ultra High Performance Concrete. In Proceedings of International Conference on Concrete and Infrastructure 2015 (pp. 44-49). Universitas Katolik Soegijapranata.

[12] Wille, K., Naaman, A. E., El-Tawil, S., & Parra-Montesinos, G. J. (2012). Ultra-high performance concrete and fiber reinforced concrete: achieving strength and ductility without heat curing. Materials and structures, 45, 309-324.

[13] Šahmenko, G., Krasnikovs, A., Lukašenoks, A., & Eiduks, M. (2015, June). Ultra high performance concrete reinforced with short steel and carbon fibers. In ENVIRONMENT. TECHNOLOGIES. RESOURCES. Proceedings of the International Scientific and Practical Conference (Vol. 1, pp. 193-199).

[14] Meng, W., & Khayat, K. H. (2018). Effect of hybrid fibers on fresh properties, mechanical properties, and autogenous shrinkage of cost-effective UHPC. Journal of Materials in Civil Engineering, 30(4), 04018030.

[15] Meng, W., & Khayat, K. H. (2016). Experimental and numerical studies on flexural behavior of ultrahigh-performance concrete panels reinforced with embedded glass fiber-reinforced polymer grids. Transportation Research Record, 2592(1), 38-44.

[16] Chen, H. J., Yu, Y. L., & Tang, C. W. (2020). Mechanical properties of ultra-high performance concrete before and after exposure to high temperatures. Materials, 13(3), 770.

[17] Ayub, T., Shafiq, N., & Nuruddin, M. F. (2014). Mechanical properties of high-performance concrete reinforced with basalt fibers. Procedia Engineering, 77, 131-139.

[18] Bheel, N., Awoyera, P., Aluko, O., Mahro, S., Viloria, A., & Sierra, C. A. S. (2020). Sustainable composite development: Novel use of human hair as fiber in concrete. Case Studies in Construction Materials, 13, e00412.

[19] Van Breugel, K., Ye, G., & Van Tuan, N. (2014, February). Ultra high performance concrete made with rice husk ash for reduced autogenous shrinkage. In Proceedings of the 4th International FIB Congress, Mumbai, India, 10–14 February 2014; Authors version. Universities Press.

[20] Tang, K., Mao, X., & Tang, X. (2018, May). Study on application of iron tailings fine aggregate in concrete. In 2018 3rd International Conference on Advances in Materials, Mechatronics and Civil Engineering (ICAMMCE 2018) (pp. 173-177). Atlantis Press.

[21] Rao, H. S., Reddy, N. T., & Ghorpade, V. G. Permeability Studies On High Performance Concrete With Replacement Of Fine Aggregate By Manufactured Sand.

[22] Bosco, E., Claessens, R. J. M. A., & Suiker, A. S. (2020). Multi-scale prediction of chemo-mechanical properties of concrete materials through asymptotic homogenization. Cement and Concrete Research, 128, 105929.

[23] Congro, M., Sanchez, E. C. M., Roehl, D., & Marangon, E. (2019). Fracture modeling of fiber reinforced concrete in a multiscale approach. Composites Part B: Engineering, 174, 106958.

[24] Bernard, F., Kamali-Bernard, S., & Prince, W. (2008). 3D multi-scale modelling of mechanical behaviour of sound and leached mortar. Cement and Concrete Research, 38(4), 449-458.

[25] Palestinian Specifications (PS-55-1-2015)

[26] Sermix Company for Ready Mix Concrete, Contracting and General Contracting

[27] Hama, S. M., & Hilal, N. N. (2019). Fresh properties of concrete containing plastic aggregate. In Use of recycled plastics in eco-efficient concrete (pp. 85-114). Woodhead Publishing.

[28] Darwin, D., Dolan, C. W., & Nilson, A. H. (2016). Design of concrete structures. New York, NY, USA:: McGraw-Hill Education.

[29] ASTM C1754 / C1754 M

[30] Babu, K. G., & Rao, G. S. N. (1996). Efficiency of fly ash in concrete with age. Cement and concrete research, 26(3), 465-474.

[31] Reinhardt, H. W. (2013). Factors affecting the tensile properties of concrete.

[32] ASTM C78/C78M

[33] ASTM C496/C496M

[34] ASTM C1583/C1583M

[35] ASTM C31/C31M

[36] ABAQUS User Manual, 2014

[37] Behnam, H., Kuang, J. S., & Huang, R. Y. (2017). Exterior RC wide beam-column connections: Effect of beam width ratio on seismic behaviour. Engineering Structures, 147, 27-44.

[38] Behnam, H., Kuang, J. S., & Samali, B. (2018). Parametric finite element analysis of RC wide beam-column connections. Computers & Structures, 205, 28-44.

[39] Jankowiak, T., & Lodygowski, T. (2005). Identification of parameters of concrete damage plasticity constitutive model. Foundations of civil and environmental engineering, 6(1), 53-69.

[40] Najafgholipour, M. A., Dehghan, S. M., Dooshabi, A., & Niroomandi, A. (2017). Finite element analysis of reinforced concrete beam-column connections with governing joint shear failure mode. Latin American Journal of Solids and Structures, 14(7), 1200-1225.

[41] Lee, J., & Fenves, G. L. (1998). Plastic-damage model for cyclic loading of concrete structures. Journal of engineering mechanics, 124(8), 892-900.

[42] Park, R., & Paulay, T. (1975). Reinforced Concrete Structures, John Wiley & Sons. NY, USA.

[43] Al-Rousan, R. Z., Alhassan, M. A., & Hejazi, M. A. (2018). Novel nonlinear stiffness parameters and constitutive curves for concrete. Computers and Concrete, 22(6), 539-550.

[44] Herrera-Franco, P. J., & Valadez-Gonzalez, A. (2004). Mechanical properties of continuous natural fibre-reinforced polymer composites. Composites Part A: applied science and manufacturing, 35(3), 339-345.

[45] AISC - Shears Moments and Deflections - BEAM DIAGRAMS AND FORMULAS 3-2 13 Table 3-23 Shears Moments and Deflections

Appendices

Appendix (A)

Figures

Figures 4.4

Stress-strain diagrams of concrete samples when adding different ratios of rivet mandrels and wires

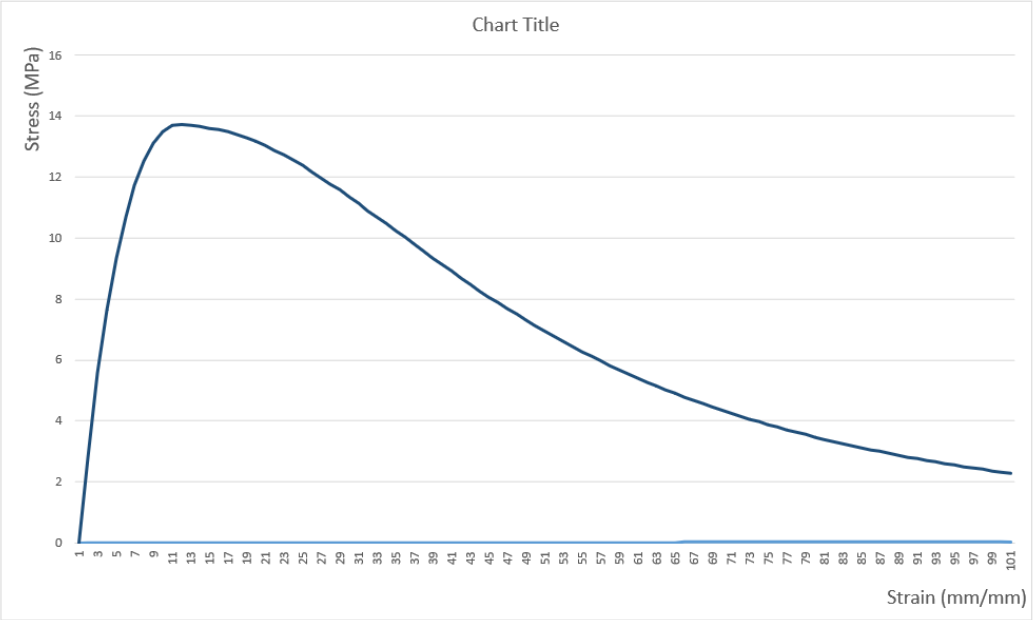

a) Stress-strain diagram of plain concrete

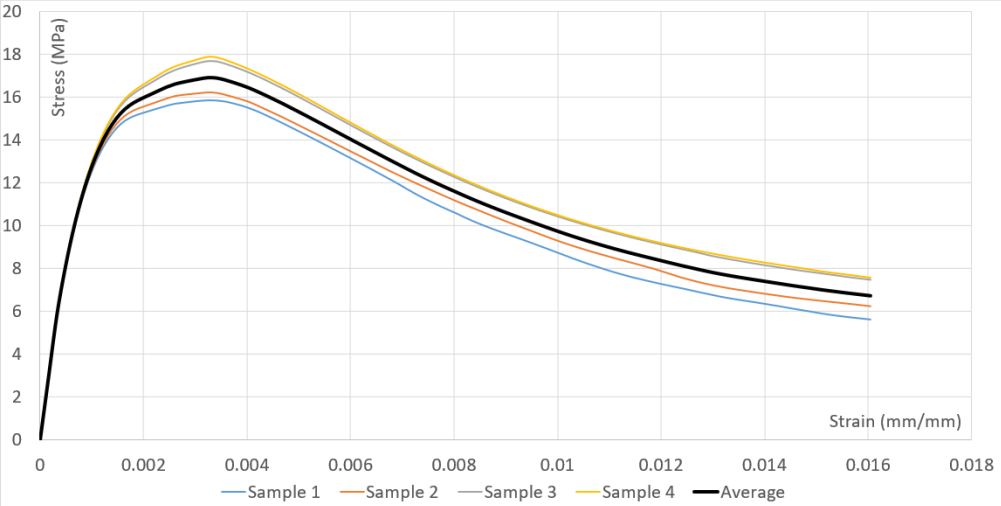

b) Stress-strain diagram of concrete samples with added 1% of rivet mandrels

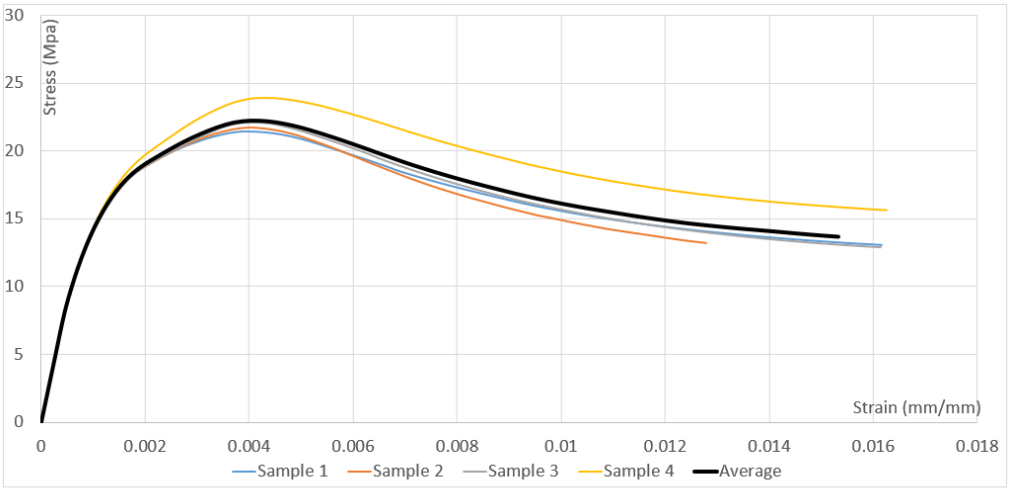

c) Stress-strain diagram of concrete samples with added 2% of rivet mandrels

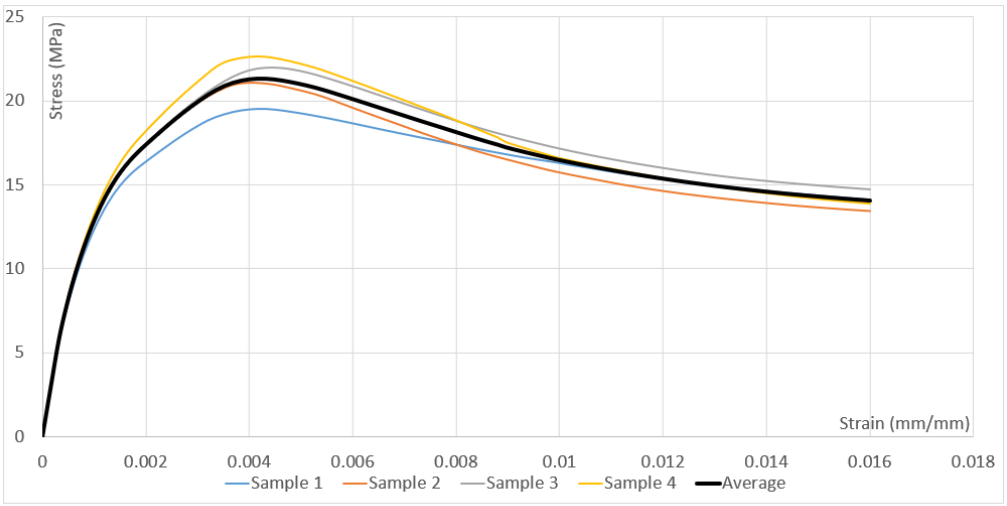

d) Stress-strain diagram of concrete samples with added 3% of rivet mandrels

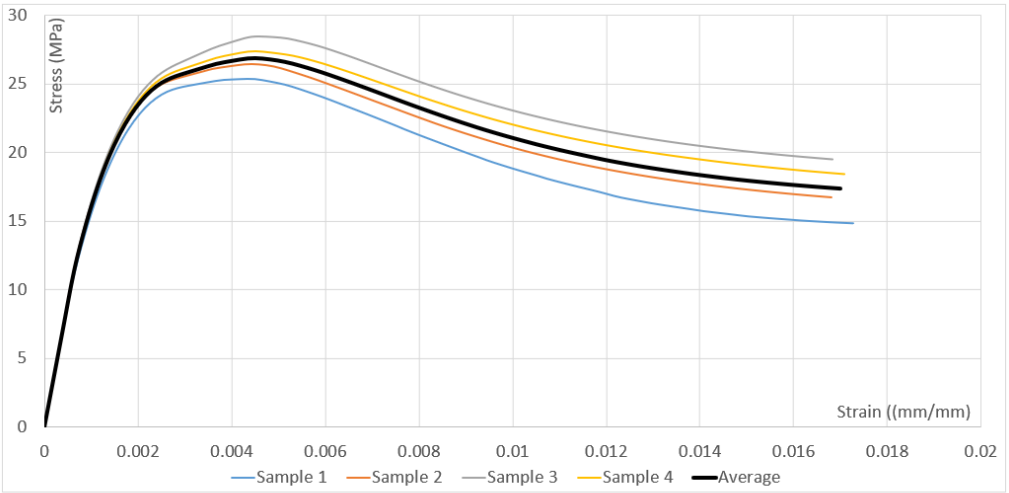

e) Stress-strain diagram of concrete samples with added 1% of wires

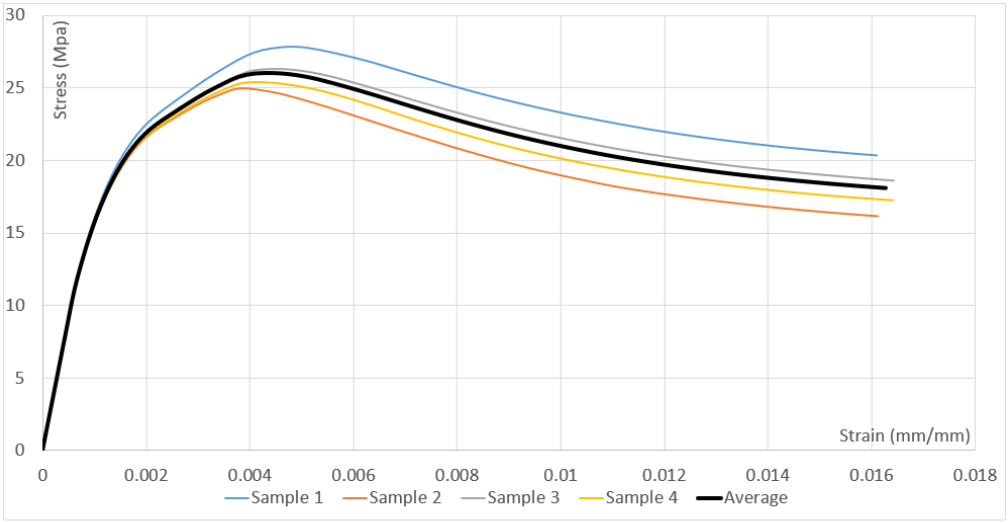

f) Stress-strain diagram of concrete samples with added 2% of wires

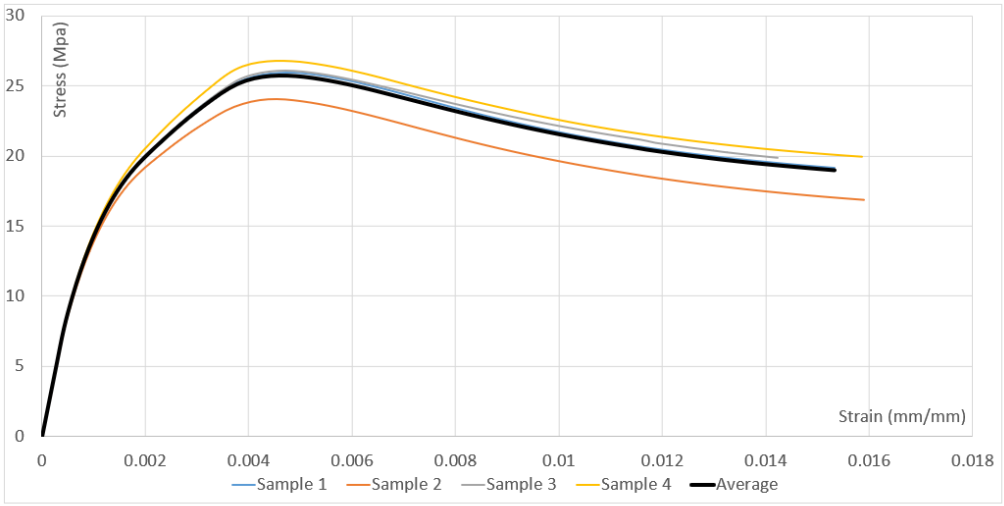

g) Stress-strain diagram of concrete samples with added 3% of wires

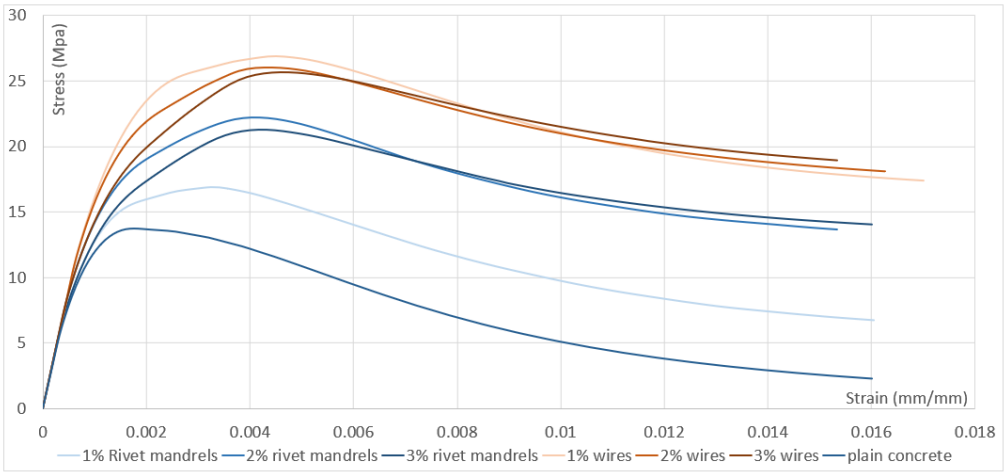

h) Comparison of stress-strain diagrams between concrete samples with added fibers of different ratios and types

Figure A1

Sample of rivets waste

Figure A2

Sample of wires waste

Figure A3

Slump Test process

Figures A4

Concrete density when adding different ratios of rivet mandrels and wires.

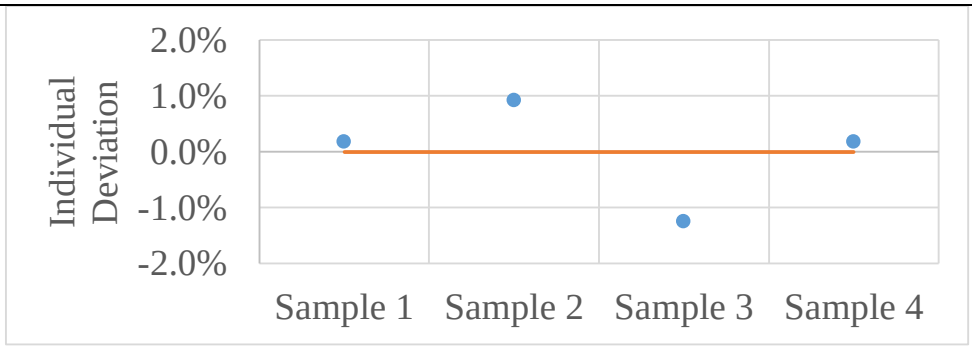

a) Density (tons) of plain concrete samples

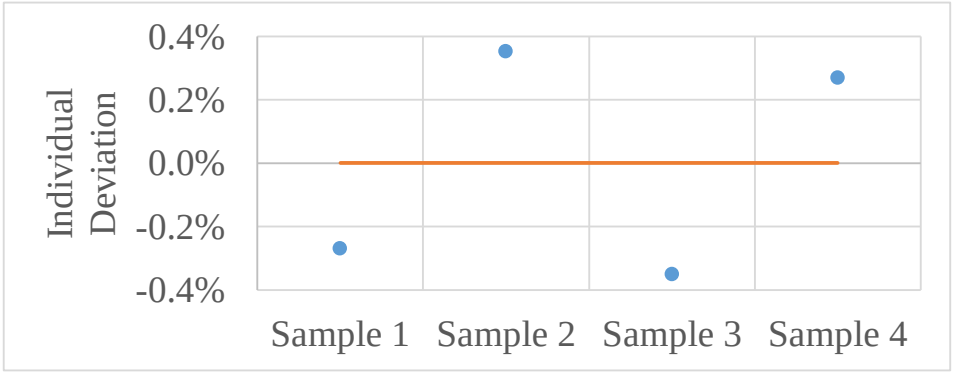

b) Density (tons) of concrete samples with added 1% of rivet mandrels

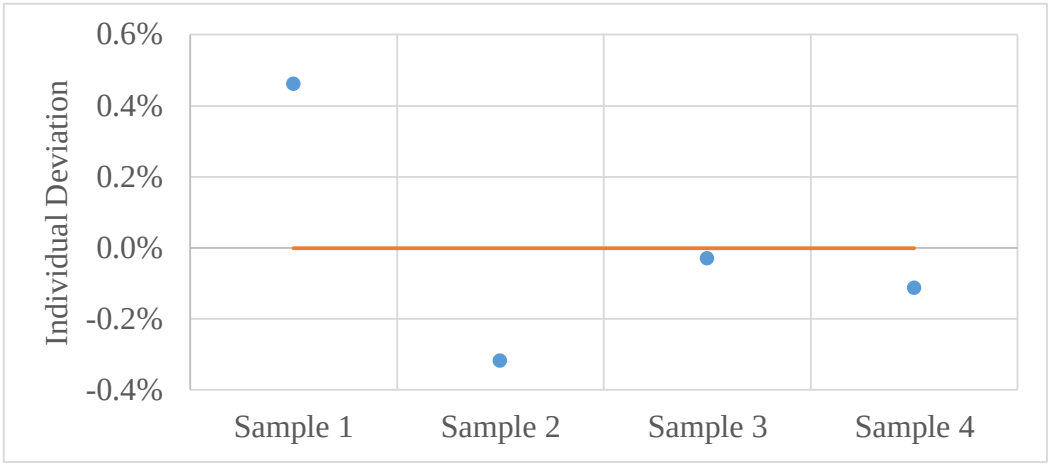

c) Density (tons) of concrete samples with added 2% of rivet mandrels

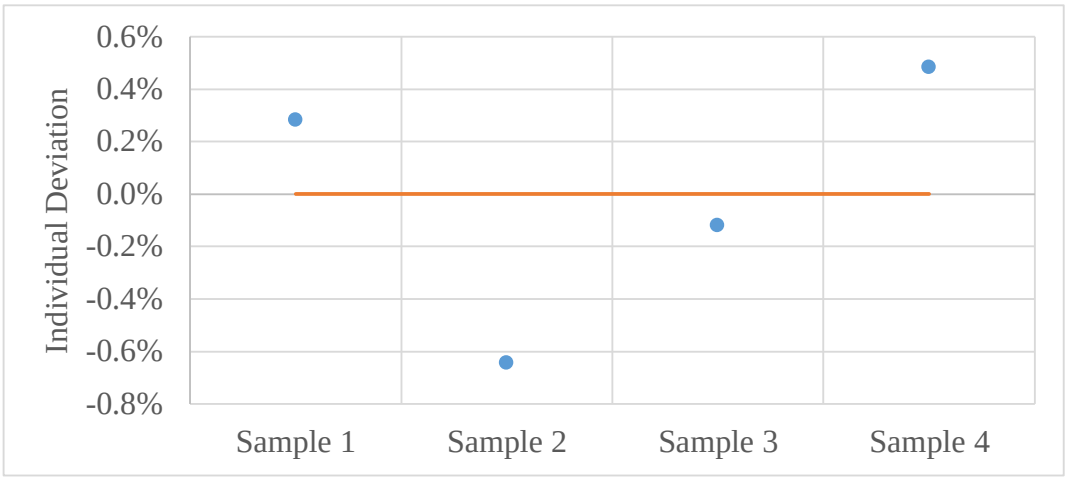

d) Density (tons) of concrete samples with added 3% of rivet mandrels

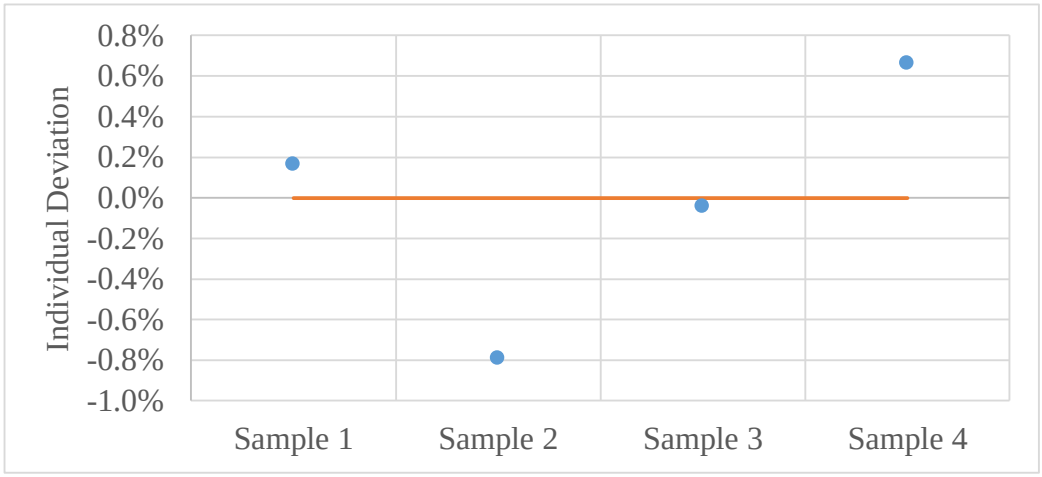

e) Density (tons) of concrete samples with added 1% of wires

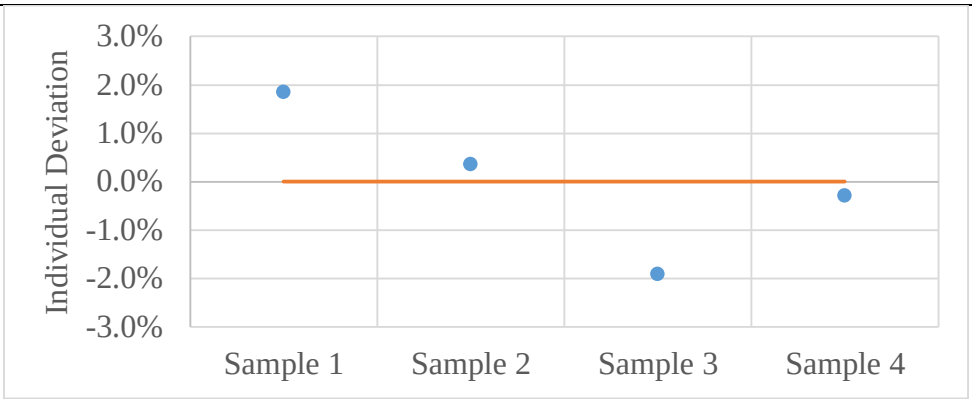

f) Density (tons) of concrete samples with added 2% of wires

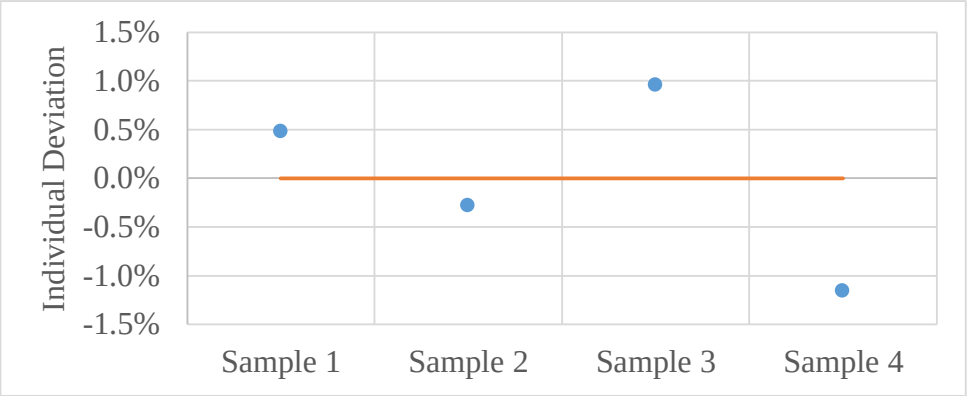

g) Density (tons) of concrete samples with added 3% of wires

Figures A5

Concrete compressive strength when adding different ratios of rivet mandrels and wires

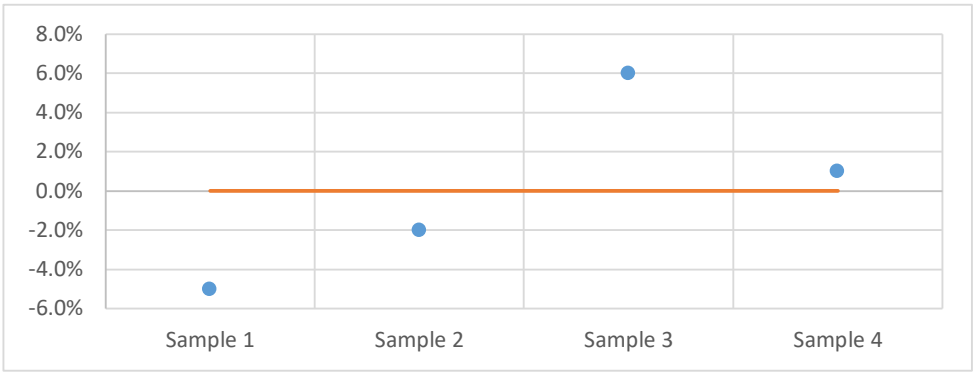

a) Compresive Strength (MPa) of plain concrete samples

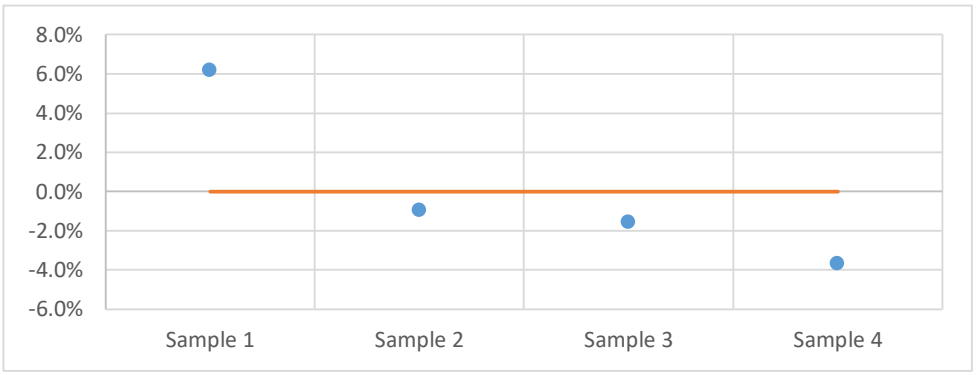

b) Compresive Strength (MPa) of concrete samples with added 1% of rivet mandrels

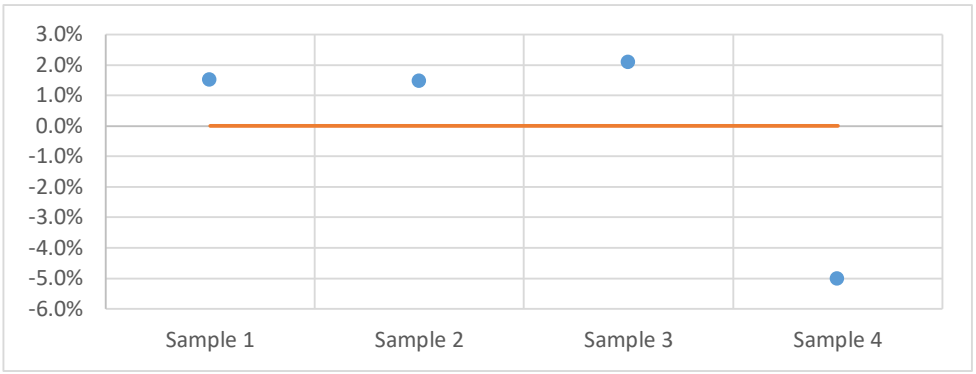

c) Compresive Strength (MPa) of concrete samples with added 2% of rivet mandrels

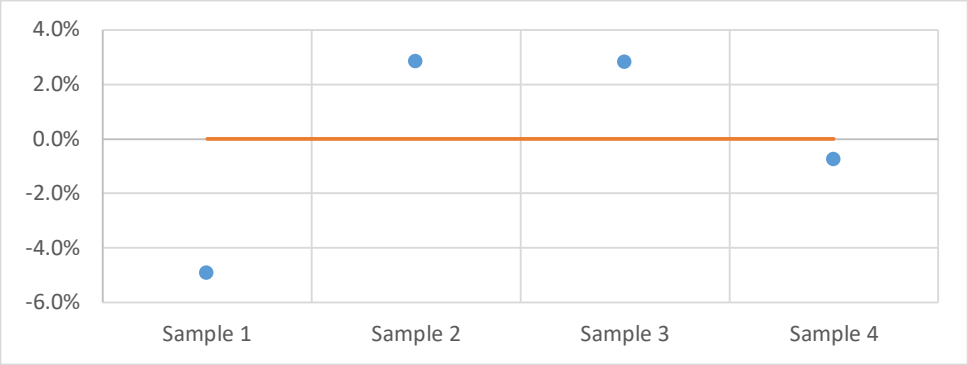

d) Compresive Strength (MPa) of concrete samples with added 3% of rivet mandrels

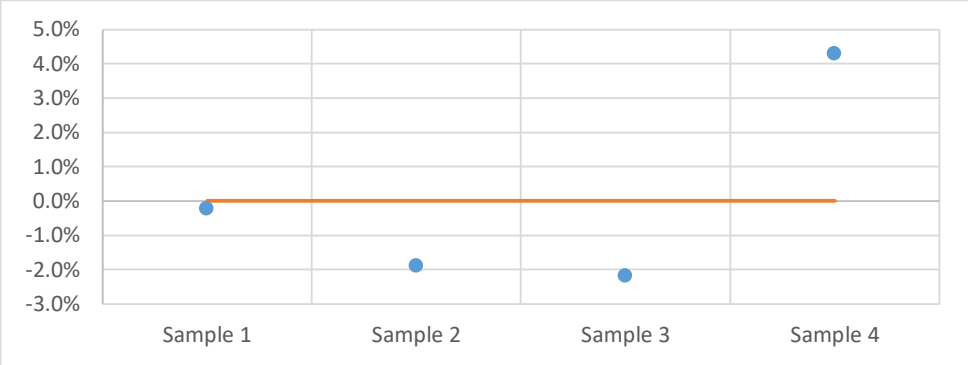

e) Compresive Strength (MPa) of concrete samples with added 1% of wires

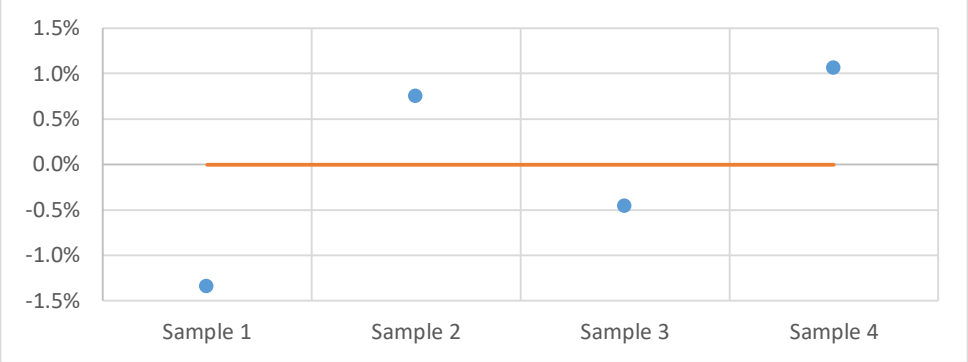

f) Compresive Strength (MPa) of concrete samples with added 2% of wires

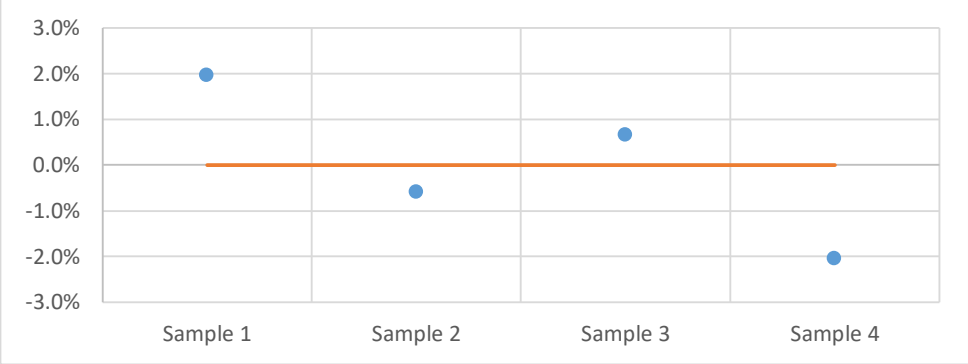

g) Compresive Strength (MPa) of concrete samples with added 3% of wires

Figures A6

Split cylinder tensile strength of concrete samples when adding different ratios of rivet mandrels and wires

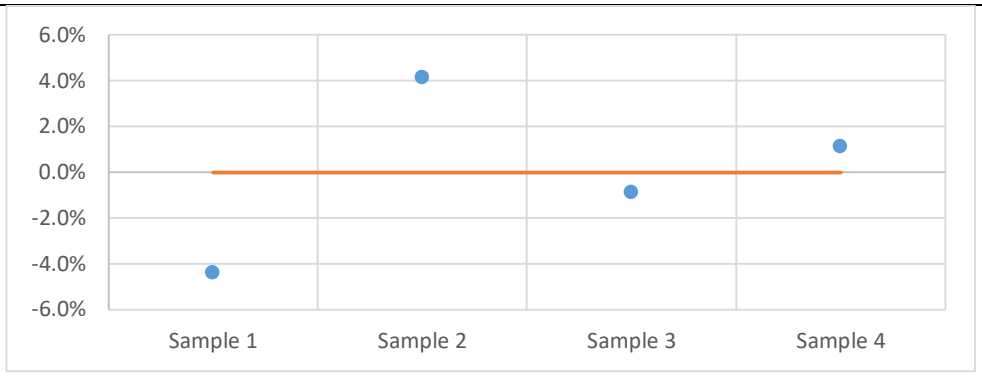

a) Split Cylinder Tensile Strength (MPa) of plain concrete samples

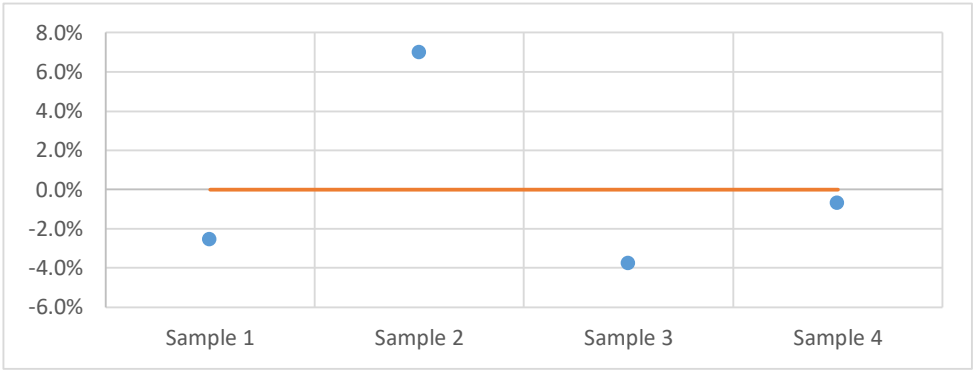

b) Split Cylinder Tensile Strength (MPa) of concrete samples with added 1% of rivet mandrels

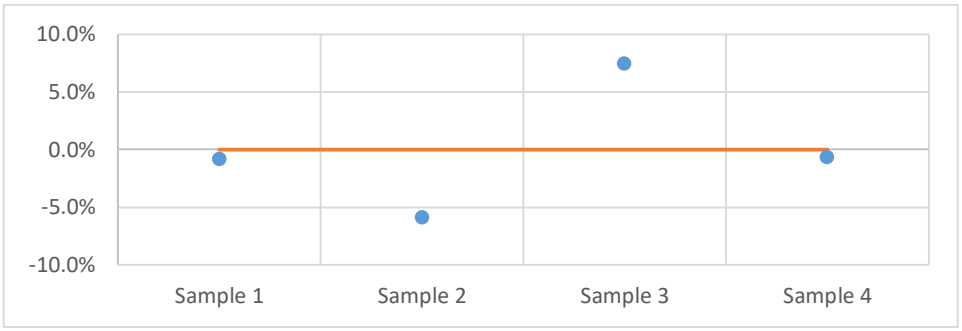

c) Split Cylinder Tensile Strength (MPa) of concrete samples with added 2% of rivet mandrels

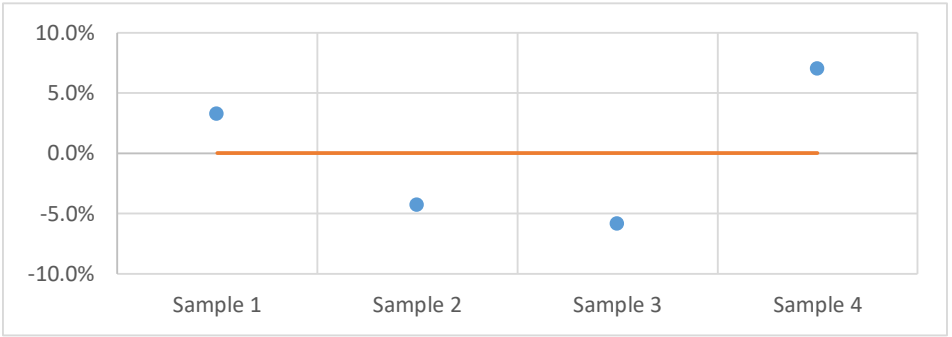

d) Split Cylinder Tensile Strength (MPa) of concrete samples with added 3% of rivet mandrels

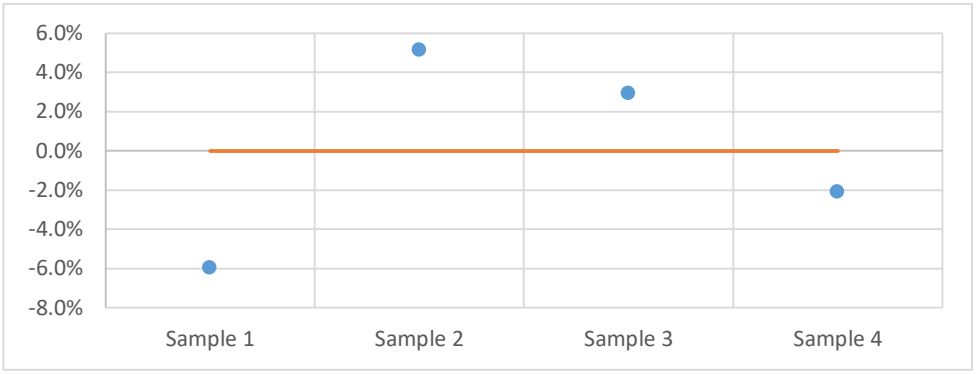

e) Split Cylinder Tensile Strength (MPa) of concrete samples with added 1% of wires

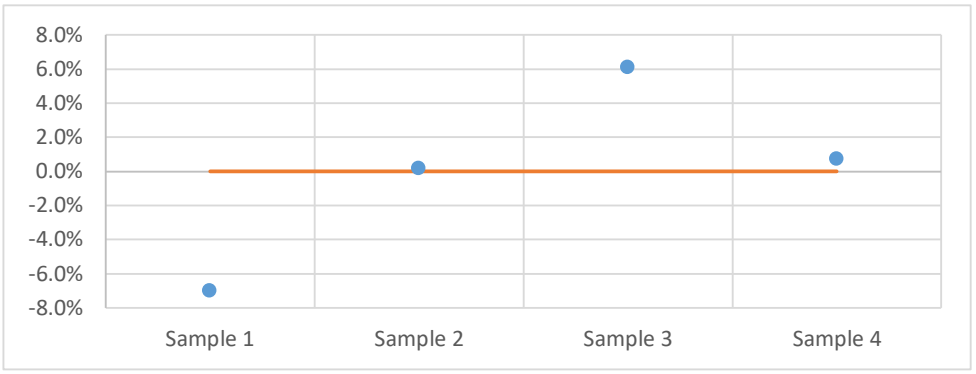

f) Split Cylinder Tensile Strength (MPa) of concrete samples with added 2% of wires

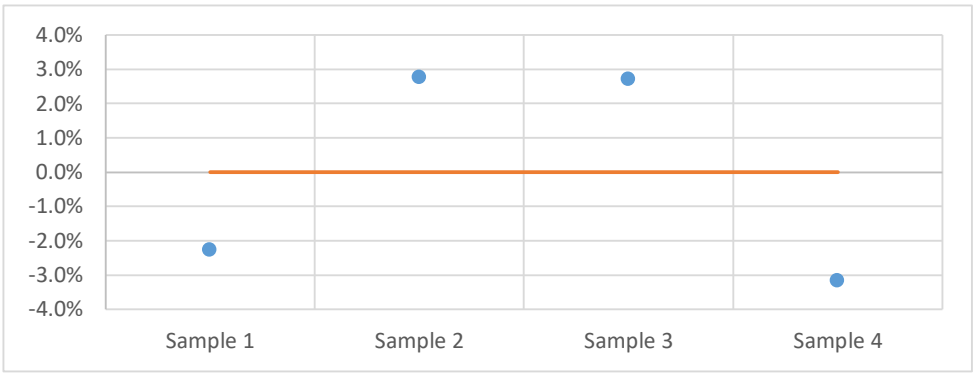

g) Split Cylinder Tensile Strength (MPa) of concrete samples with added 3% of wires

Figures A7

Modulus of rupture of concrete samples when adding different ratios of rivet mandrels and wires

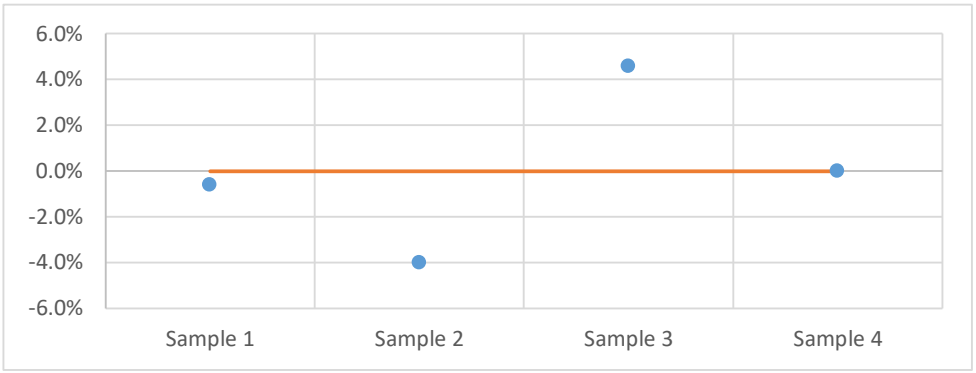

a) Modulus of Rapture (MPa) of plain concrete samples

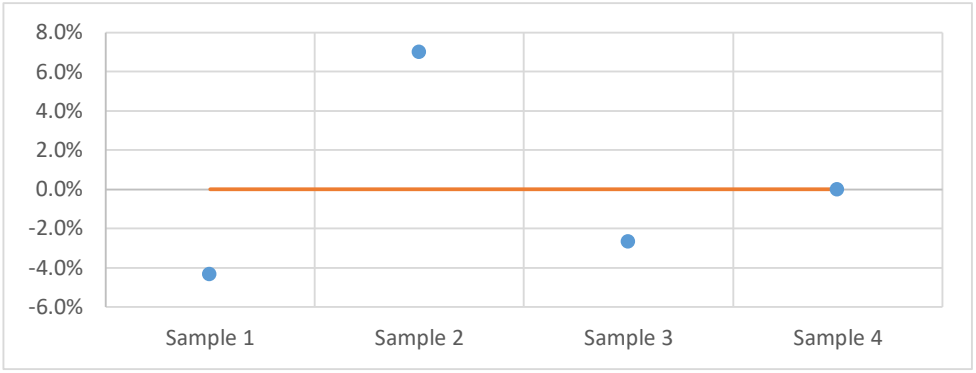

b) Modulus of Rapture (MPa) of concrete samples with added 1% of rivet mandrels

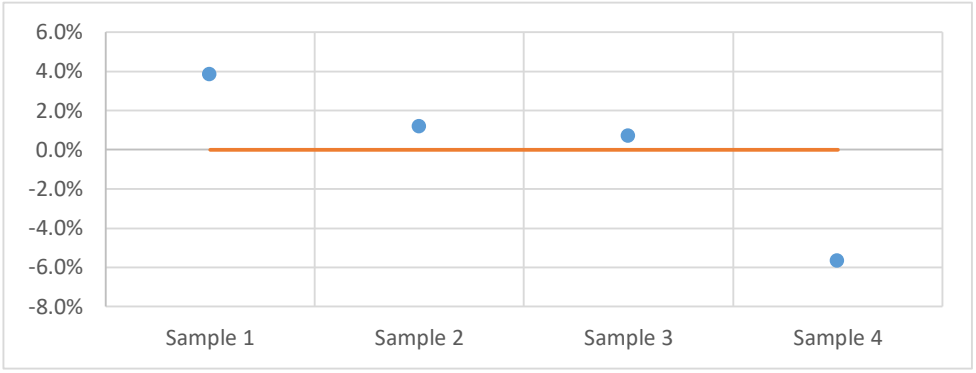

c) Modulus of Rapture (MPa) of concrete samples with added 2% of rivet mandrels

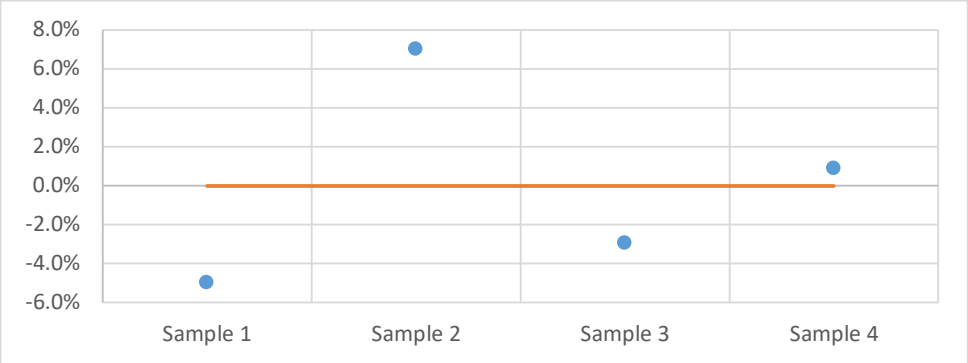

d) Modulus of Rapture (MPa) of concrete samples with added 3% of rivet mandrels

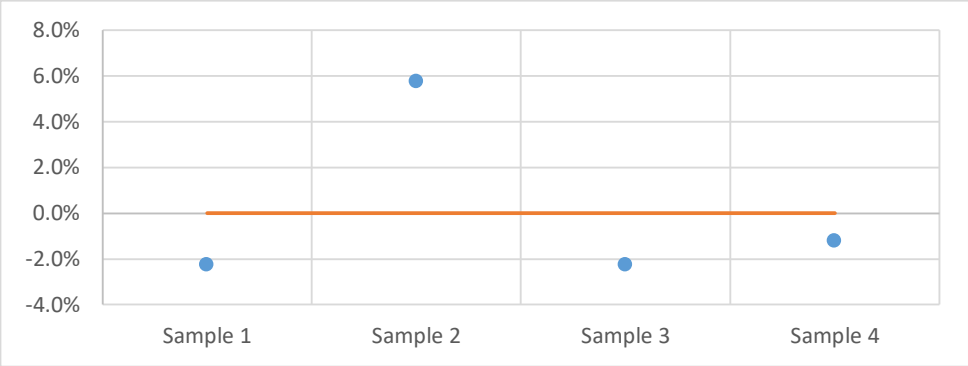

e) Modulus of Rapture (MPa) of concrete samples with added 1% of wires

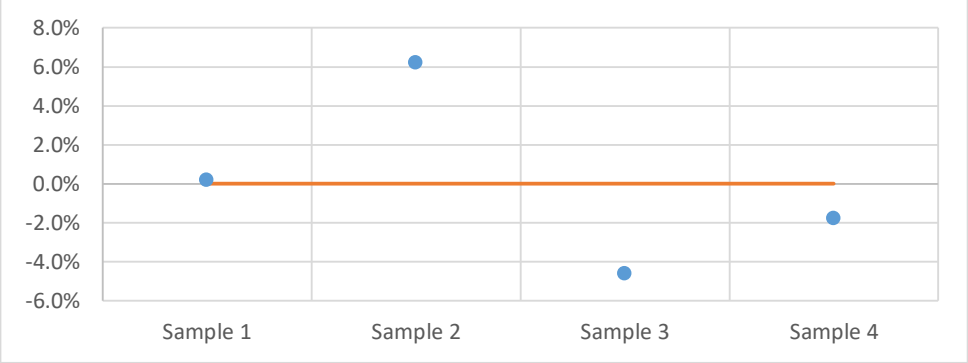

f) Modulus of Rapture (MPa) of concrete samples with added 2% of wires

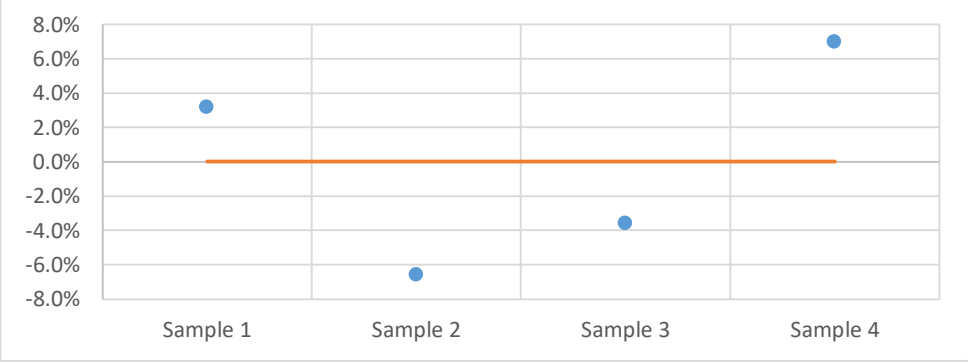

g) Modulus of Rapture (MPa) of concrete samples with added 3% of wiresss

Figure A8

Shears, moments and deflections equations – two equal concentrated loads symmetrically placed. [45]

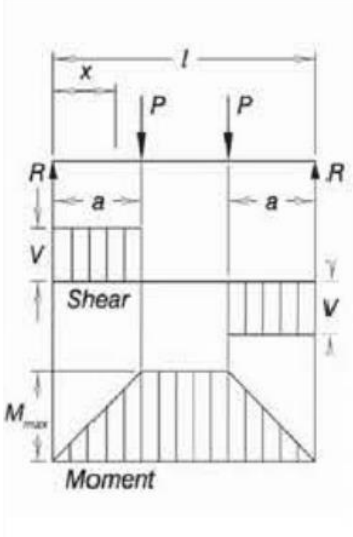

Total Equiv. Uniform Load ..... $= \frac{8Pa}{l}$

$R=V$ ..... $= P$

M_{max} (between loads) ..... $= Pa$

M_x (when $x < a$) ..... $= Px$

Δ_{max} (at center) ..... $= \frac{Pa}{24EI}\left(3l^2 - 4a^2\right)$

Δ_{max} (when $a = \frac{l}{3}$) ..... $= \frac{Pl^3}{28EI}$

Δ_x (when $x < a$) ..... $= \frac{Px}{6EI}\left(3la - 3a^2 - x^2\right)$

Δ_x (when $a < x < (l - a)$) ..... $= \frac{Pa}{6EI}\left(3lx - 3x^2 - a^2\right)$

Figures A9

Load/deflection relationships and elastic modulus of concrete samples when adding different ratios of rivet mandrels and wires

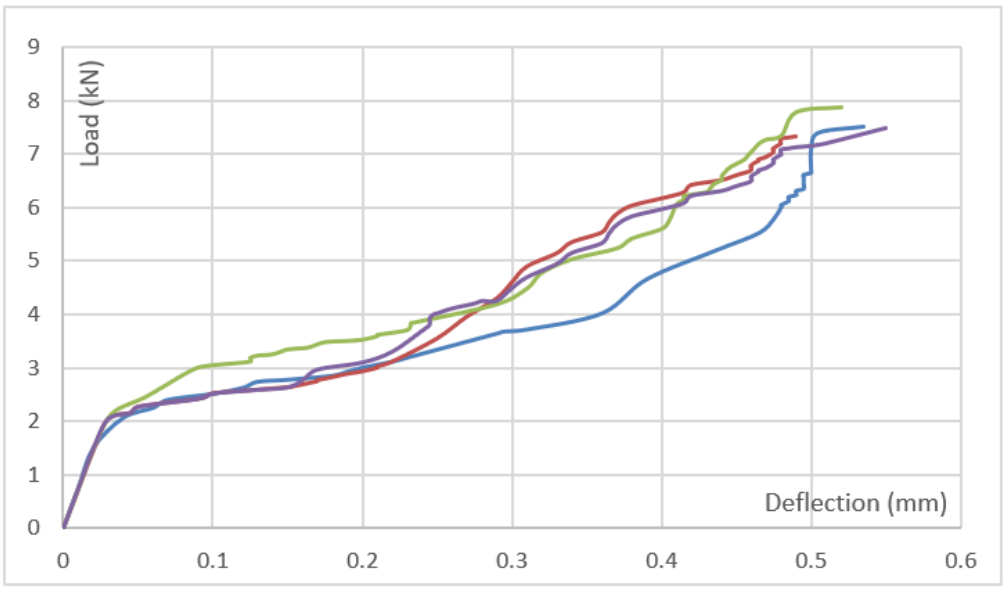

a) Load/deflection diagram of plain concrete samples

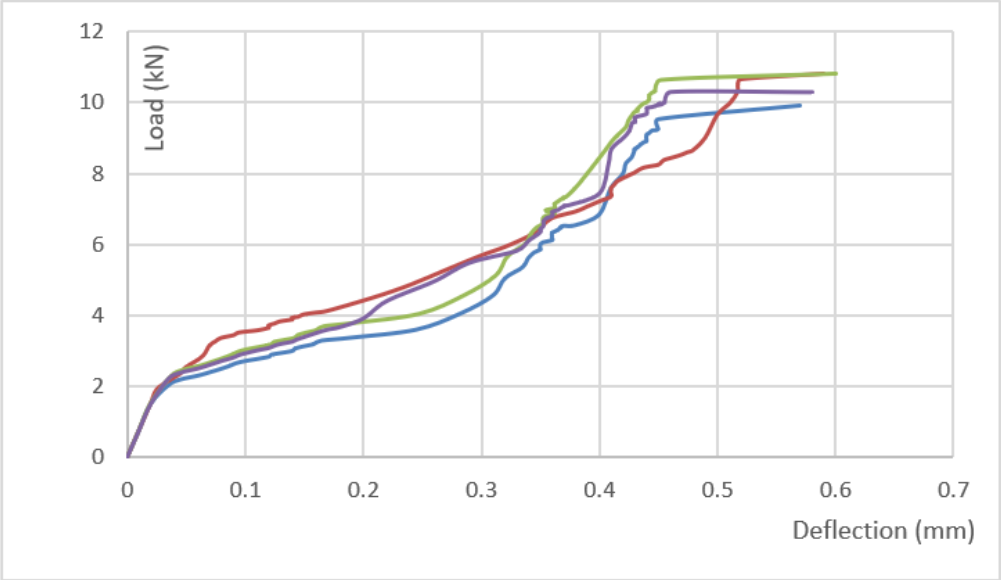

b) Load/deflection diagram of concrete samples with added 1% of rivet mandrels

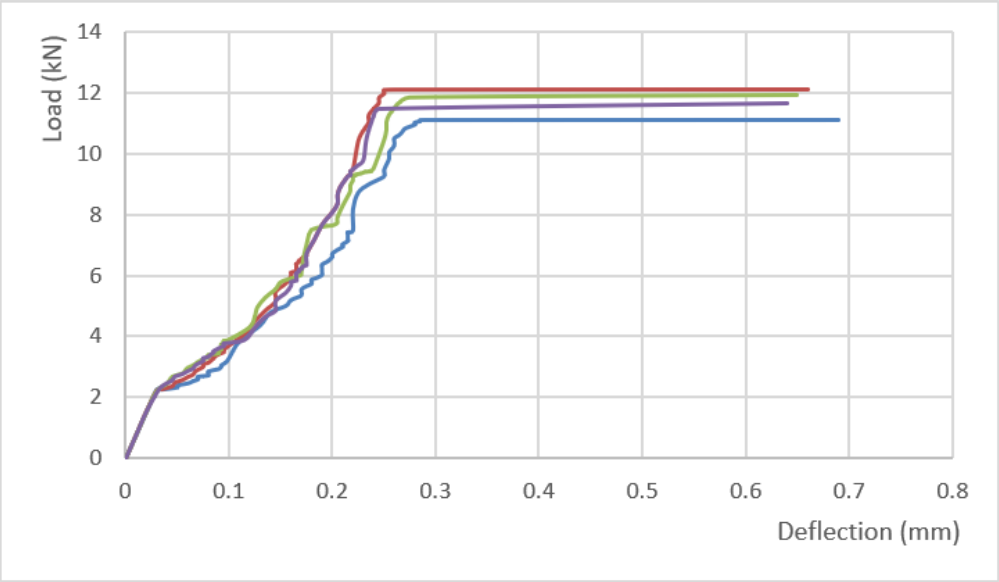

c) Load/deflection diagram of concrete samples with added 2% of rivet mandrels

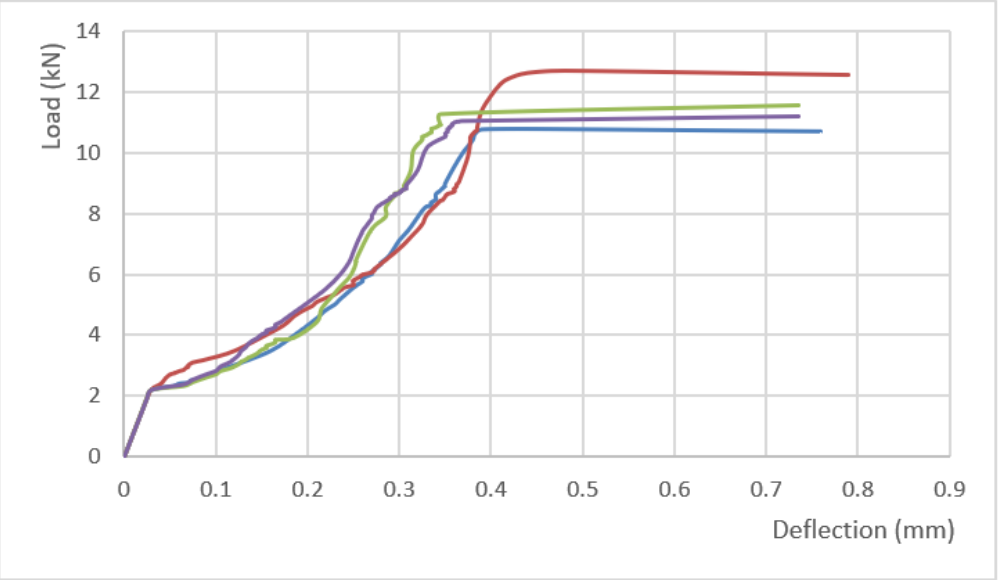

d) Load/deflection diagram of concrete samples with added 3% of rivet mandrels

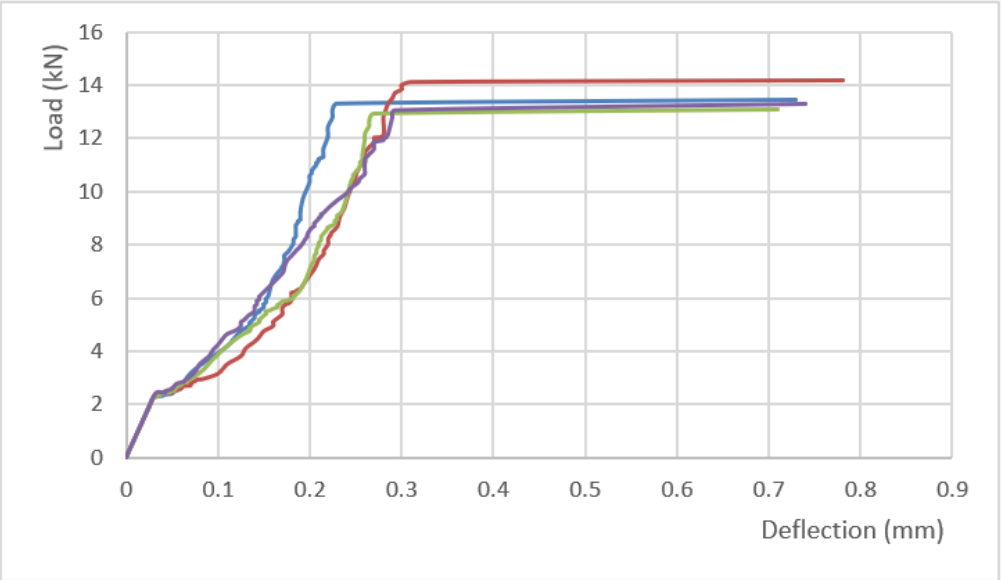

e) Load/deflection diagram of concrete samples with added 1% of wires

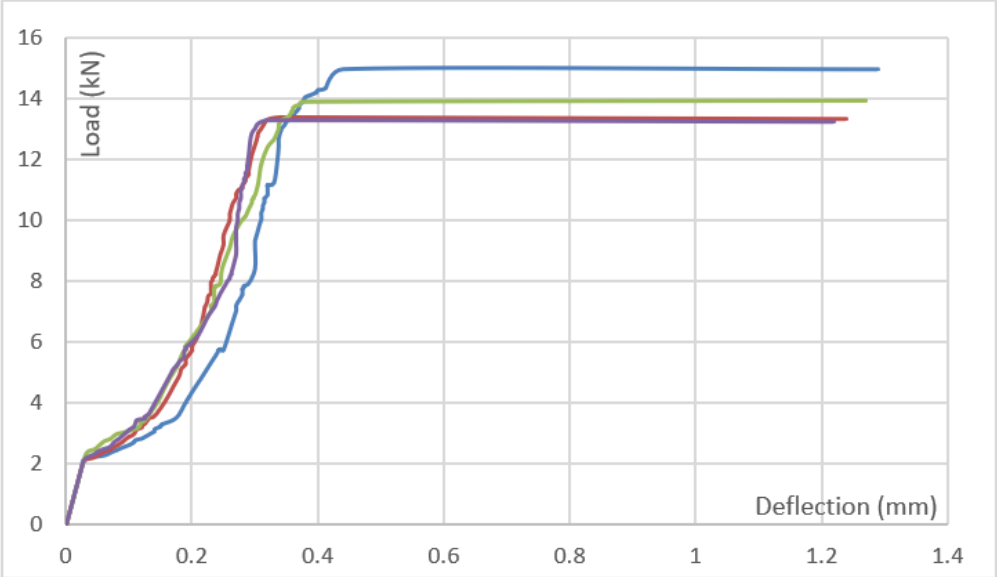

f) Load/deflection diagram of concrete samples with added 2% of wires

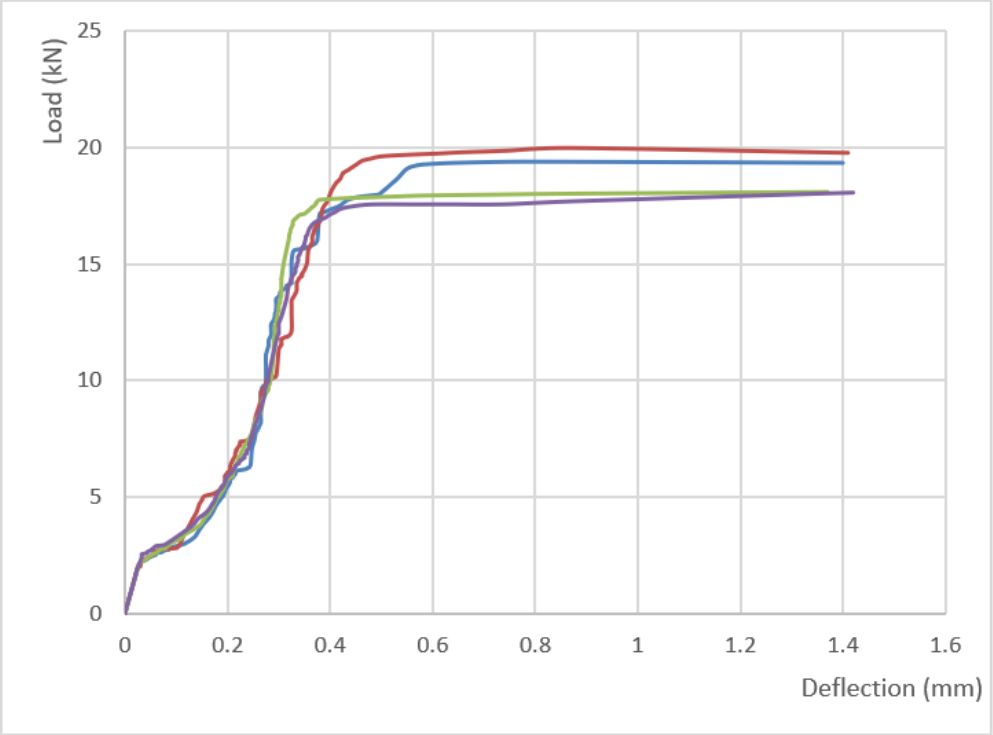

g) Load/deflection diagram) of concrete samples with added 3% of wires

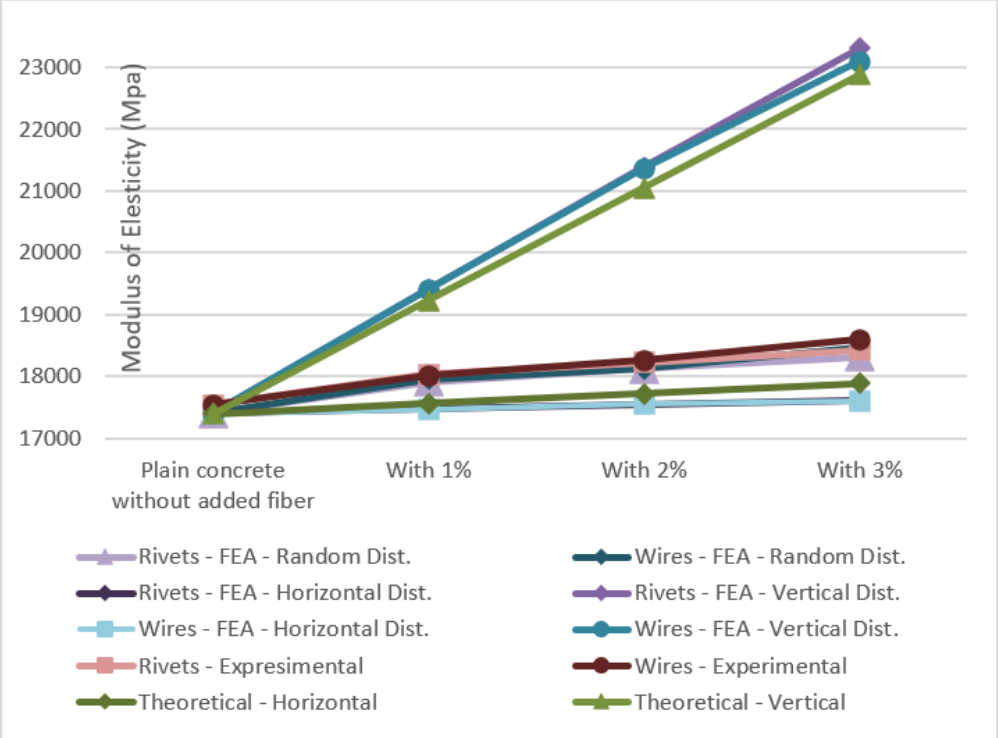

h) Modulus of elasticity (MPa) comparison between adding rivet mandrels and wires at different ratio

Figures A10

Time/deflection relationships of concrete samples when adding different ratios of rivet mandrels and wires.

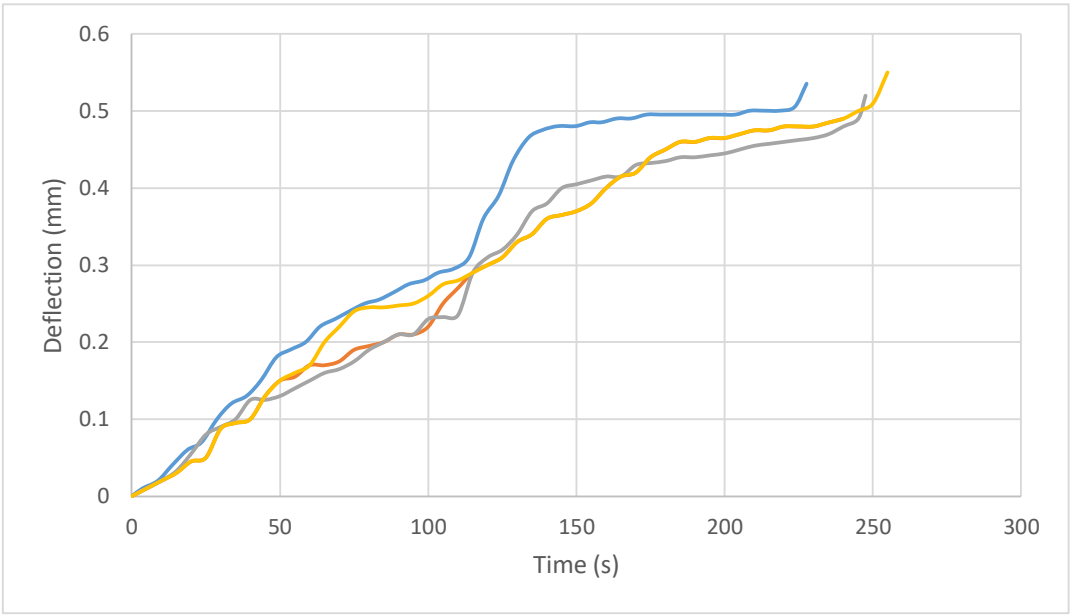

a) Time/deflection diagram of plain concrete samples

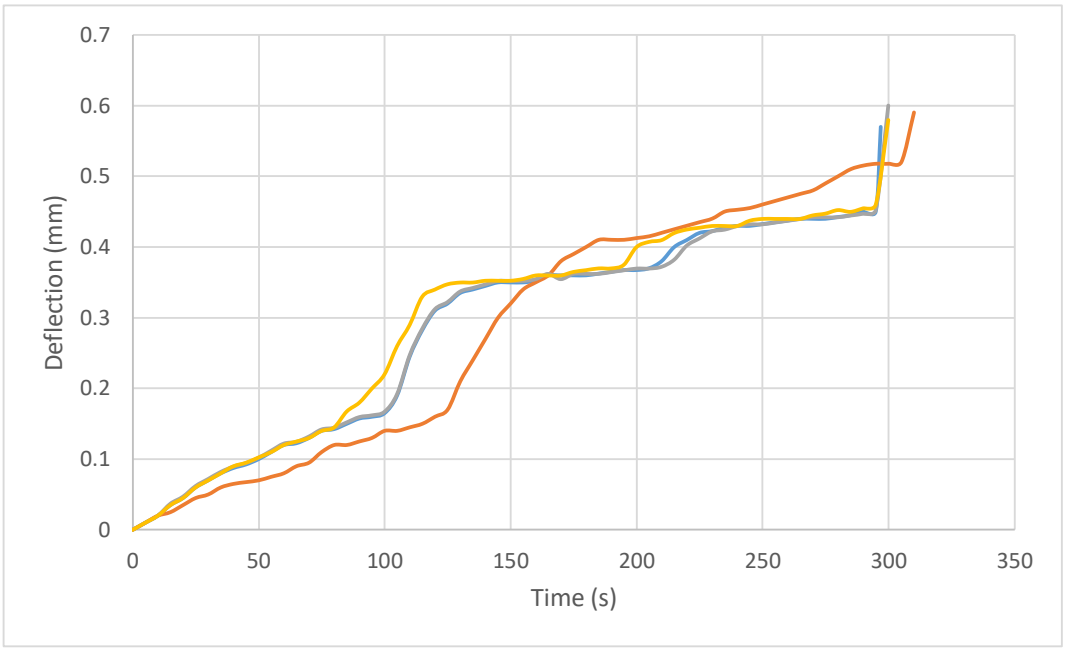

b) Time/deflection diagram of concrete samples with added 1% of rivet mandrels

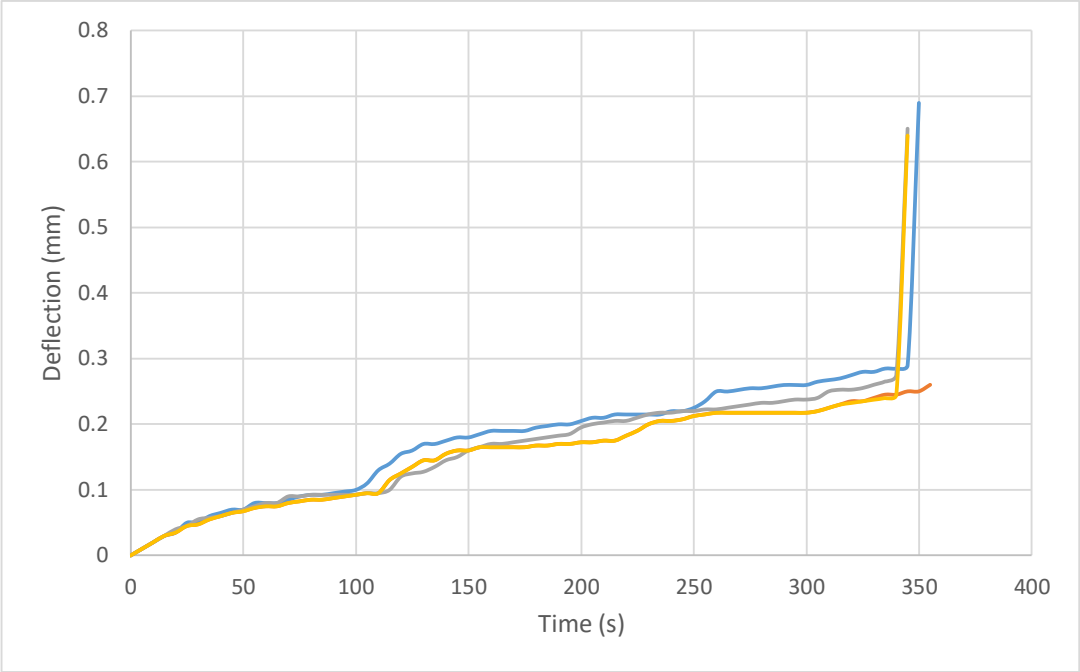

c) Time/deflection diagram of concrete samples with added 2% of rivet mandrels

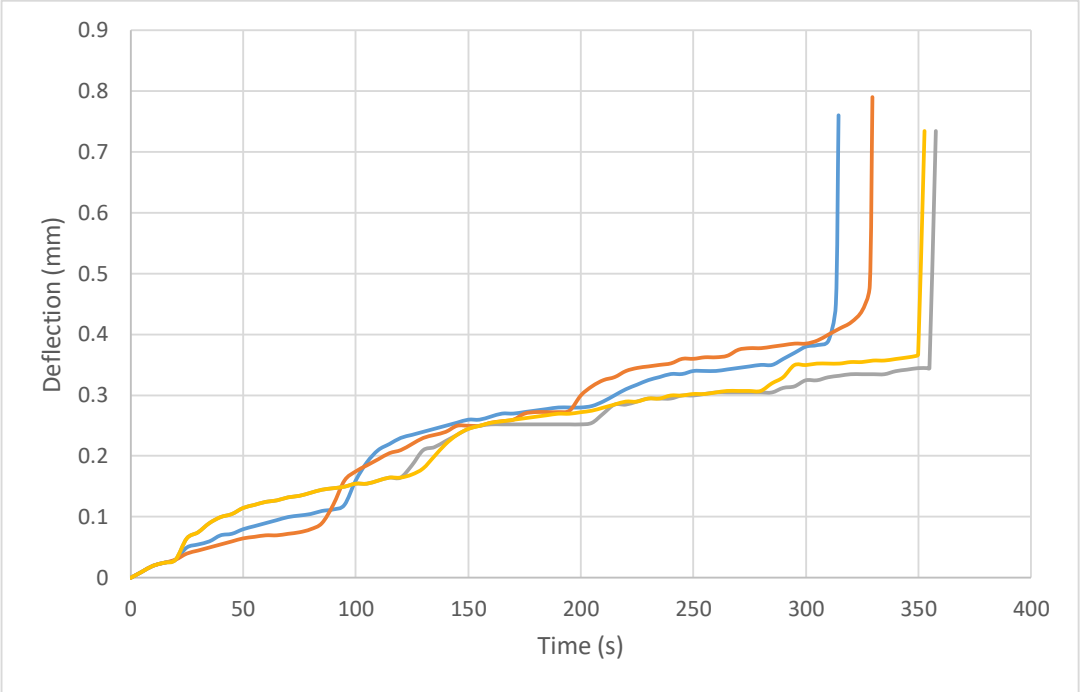

d) Time/deflection diagram of concrete samples with added 3% of rivet mandrels

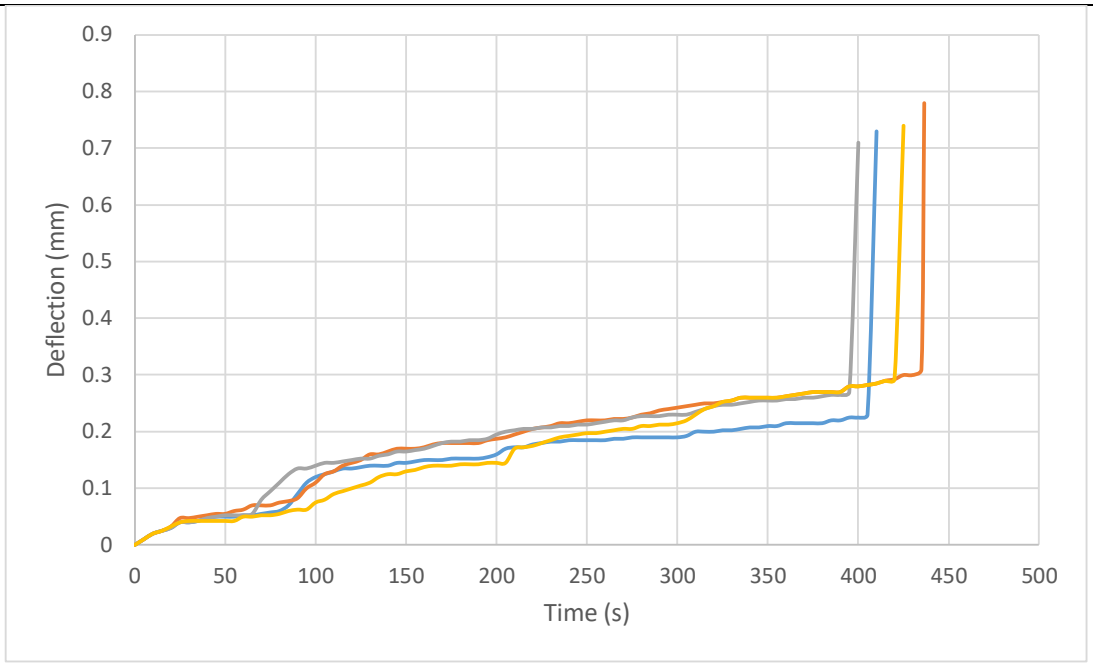

e) Time/deflection diagram of concrete samples with added 1% of wires

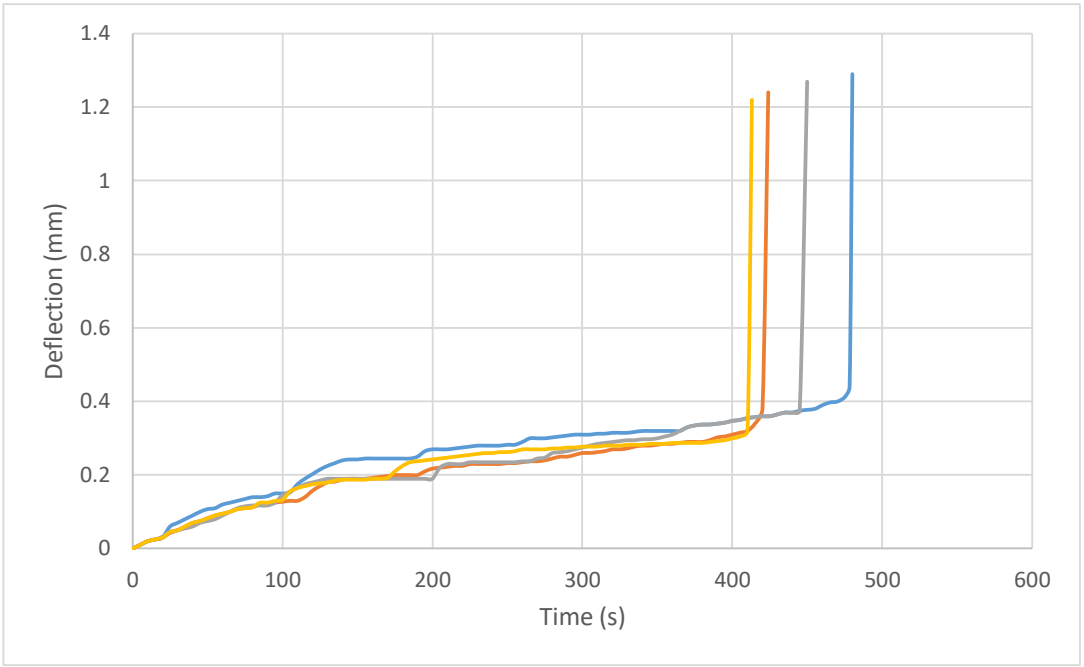

f) Time/deflection diagram of concrete samples with added 2% of wires

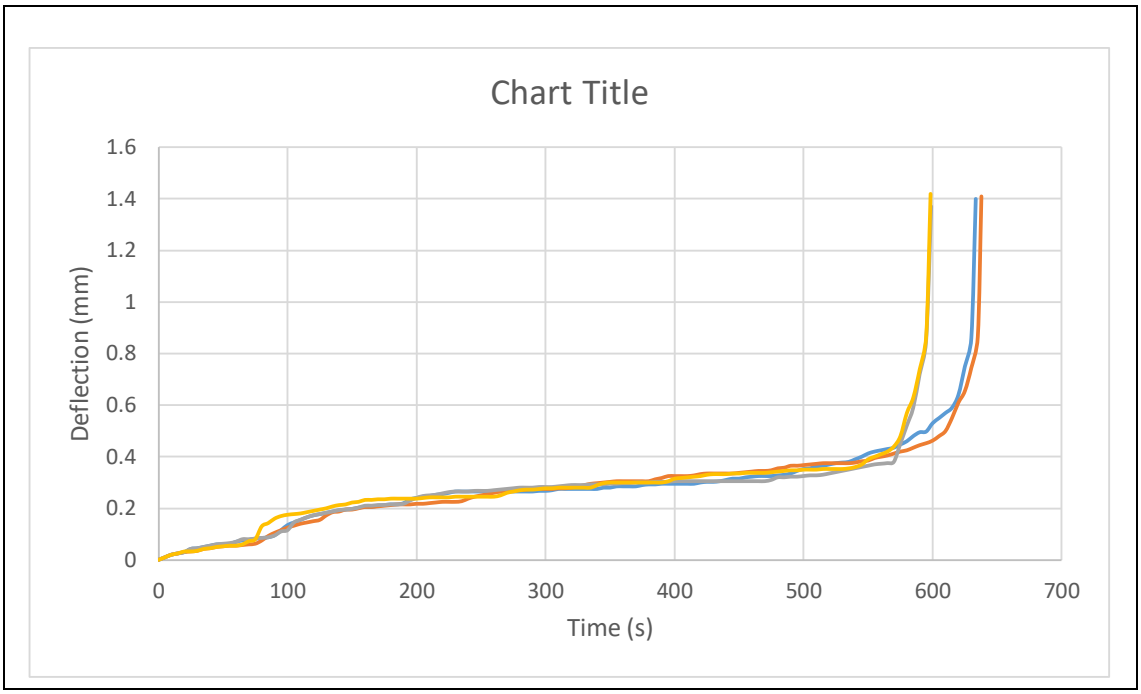

g) Load/deflection diagram) of concrete samples with added 3% of wiress

Figures A11

Load/Time relationships of concrete samples when adding different ratios of rivet mandrels and wires.

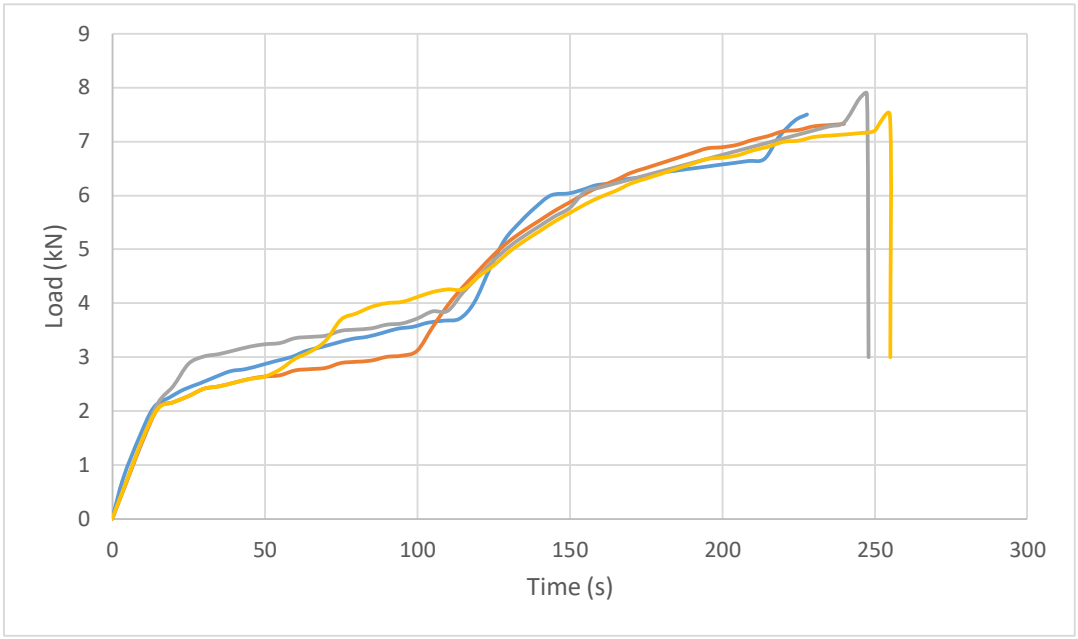

a) Load/Time diagram of plain concrete samples

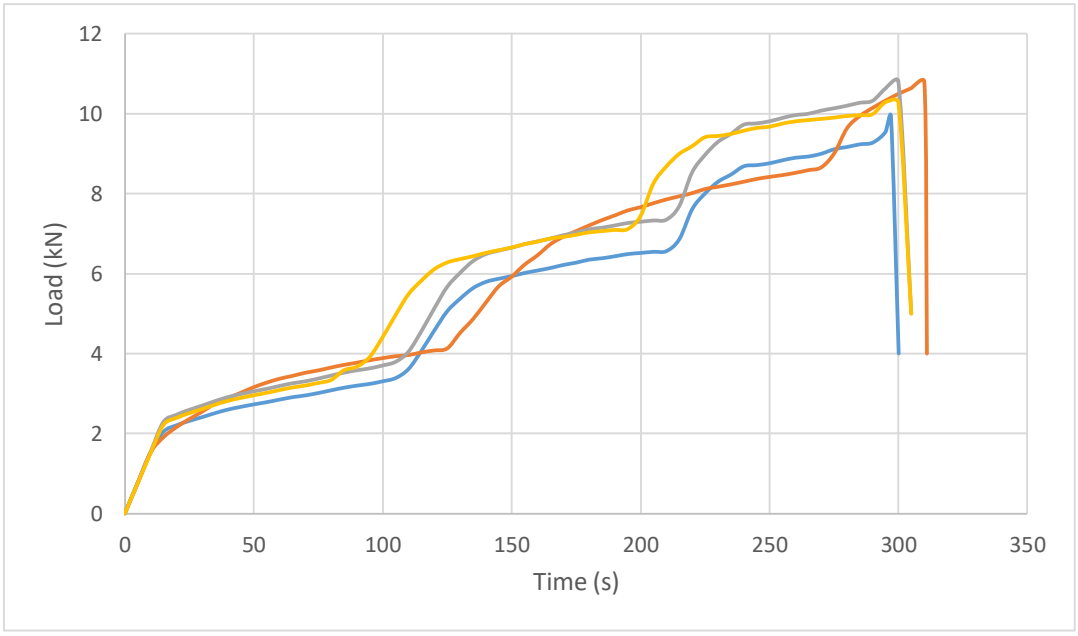

b) Load/Time diagram of concrete samples with added 1% of rivet mandrels

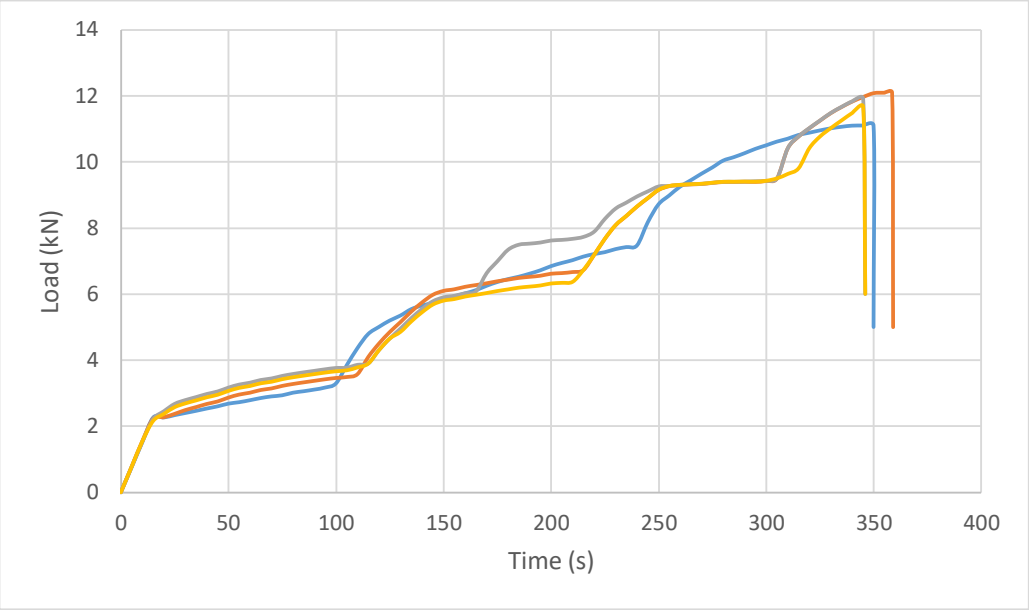

c) Load/Time diagram of concrete samples with added 2% of rivet mandrels

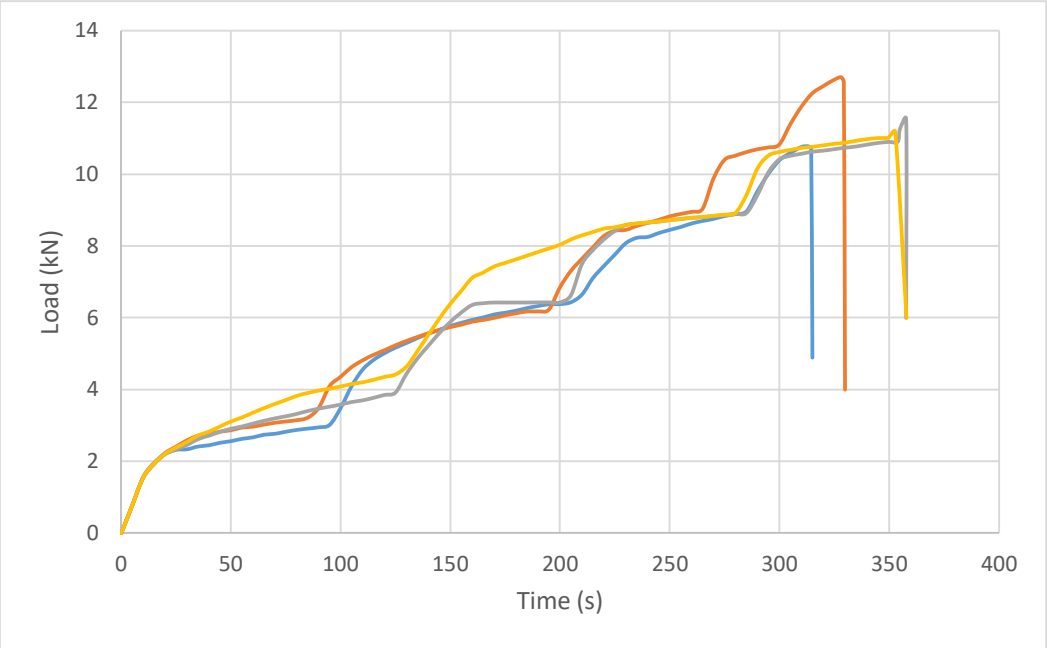

d) Load/Time diagram of concrete samples with added 3% of rivet mandrels

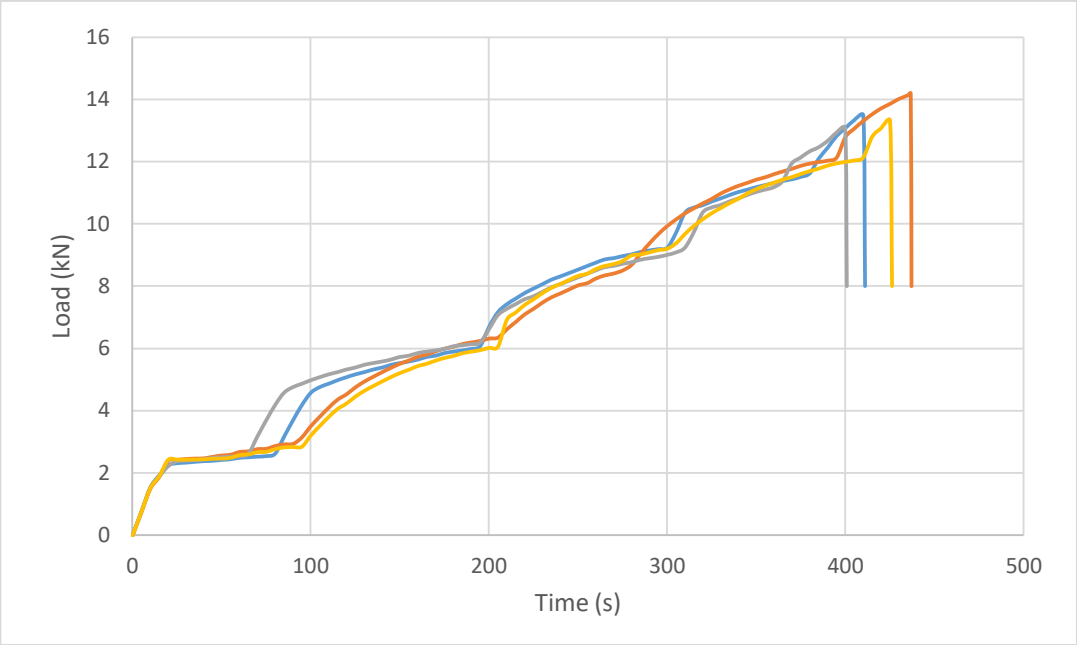

e) Load/Time diagram of concrete samples with added 1% of wires

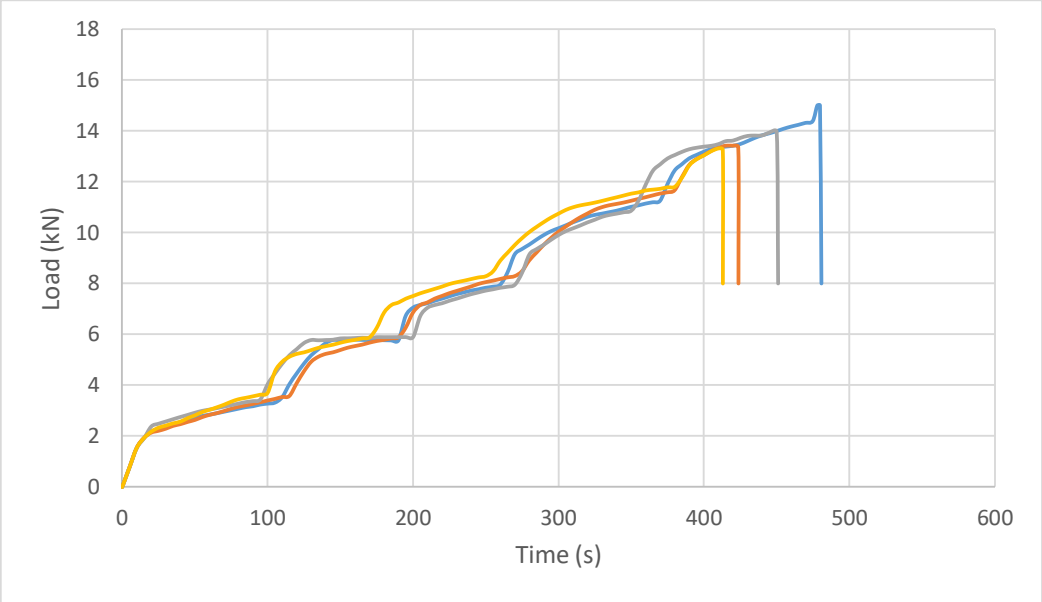

f) Load/Time diagram of concrete samples with added 2% of wires

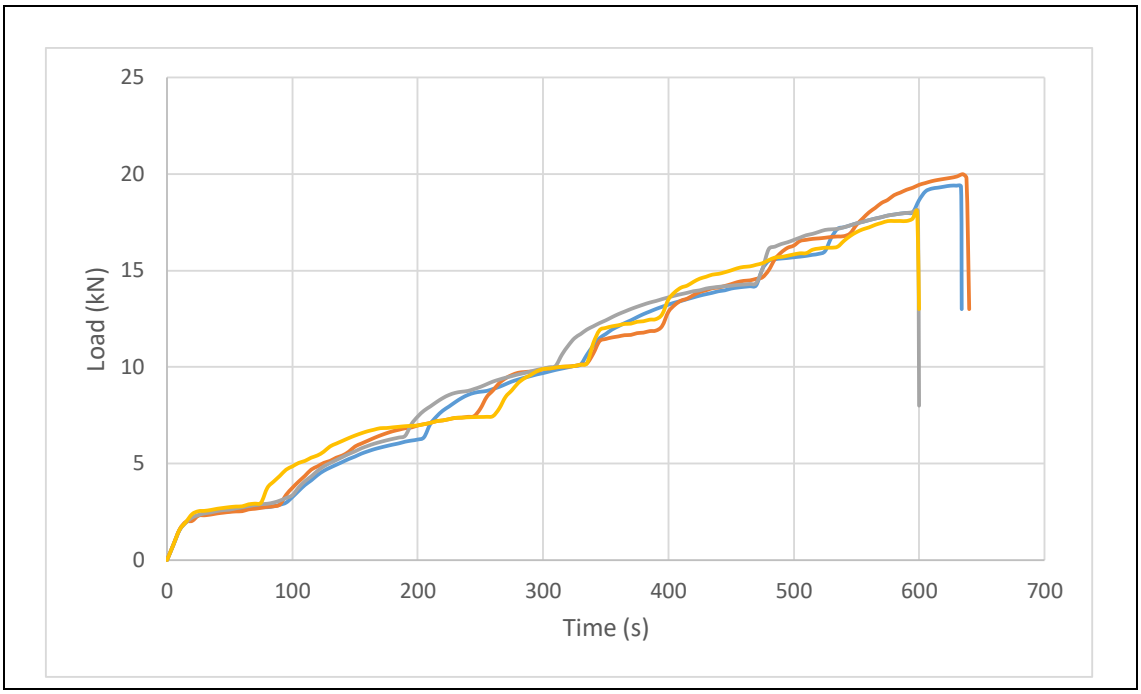

g) Load/Time diagram) of concrete samples with added 3% of wires

Figure A12

Remaining fiber models (see figure 3.1c)

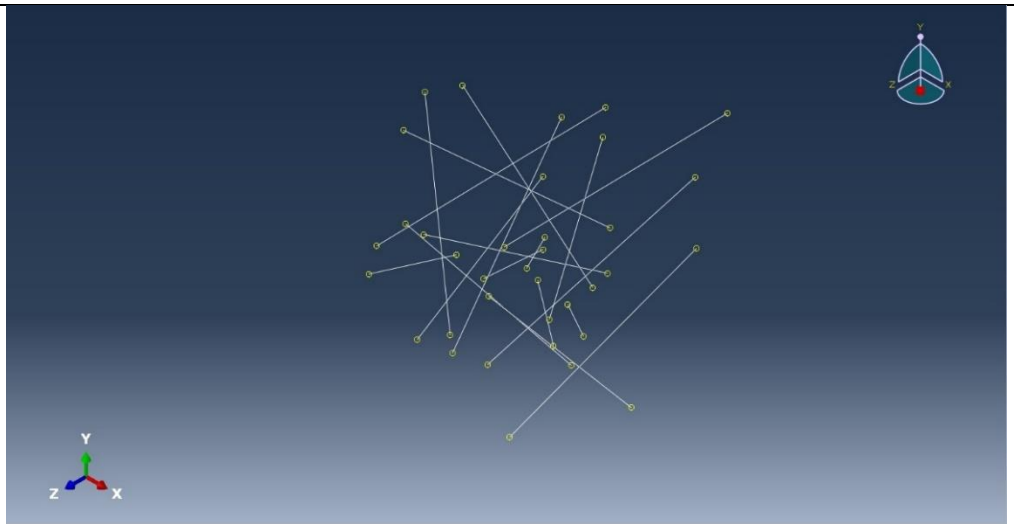

a) Model of rivet 2% fibers (18 pieces)

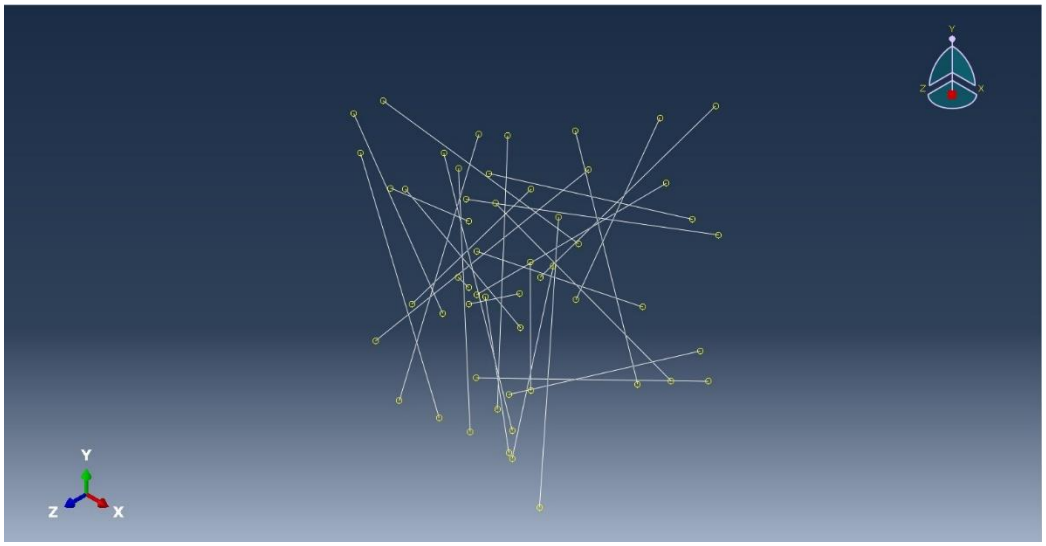

b) Model of 3% rivet fibers (27 pieces)

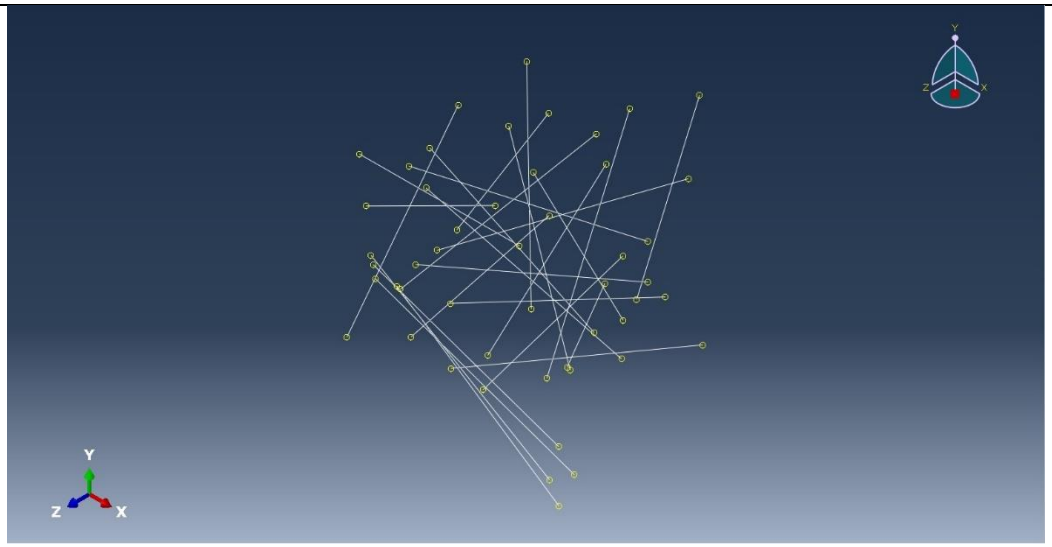

c) Model of 1% of wires fiber (25 pieces)

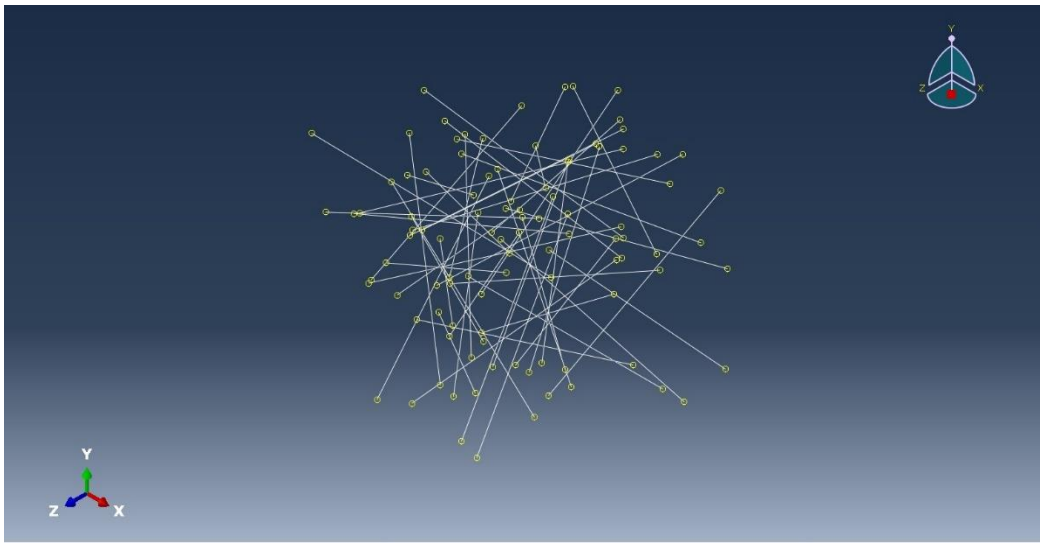

d) Model of 2% of wires fiber (50 pieces)

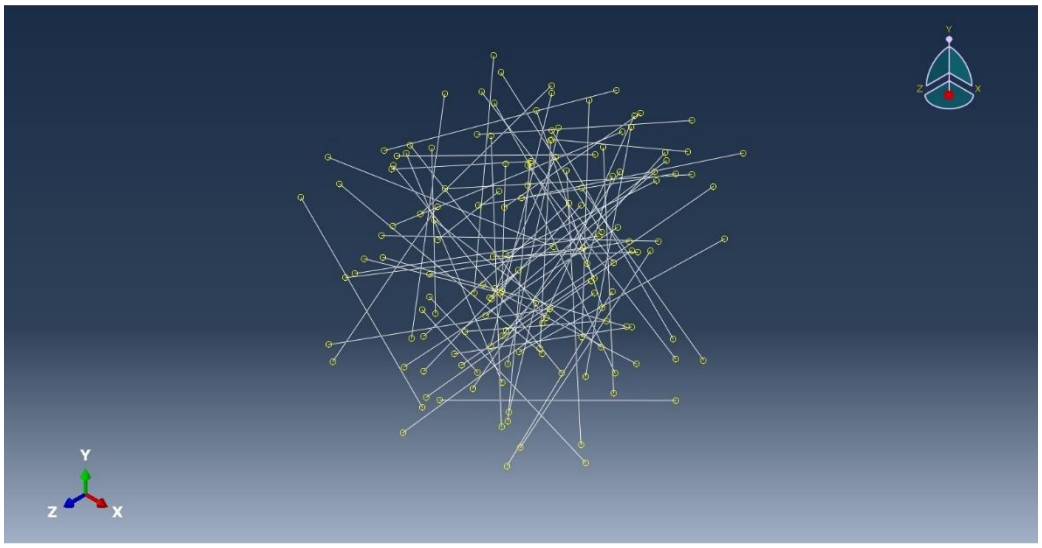

e) Model of 3% of wires fiber (75 pieces)

Figure A13

Concrete damage plasticity model: a yield surface in plane stress and b yield surface in the deviatoric plane

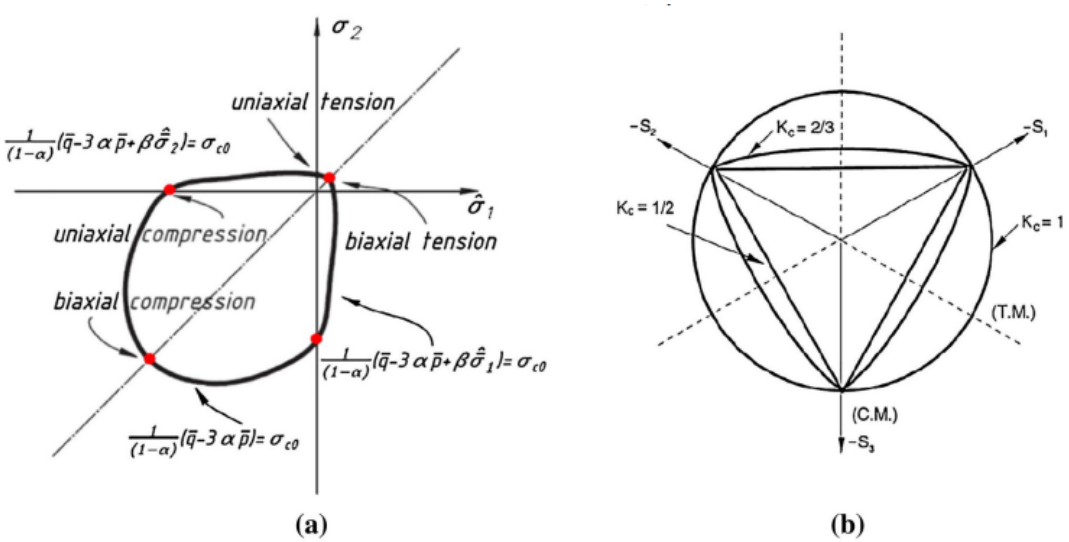

Figure A14

Uniaxial compressive stress–strain relationship for concrete

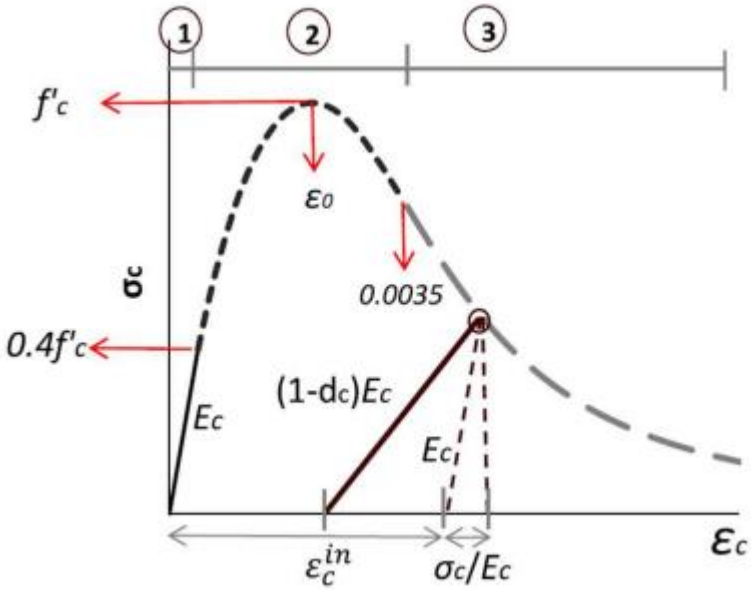

Figure A15

Uniaxial tensile stress–strain behavi9or for concrete and its softening branch assumptions

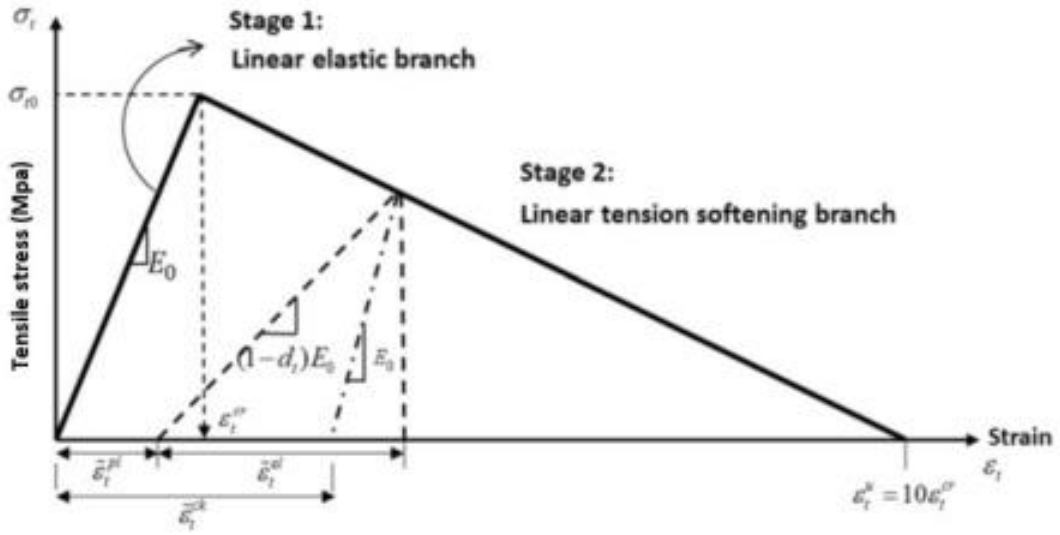

Figure A16

Uniaxial stress–strain behavior of reinforcements bars

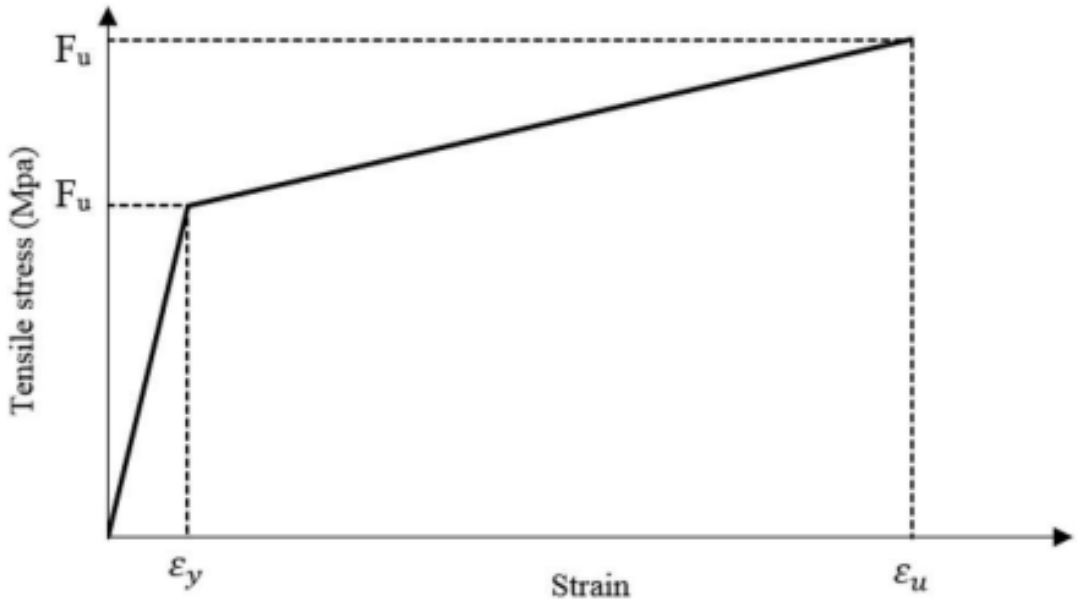

Figure A17

Embedded region interaction between fibers and concrete models in ABAQUS software

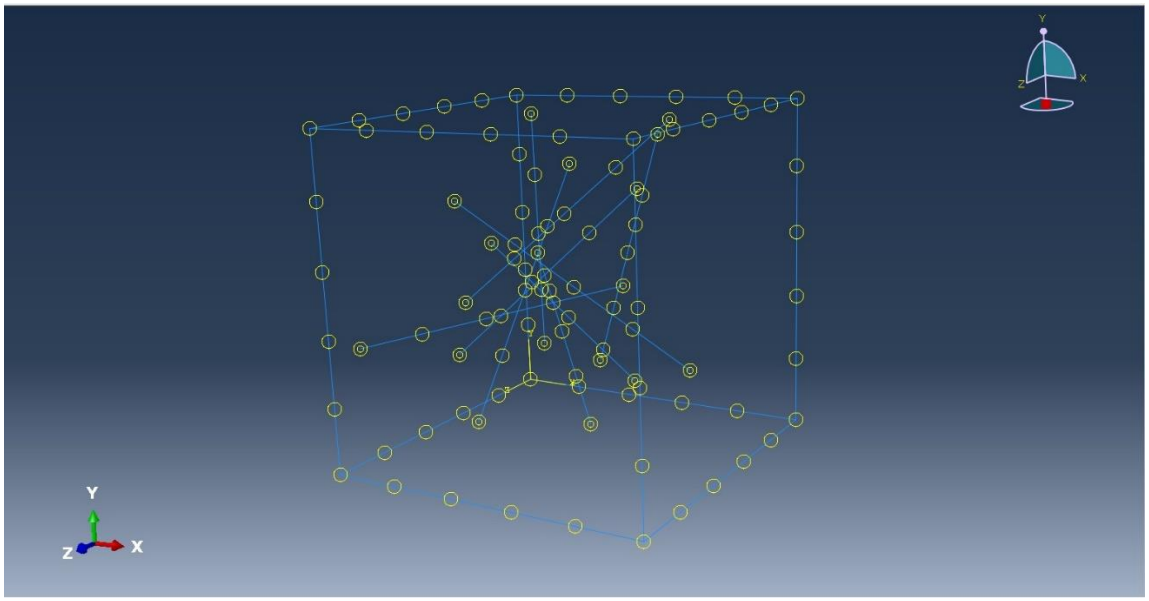

Figure A18

Applied boundary conditions to the concrete model.

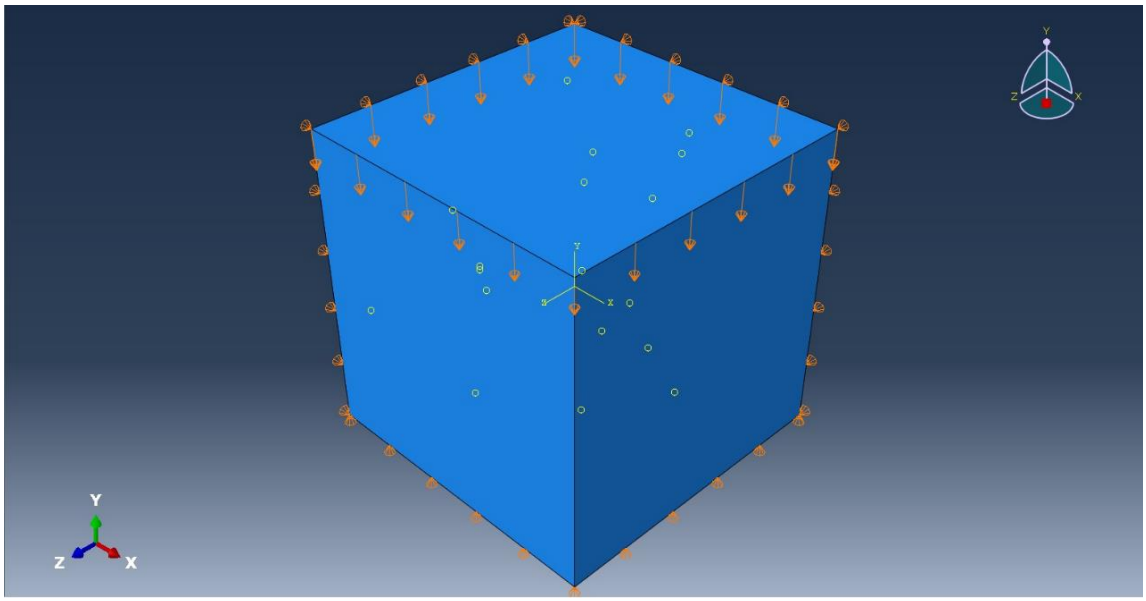

جـامعـــة النجاح الوطنية
كليـــة الدراســـات العليـــا

تحسين خصائص الخرسانة باستخدام النفايات

إعداد
رجاء خالد رجا صبره

إشراف
د. منذر دويكات
د. محمود دويكات

قدمت هذه الرسالة استكمالا لمتطلبات الحصول على درجة الماجستير في هندسة الإنشاءات، من كلية الدراسات العليا، في جامعة النجاح الوطنية، نابلس –فلسطين.

2023

تحسين خصائص الخرسانة باستخدام النفايات

إعداد

سماهر عبد الحفيظ حمدان

إشراف

د. أيمن رفيق نزال

الملخص

خلفية الدراسة: الخرسانة هي أكثر مادة مستخدمة في البناء، خصوصاً في فلسطين. لكنها تواجه بعض المشاكل والمعوقات عند بناء الأبنية العالية والأرضيات الكبيرة والطوابق الخاصة ذوات الحمولة العالية، إلخ. المواد المستخدمة لإنتاج الخرسانة عالية الأداء تأتي بتكاليف باهظة، مما جعل الحاجة إلى إيجاد بدائل عن المواد الشائعة المستخدمة لإنتاج هذا النوع من الخرسانة.

أهداف الدراسة: التباشيم وأسلاك الربط متوفرة بشكل واسع كفضلات، وهذا البحث يدرس تأثير هذه المواد على الخصائص الميكانيكية للخرسانة، للتحقق من مناسبة استخدام هذه المواد لإنتاج خرسانة عالية الأداء.

المنهجية: تم استخدام مهنجيتين لدراسة تأثير إضافة الألياف إلى الخرسانة. الأولى هي باستخدام تحليل العناصر المحددة ومحاكاة تصرف المادة الخرسانية عند إضافة نسب مختلفة من الألياف. وأيضاً تم عمل تجارب مختبرية للتحقق من نتائج تحليل العناصر المحددة وإيجاد بعض الخصائص الأخرى ككثافة المادة وقابليتها التشكيل.

النتائج: تشير النتائج إلى أن إضافة ألياف النفايات مثل التباشيم والأسلاك ساعدت على تحسين قدرة تحمل الضغط والشد ومرونة المادة الخرسانية. ولكن، توجد حدود تمثل ذروة تحمل الخرسانة للضغط والشد، وتجاوز هذه الحدود يبدأ بإضعاف المادة.

الكلمات المفتاحية: خرسانة، خرسانة عالية الأداء، ألياف، أسلاك الربط، تباشيم.